ESTIMATING PILE SHAFT CAPACITIES BY USE OF DIRECT CPT/CPTu-BASED METHODS FOR CONTINOUS FLIGHT AUGER PILES IN SILTS AND SANDS

A Thesis

Submitted to the Faculty of Graduate Studies

in Partial Fulfillment of the Requirements

for the Degree of Master of Science

in the

Department of Civil Engineering

University of Manitoba, Winnipeg, Canada

By Patrick W. Machibroda

August, 2023

Contents

List of Figures

List of Tables

ABSTRACT

Cone penetrometer (CPT) and piezometric cone (CPTu) test methods are widely used to estimate pile shaft resistances with depth, but these methods are typically derived from empirical correlations to reference load tests. They may not be applicable to all geological conditions and pile types. Thus, developing correlations for specific geographic areas and pile types can be beneficial. In this study, the accuracy and precision of five applicable direct CPT/CPTu methods were evaluated for continuous flight auger (CFA) piles in predominantly silt and sand soils of the Condie aquifer near Regina, Saskatchewan. Six instrumented CFA test piles were evaluated through a combination of CPTu testing and instrumented static axial load testing to determine reference shaft capacities. The direct CPT/CPTu method determined shaft capacity estimates were compared to refence shaft capacities, and the relative performances of the methods were evaluated using statistical and non-statistical quantitative evaluation criteria. The best performing methods (Modified Unicone and KTRI) were then calibrated by minimizing the square root of the residual sum of squares between the predicted and measured shaft capacities. Once calibrated, the methods were re-evaluated using the initial criteria. It was found that all methods overestimated the unit shaft resistance in the upper 1.5 m, but the calibrated KTRI method provided the best overall fit. The calibrated Modified Unicone method was found to be slightly less accurate but more conservative in its predictions of shaft capacity. These findings can be used to improve pile design in the Condie aquifer region and other areas with similar geological conditions.

ACKNOWLEDGMENTS

I would like to acknowledge the contributions made in the way of opportunities, guidance, and suggestions by Dr. J.A Blatz and Mr. K. Pardoski, P.Eng. I would like to thank Mr. K. Mason, P.Eng. for his co-operation and support in allowing me to use the data and tag along with project field work. I am appreciative of Dr. D. Elwood and Dr. I. Fleming as well for allowing me to take courses at the University of Saskatchewan so I could be involved in the fieldwork. This was an invaluable experience that has greatly impacted my fledgling career.

Technical discussions and inspiration garnished from my father; Ray were also greatly appreciated. Motivation came from my late grandfather Paul as well. Kudos to Georgia as well. You did not actually read my thesis, but you did have to endure listening to me talk about piles and cones.

NOMENCLATURE

ROMAN SYMBOLS

A_c	Projected area of the CPTu cone
$A_{concrete}$	Cross-sectional area of the concrete shaft at the plain of the strain gauges
A_s	Surface area of the CPTu friction sleeve
A_s	Surface area of the pile shaft
A_{steel}	Cross-sectional area of the reinforcing steel at the plain of the strain gauges
D	Nominal pile diameter
E	Young's modulus
E_c	Young's modulus for concrete
E_s	Young's modulus for steel reinforcement
F_r	Normalized friction
F_s	Total force acting on the CPTu friction sleeve
f_s	Sleeve friction of the CPTu
I_c	CPT material index
k_1	Togliani unit shaft resistance factor
k_3	Togliani unit end bearing resistance factor
k_b	Price and Wardle unit end bearing resistance factor for pile type
k_c	LCPC bearing capacity factor for soil and pile type
k_s	Price and Wardle unit shaft resistance factor for pile type
L	Length of pile embedded below grade
n	Stress ratio exponent for normalized tip resistance determination
P	Force acting along pile cross-section
P_a	Atmospheric pressure
Q_b	End bearing capacity of a pile
Q_c	Total force acting on the CPTu cone
q_c	Cone resistance of the CPTu
q_{ca}	The averaged cone tip resistance as described by Bustamante and Gianeselli (1982)
q_E	Effective tip resistance (using dynamic porewater pressure)

Q_s	Shaft capacity of a pile
$Q_{s(m)}$	Pile shaft capacity obtained from static axial load test
$Q_{s(p)}$	Pile shaft capacity predicted from direct CPT/CPTu method
Q_t	Total axial pile capacity
q_t	Corrected cone tip resistance for porewater pressure effect
Q_{tn}	Normalized tip resistance
Q_p	Predicted total pile capacity
Q_m	Measured total pile capacity
R_f	Friction ratio
r_s	Unit shaft resistance of a pile
r_t	Unit end bearing resistance of a pile
u_2	Dynamic porewater pressure
u_o	Equilibrium porewater pressure
Δu	Excess porewater pressure

GREEK SYMBOLS

α_{LCPC}	LCPC method friction coefficient
λ	Togliani method unit end bearing resistance coefficient for pile type
β	Togliani method unit shaft resistance coefficient for pile type
Θ_{PT}	Modified Unicone method pile type coefficient
Θ_{TC}	Modified Unicone method loading direction coefficient
Θ_{Rate}	Modified Unicone method cone penetration rate coefficient
σ_{atm}	Atmospheric pressure
σ_v	Total vertical overburden stress at mid-layer depth
σ'_v	Effective vertical overburden stress at mid-layer depth
ε	Measured strain from strain gauges
σ	Standard deviation of predicted vs. measured pile shaft capacities
μ	Mean of predicted vs. measured pile shaft capacities

ACRONYMS

CPT	Cone penetration or cone penetrometer test
CPTu	Piezocone penetration test
CFA	Continuous flight auger pile
RSS	Residual sum of squares
mbg	Meters below grade
LVDT	Linear variable differential transformers
COV	Coefficient of variation
KTRI	Kajima Technical Research Institute (Takesue et al., 1998 method)
LCPC	Laboratoire Central des Ponts et Chausees (Bustamante and Gianeselli, 1982 method)

CHAPTER 1. INTRODUCTION

1.1 BACKGROUND

Deep foundation units such as piles are commonplace amongst the landscapes of the Canadian prairies. Historically, these deep foundation units have supported structures by transferring applied loads to deeper and stronger soil layers (Terzhagi and Peck, 1968). In recent decades, the applications of piles have expanded to absorbing tensile and lateral loads, supporting loads by shaft resistance, and to reducing settlements (Salgado, 2008). There are many types of pile foundation, and they are typically classified based on the following:

- Method of fabrication and installation process
- Pile material
- Pile loading mode

Under the method of fabrication and installation process, the classification of piles are divided into non-displacement and displacement piles. The classification of piles by these considerations are radically important from a design perspective because the response of the piles is characterized due to the state of the soil around the pile after installation. In the case of non-displacement piles, a volume of soil is removed from the ground and the pile is cast in-situ. Displacement piles are piles that are inserted into the soil by either driving or jacking. There is little to no soil removal in the installation of displacement piles. A displacement pile to some degree will have preloaded the soil surrounding the pile, whereas the non-displacement pile will preserve the state and density of the surrounding soil.

The continuous flight auger pile (CFA) is a type of pile that combines certain properties from the displacement and non-displacement piles. Originally these piles were introduced in the 1950's (Van Impe, 2004), however they were not widely used until the 1980's (Fleming, 1995). These piles are bored similar to bored piles, where they are installed by rigs typically crawler mounted. During installation the auger is first positioned above the desired pile location, establishing auger verticality, and then drilling to a final depth. During drilling, the auger transports the soil upwards along its flights. These piles are installed much faster than a typical non-displacement pile. After the desired depth is reached, a seal at the bottom of the auger opens and concrete is pumped through the hollow stem of the auger. As concrete is pumped, the auger is brought up

without rotation, or in the case of sandy soils there is a very slow rotation in the same direction that the pile was bored. The rate of ascension for the auger is monitored so that the pumping rate of the concrete can ensure pile continuity and support of the surrounding soil. The volume of concrete pumped per unit of time is measured directly by use of sensors placed just before the concrete enters the auger. This volume is often compared to an estimated volume that is correlated to the counting of pump strokes (Salgado, 2008; Neely, 1991). If steel reinforcement is required for the design, then it is introduced by pushing it down into the placed concrete by either vibrating or driving.

The main focus of the geotechnical design of a pile foundation is to establish a secure threshold for the external load that it can withstand without compromising the stability of the structure it supports. To accomplish this, a factor of safety or resistance factor is applied to the projected ultimate or nominal bearing capacity (also known as pile capacity), which represents the amount of load that would trigger shear failure of the foundation. Depending on the pile type used, these capacities can predominantly be derived through shaft and/or toe resistances. These capacities are determined based on the following methods (Chung et. al, 2019):

- Static analysis (analytical)
- Full-scale field loading tests
- Pile driving formulae
- Analysis based on in-situ sounding tests

Recently, in-situ sounding tests have gained popularity as a means of determining pile capacity. This trend can be attributed to the advancements in testing equipment, improved understanding of the tests' mechanics and interpretation, and reduced costs in comparison to full-scale pile loading tests (Eslami and Gholami, 2006; Eslami et al., 2011). The most commonly used in-situ sounding tests are the standard penetration test (SPT) and the cone penetration test (CPT) (Salgado, 2008). When it comes to pile analysis and design, the CPT is generally considered superior to SPT. This is because the data obtained from the CPT is repeatable, reliable (not influenced by the operator), and provides quick continuous readings of soil behavior with depth (Robertson, 2012; Bartz and Blatz, 2021). One of the earliest applications of the CPT was to estimate axial pile capacity. The cone penetrometer was used as a model pile, and the data

obtained from it was utilized to provide the necessary parameters for capacity estimation (Eslami, 1997).

There are two main approaches to prediction methods based on CPT data: direct and indirect. In the direct approach, pile capacities are directly correlated to CPT cone resistance (q_c), and/or the local sleeve friction (f_s) measurements. In contrast, the indirect approach involves using q_c and f_s to evaluate soil strength parameters, which are then utilized in static analysis to determine pile capacity (Cai et al., 2009; Niazi and Mayne, 2013). Direct methods do not require laboratory testing to determine intermediate values to supplement the field data, unlike indirect methods. Some of the original direct CPT-based pile design and analysis methods include Schmertmann (1978), De Ruiter and Beringen (1979), and Bustamante and Gianeselli (1982).

In the 1980-90's, improvements to CPT would lead to the capability of pore water pressure measurement (u). These improved CPT units would become known as the piezocone (CPTu) (Eslami, 1997). The inclusion of CPTu lead to proposed CPTu pile design and analysis methods which included pore pressure measurements. Increasing demand for deep foundation units, as well as the reliable and cost-efficient pile design methods have led to frequent evaluations of CPT/CPTu methods in comparison to the more reliable results of static load tests for local calibrations (Briaud and Tucker, 1998; Abu-Farsakh and Titi, 2004; Cai et al., 2009; Bartz and Blatz, 2021).

In Fall of 2022, a static axial load testing program was carried out near Regina, Saskatchewan. The axial capacities of six instrumented CFA test piles of 450-500 mm diameter and 15-22.55 m length were evaluated in mixed soils of predominantly silts and sands. From this testing program, only one pile met failure criteria (pile head deflection >10% of pile shaft diameter) – the capacities for the other piles would be considered underestimated. The maximum applied loads applied to the piles were in the range of 4500-5235 kN (459,000 – 534,000 kg). The results from the load testing program were then applied to the several applicable CPT/CPTu design methods. The methods showing the best correlation to the load test results were then considered for site specific improvements.

1.2 PROBLEM STATEMENT

The direct methods that are based on CPT/CPTu are utilized to determine the toe and shaft resistances of piles. Each method has its own advantages and limitations, which are closely tied to the type of pile and soil conditions. Hence, it is essential to undertake a thorough evaluation and proper calibration of these methods to ensure their suitability for the soil conditions in Saskatchewan.

In Saskatchewan, incorporating CPT/CPTu based direct methods into pile design practices has the potential to greatly improve bearing capacity predictions. This is achieved by utilizing shear strength measurements obtained from in-situ tests, as opposed to relying on laboratory tests that are based on soil samples which may undergo disturbances during sampling and transportation and may not accurately represent the actual in-situ conditions.

In addition, using CPT/CPTu based methods would result in a higher resolution of bearing capacity predictions, as the pile capacity can be estimated at the 0.025 m intervals of the CPT/CPTu data. This would provide a more precise prediction of bearing capacity at a considerably lower design cost, compared to traditional laboratory testing methods.

1.3 OBJECTIVES OF THIS STUDY

This research aimed to evaluate the performance of three CPT based and two CPTu based pile capacity prediction methods for CFA piles and to propose a CPT/CPTu based pile design method. The evaluated CPT methods were Price and Wardle (1982), Bustamante and Gianeselli (1982), and Togliani (2008). The evaluated CPTu methods were Niazi and Mayne (2015) and Takesue et al. (1998). The data used for the evaluation included the following:

- Records of the CFA test pile installations.
- Results from the instrumented static axial load tests performed on the test piles.
- Auger boring information from the site.
- CPTu data collected at the exact location of the test piles.

The CPTu data contained depth, inclination, average tip resistance (q_c), average sleeve friction (f_s), and average dynamic pore pressure (u_2). To evaluate the pile bearing capacities, instrumented static load test data was used as a reference. However, due to the test piles having high capacities exceeding the force that could be applied by the jack, only one pile met the

failure conditions. Therefore, the capacities of the other five piles were assumed to be underestimated, which limited the evaluation to the shaft capacities of the piles. The evaluation and suggestion of a bearing capacity determination method were conducted in two stages.

In the first stage, calibration factors were calculated for the CFA piles and applied to the shaft friction resistances obtained from the CPT/CPTu methods. This was accomplished by optimizing the predicted shaft capacities to the measured pile capacities from the static axial load test. In the second stage, the best performing methods were determined using a rank index (RI) based on techniques utilized by Abu-Farsakh and Titi (2004), Eslami et al. (2011) and Chung et al. (2019). The RI was calculated by considering the following criteria:

1. The slope of the best fit line between $Q_{s(p)}$ and $Q_{s(m)}$ and the square root of the residual sum of squares ($\sqrt{RSS}$) between predicted and actual shaft capacities ($Q_{s(p,best)}$) and $Q_{s(p)}$.
2. The coefficient of variation (COV) of the predicted vs. actual shaft capacity ratios.
3. The 50% (P_{50}) and 90% (P_{90}) cumulative probabilities for the predicted vs. actual shaft capacity ratios.

The RI for a given method was computed by summing the ranks obtained from each criterion mentioned above. The method with the lowest RI was deemed to be the best performing method.

CHAPTER 2. LITERATURE REVIEW

2.1 INTRODUCTION

Determining the capacity of piles can be a challenging task due to the presence of various factors that can influence the capacity, coupled with inherent uncertainties. Static analysis of pile capacity can be impractical as it incorporates numerous assumptions and simplifications that may not always be accurate, leading to accumulated errors over time (Chung et al., 2019). In order to improve the accuracy of pile capacity predictions, site-specific field load tests, such as instrumented static axial load tests are conducted. These tests offer several benefits to large-scale projects, as highlighted by Brown et al. (2018):

a) Field load tests provide direct measurements of resistance in specific geological formations where the piles will be installed. This information is valuable as it offers insight into the soil conditions, which can impact the capacity of the piles.
b) The tests offer direct assessments of pile performance using the actual construction methods and materials planned for the project. This ensures that the pile design is suitable for the specific project and can perform as expected.
c) Field load tests offer an opportunity to refine the design methodology based on the local geological conditions. This can lead to an optimized design that is tailored to the site-specific requirements.
d) Site-specific verification of design and construction methods through field load tests can significantly improve the overall reliability of the pile foundation. This can lead to a safer and more durable foundation for the project.
e) Improved reliability of the pile foundation through site-specific verification of a design and construction methods can also increase confidence in the project's success.
f) In some cases, field load tests can help determine whether a reduction in pile shaft length is possible. This can reduce the risks associated with construction difficulties, leading to a more cost-effective and efficient project.

Although field load tests offer several benefits to large-scale projects, they also have some limitations that must be taken into account (Brown et al., 2018; Eslami et al., 2011):

a) In sites where there are highly variable geological conditions, one or few tests may not be sufficient to evaluate the performance of the piles on the site.
b) Field load tests require a significant investment of resources and time, which can cause delays that are more costly than additional pile shaft embedment resulting from a conservative design with lower resistance factors – especially the case for projects on tighter schedules.
c) Projects with a relatively small number of piles may not derive sufficient improvements in economy and efficiency to offset the costs of the load testing.

To overcome these limitations, researchers have attempted to correlate the results of pile load tests with in-situ sounding tests such as SPT and CPT/CPTu, which are more versatile and cost-effective methods for determining pile capacity. Of these methods, CPT/CPTu is generally considered to be the superior option due to its closer resemblance to a pile and the higher resolution it provides in the form of continuous sounding results with 0.025 m discretization, compared to the discrete results obtained from SPT (Eslami and Fellenius, 1997; Chung et al., 2019). This chapter provides a comprehensive review of the relevant direct pile capacity prediction methods based on CPT/CPTu, as well as an overview of the fundamentals of static axial load testing, which was used to obtain the reference pile capacities in this study.

2.2 PILE CAPACITY FROM CPT/CPTu RESULTS

The CPT/CPTu device itself is a cone on the end of a series of rods that is pushed into the ground at a constant rate (2 cm/s). As the cone is pushed into the ground, continuous measurements are made of the resistance to penetration of the cone and of the surface sleeve. In the case of the CPTu, a dynamic pore pressure measurement (u_2) is also continuously taken.

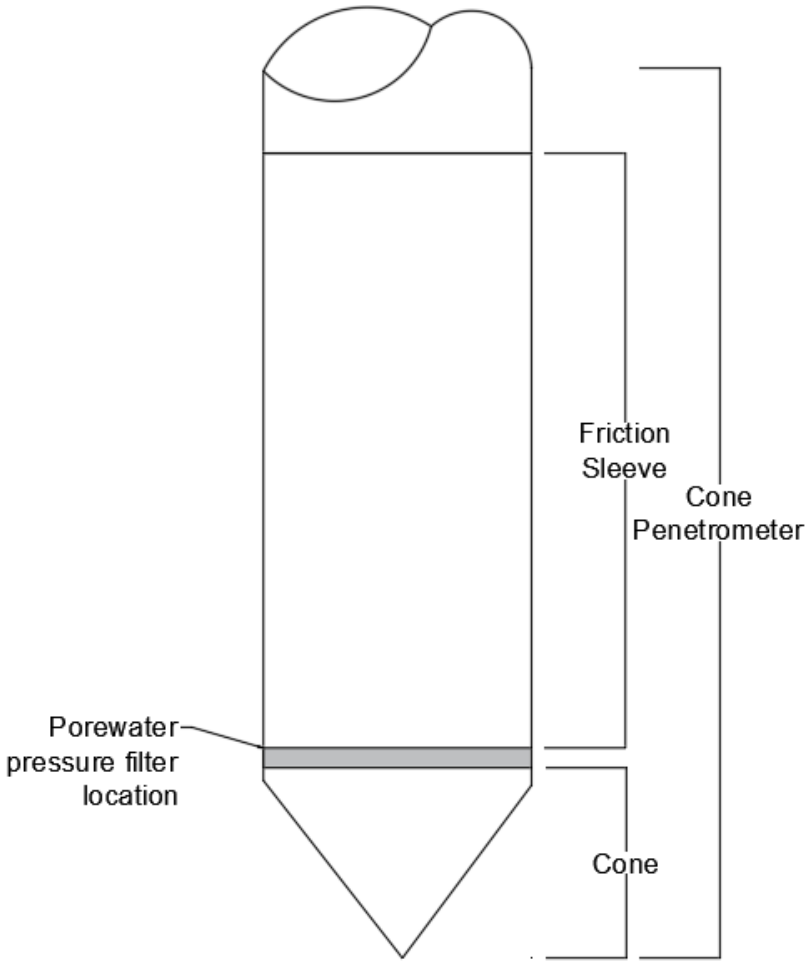

Figure 2.1. CPTu components schematic

The total force acting on the cone, Q_c, is divided by the projected area of the cone, A_c, to produce the cone resistance, q_c. The total force acting on the friction sleeve, F_s, divided by the surface area of the friction sleeve, A_s, produces the sleeve friction, f_s. In the CPTu, a pore pressure filter is located behind the cone as shown in Figure 2.1.

As specified in most standards, the cone areas are typically 10 cm^2 and 15 cm^2. However specific applications such as shallow investigations or gravely soils may see 2 cm^2 and 40 cm^2, respectively (Robertson and Kabal, 2010). The cones are usually pushed by specially built units that are either truck or track mounted. They may also be carried out on modified anchored drill rigs.

Figure 2.2. Truck mounted CPTu unit

In comparison to other in-situ tests, cone testing is generally advantageous in the following ways (Robertson and Kabal, 2010):

1. Fast and continuous profiling
2. Repeatable and reliable data (operator-independent)
3. Economical and productive
4. Strong theoretical basis for interpretation

By the same comparison, the general limitations are as follows (Roberson and Kabal, 2010):

1. High capital investment
2. Requires skilled operators
3. No soil sample
4. Penetration can be restricted in gravel/cemented layers

The estimation of pile capacity has been a longstanding application of CPT/CPTu data, as noted by Eslami and Fellenius (1997) and Abu-Farsakh and Titi (2004). The cone resistance and sleeve friction measurements obtained during CPT/CPTu testing are often viewed as analogous to the load bearing mechanisms of piles through toe and shaft resistance, respectively. However, since

there is a difference in scale between the cone equipment and the piles, correlation factors are required to provide accurate capacity predictions as emphasized by Song et al. (2019).

The methods for applying cone data to pile design are generally classified as direct or indirect in their determinations, according to Eslami and Fellenius (1997). Indirect CPT/CPTu methods rely on soil parameters, such as friction angle and undrained shear strength, estimated from cone data and evaluated from bearing capacity theories. However, the accumulated errors and empiricism involved in CPT/CPTu determinations of shear strength properties make them less desirable. On the other hand, direct CPT/CPTu methods equate cone resistance and sleeve friction to determine pile capacity. By skipping the intermediate steps required by the indirect methods, direct approaches reduce the errors induced in the estimation of bearing capacity, as noted by Eslami and Fellenius (1997) and Song et al. (2019).

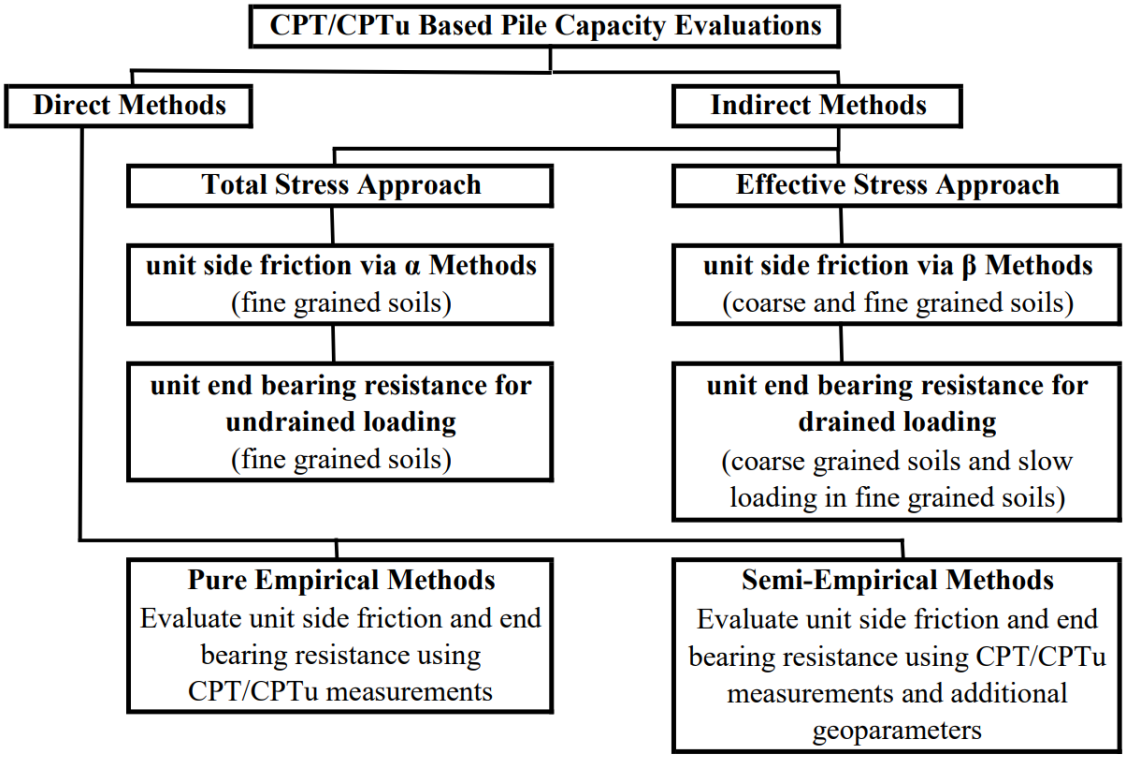

Figure 2.3. Breakdown of CPT/CPTu Based Pile Capacity Evaluations

2.3 PILE CAPACITIES BASED ON DIRECT APPROACH

The determination of the axial compression capacity of a single pile comprises of two components: the side or shaft component and the end-bearing component at the base. In the case of a circular pile, the shaft capacity (Q_s) is calculated by multiplying the unit side friction (r_s) with the surface area of the shaft (A_s).

$$A_s = \pi dL \tag{1}$$

Where d is the pile diameter, and L is the length embedded below grade.

If the magnitude of side friction is uniform and constant with depth, the side capacity is simply found as:

$$Q_s = r_s A_s \tag{2}$$

However, many piles extend through multiple layers and a summation of unit side frictions acting on various pile segments must be tabulated over the length of the pile:

$$Q_s = \int r_s dA_s \tag{3}$$

The unit-end bearing resistance (r_t) acts over the base of the pile tip, where the area of a circular pile at the base (A_b) is given by:

$$A_b = \pi\, d^2/4 \tag{4}$$

For piles in compression loading, the base capacity (Q_b) is determined as:

$$Q_b = r_t A_b \tag{5}$$

The summation of Q_s and Q_b provides the total axial pile capacity (Q_t).

$$Q_t = Q_s + Q_b \tag{6}$$

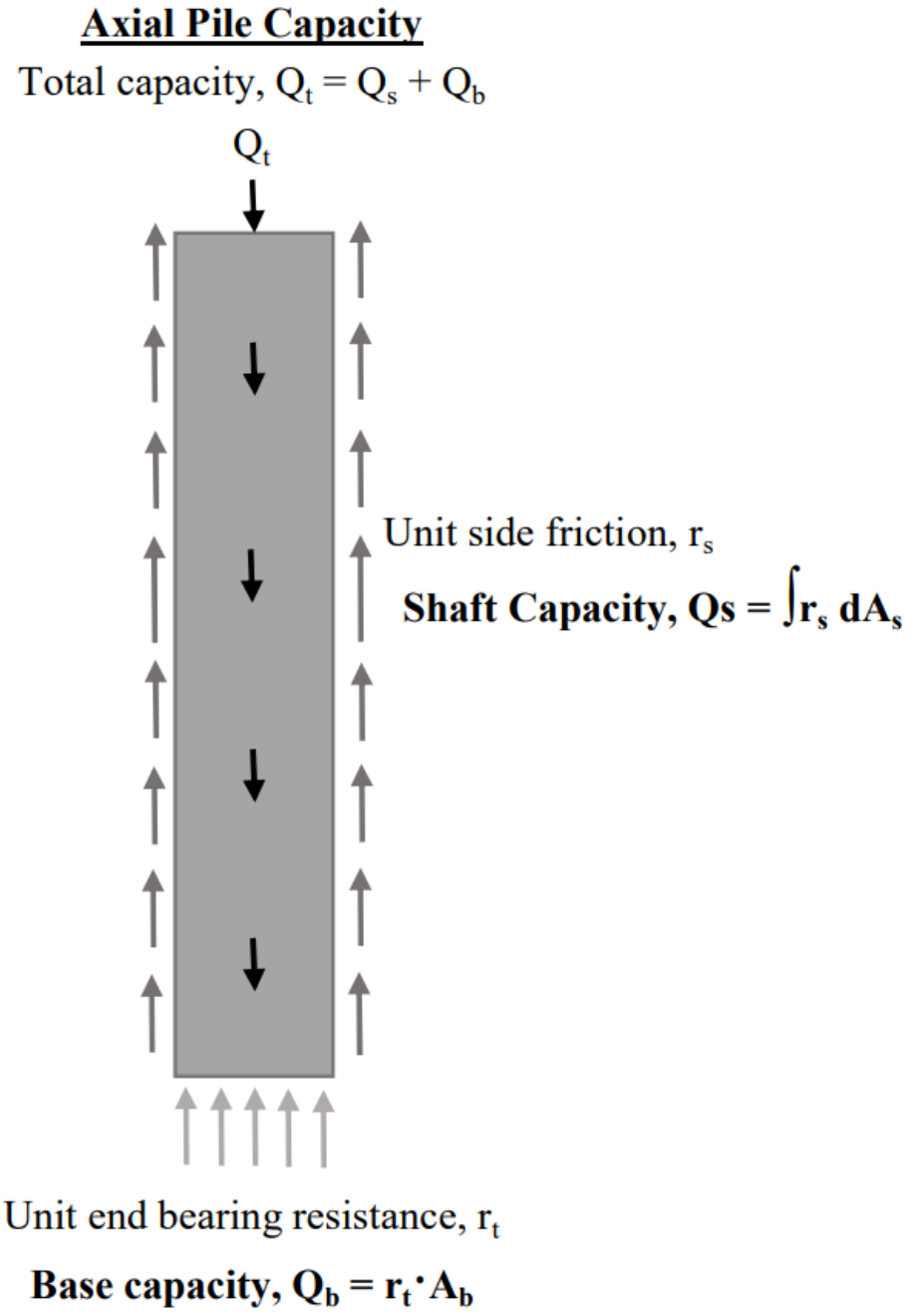

Figure 2.4. Components of axial pile capacity

Several direct cone test methods were selected for comparison to the measured capacities from the static load testing. As many as 40 different direct CPT methods have been developed over the past five decades, as summarized by Niazi & Mayne (2013). However, many of these methods

predate the mid-1990's which was when the modern electric piezometer (CPTu) was implemented.

The comparison in this study is not exhaustive of all methods, rather several common methods applicable to the evaluation of continuous flight auger piles in mixed soils of primarily silts/sands were compared. Three CPT methods and two CPTu methods were selected, a detailed summary of the selected methods is presented in Table 2.1.

Table 2.1. Summary of selected direct CPT/CPTu methods

Method	r_t (unit base resistance)	r_s (unit shaft resistance)	Note
Price and Wardle (1982)	$r_t = k_b q_c \leq 15\ MPa$ k_b=0.35 for driven piles and 0.3 for jacked piles	$r_s = k_s f_s \leq 120\ kPa$ k_s=0.53 for driven piles, 0.62 for jacked piles, and 0.49 for bored piles	CPT based
LCPC, Bustamante and Gianeselli (1982)	$r_t = k_c q_{ca}$ where k_c is bearing capacity factor, and q_{ca} is the averaged cone tip resistance as described by Bustamante and Gianeselli (1982)	$r_s = \frac{q_c}{\alpha_{LCPC}}$ where α_{LCPC} is a friction coefficient	CPT based
Penpile, Clisby et al. (1978)	$r_t = 0.25 q_c\ (clay\ soils)$ $r_t = 0.125 q_c\ (sand\ soils)$	$r_s = \frac{f_s}{1.5 + 0.0145 f_s}$ where f_s is in kPa	CPT based
Togliani (2008)	$r_t = k_3 q_{c_{toe}}$ $k_3 = \{\lambda + [0.01(L_{pile}/d_{toe})]\}$ λ being 0.2 for all driven piles, and 0.1 for all bored piles	$r_s = \sqrt{k_1 q_c}$ $k_1 = \left[1.2\left(0.8 + (R_f/8)\right)\right]\beta\ if\ R_f < 1$ $k_1 = \left[1.1\left(0.4 + Ln(R_f)\right)\right]\beta\ if\ R_f \geq 1$ $Friction\ ratio, R_f = (f_s/q_c)$ β is 1 for displacement driven piles, 0.6 for non-displacement piles and CFA, 0.5 for bored piles	CPT based

KTRI, Takesue et al. (1998)	$r_t = 0.1q_t\ (sands)$ otherwise by UniCone Method	$r_t = \frac{\Delta u + 950}{1250} f_s\ if\ \Delta u < 300\ kPa$ $r_t = \frac{\Delta u - 100}{200} f_s\ if\ 300\ kPa < \Delta u < 1250\ kPa$ $\Delta u = u_2 - u_o$	CPTu based
Enhanced UniCone, Niazi and Mayne (2015)	$r_t = q_E 10^{(0.325 I_c - 1.218)}$ For I_c values read details in section below.	$r_s = q_E \theta_{PT} \theta_{TC} \theta_{Rate} 10^{0.732 \cdot I_c - 3.605}$ Where θ_{PT} is the coefficient for pile type (0.84 for bored piles, 1.02 for jacked piles, and 1.13 for driven piles), θ_{TC} is the coefficient for loading direction (1.11 for compression and 0.85 for tension/uplift), θ_{Rate} is the rate coefficient applied to the soils (1.09 for constant rate of penetration and 0.97 for maintained load test). For I_c values read details in section below.	CPTu based

2.3.1 Price and Wardle Method (1982)

In 1982, Price and Wardle conducted pile load tests in stiff London clay. Based on their analysis they developed the following relationships for determining unit end bearing capacity and unit shaft resistance. These relationships make use of pile type dependent factors. To evaluate the unit end bearing capacity (r_t) of the pile from the cone tip resistance (q_c), the following relationship is applied (Titi and Abu-Farsakh, 1999; Chung et al., 2019):

$$r_t = k_b q_c \leq 15\ MPa \tag{7}$$

Where k_b is a factor that is dependent on the pile type (k_b=0.35 for driven piles and 0.3 for jacked piles). The unit shaft resistance (r_s) is obtained from the local sleeve friction (f_s) by the following relationship (Titi and Abu-Farsakh, 1999; Chung et al., 2019):

$$r_s = k_s f_s \leq 120\ kPa \tag{8}$$

Where k_s is a factor that is dependent on the pile type (k_s=0.53 for driven piles, 0.62 for jacked piles, and 0.49 for bored piles). The values for these factors were based on analysis conducted on pile load tests in stiff London clay (Titi and Abu-Farsakh, 1999).

2.3.2 Clisby and Scholtes (1978)

The Penpile method, also referred to as the method developed for the Mississippi Department of Transportation (Clisby and Scholtes, 1978), calculates the unit end bearing capacity of the pile using the following relationship (Titi and Abu-Farsakh, 1999; Chung et al., 2019):

$$r_t = 0.25 q_c\ (clay\ soils) \tag{9}$$

$$r_t = 0.125 q_c\ (sand\ soils) \tag{10}$$

The unit shaft resistance (r_s) is determined by the following relationship where the local sleeve friction (f_s) is in kPa (Titi and Abu-Farsakh, 1999; Chung et al., 2019):

$$r_s = \frac{f_s}{1.5 + 0.0145 f_s} \tag{11}$$

2.3.3 LCPC Method, Bustamante and Gianeselli (1982)

The LCPC method, otherwise known as the French method, is based on the analyses of 197 pile loading tests with various bearing strata conditions. This work was done by Bustamante and Gianeselli at the Laboratoire Central des Ponts et Chausees (LCPC) (Eslami and Fellenius, 1997; Chung et al., 2019). By this method, the sleeve friction (f_s) is neglected, and the unit toe and unit shaft resistance are both determined from the average cone resistance (q_c). By this method the unit toe resistance (r_t) is determined by the following (Eslami and Fellenius, 1997; Chung et al., 2019):

$$r_t = k_c q_{ca} \tag{12}$$

Here k_c is a bearing capacity factor that is selected from Table 2.2, and q_{ca} is the average cone tip resistance based on the procedure outlined in Figure 5.

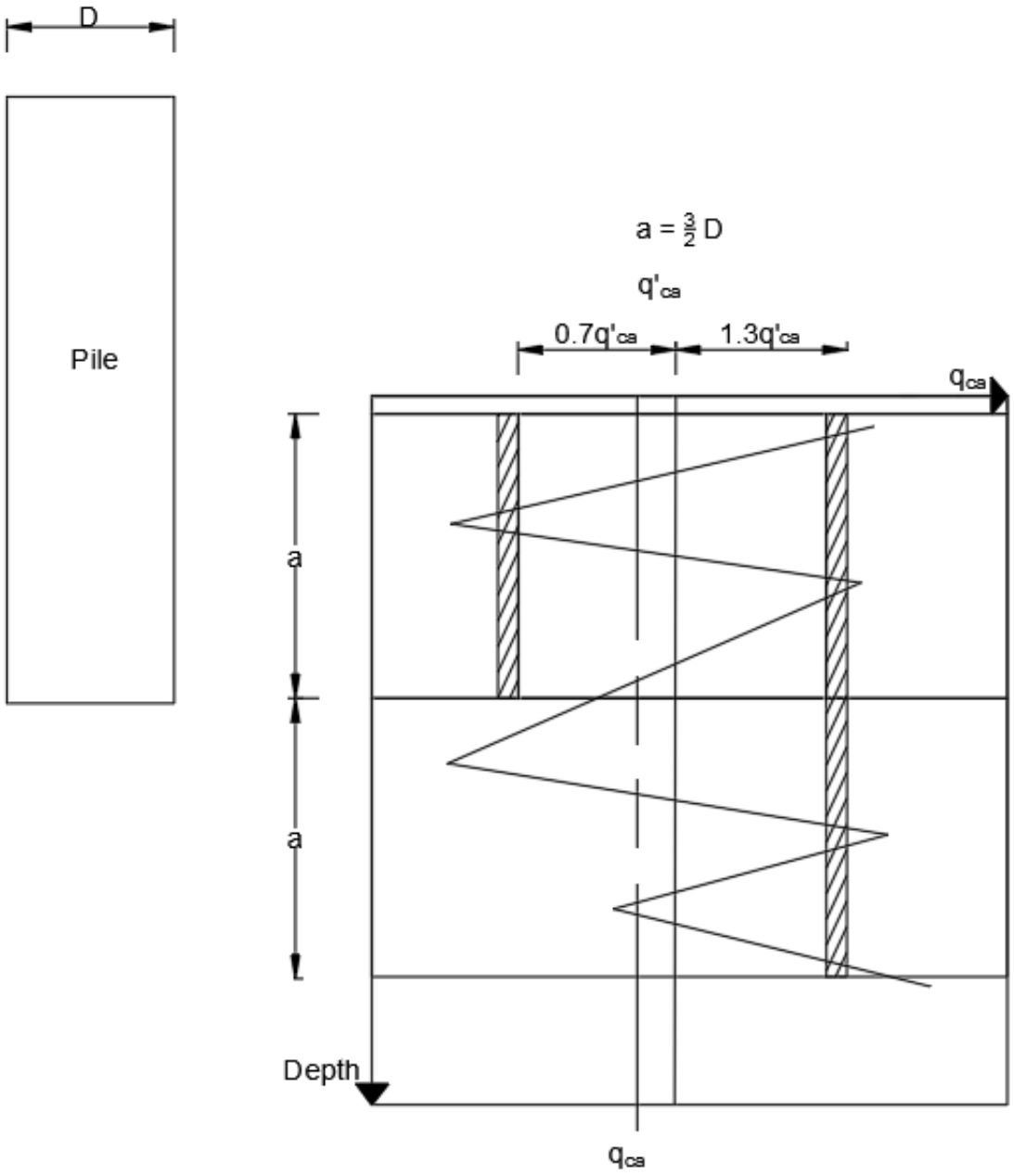

Figure 2.5. Determination of q_{ca} after Bustamante and Gianeselli (1982)

Table 2.2. k_c as a function of soil and pile type (from Bustamante and Gianeselli, 1982)

Nature of soil		k_c	
	q_c [Mpa]	Group I[1]	Group II[2]
Soft clay and mud	1	0.40	0.50
Moderately compacted clay	1 to 5	0.35	0.45
Silt and loose sand	5	0.40	0.50
Compacted to stiff clay and compacted silt	5	0.45	0.55
Soft chalk	5	0.20	0.30
Moderately compacted sand and gravel	5 to 12	0.40	0.50
Weathered to fragmented chalk	5	0.20	0.40
Compacted to very compact sand and gravel	12	0.30	0.40

1. Plain bored piles; mud bored piles; micro piles (grouted under low pressure); cased bored piles; hollow auger bored piles; piers; barrettes.

2. Cast screwed piles; driven precast piles; prestressed tubular piles; driven cast piles; jacked metal piles; micro piles (small diameter piles grouted under high pressure with diameter <250 mm); driven grouted piles (low pressure grouting); driven metal piles; driven rammed piles; jacket concrete piles; high pressure grouted piles of large diameter.

The unit shaft resistance is determined from relation where a friction coefficient (α_{LCPC}) is applied to the cone tip resistance (Eslami and Fellenius, 1997; Chung et al., 2019):

$$r_s = \frac{q_c}{\alpha_{LCPC}} \tag{13}$$

Table 2.3. α_{LCPC} as a function of soil and pile type (from Bustamante and Gianeselli, 1982)

Nature of soil	q_c[Mpa]	Category									
		Coefficients, α_{LCPC}				Maximum Limit of r_s					
		I		II		I		II		III	
		A[1]	B[2]	A[3]	B[4]	A	B	A	B	A[5]	B[5]
Soft clay and mud	5	30	90	90	30	0.015	0.015	0.015	0.015	0.035	≤0.12
Moderately compact clay	1 to 5	40	80	40	80	0.035 (0.08)	0.035 (0.08)	0.035 (0.08)	0.035	0.08	≤0.12
Silt and loose sand	≤5	60	150	60	120	0.035	0.035	0.035	0.035	0.08	N/A
Compact to stiff clay and compact silt	>5	60	120	60	120	0.035 (0.08)	0.035 (0.08)	0.035 (0.08)	0.035	0.08	≥0.2
Soft chalk	5	100	120	100	12	0.035	0.035	0.035	0.035	0.08	N/A
Moderately compact sand and gravel	5 to 12	100	200	100	200	0.08 (0.12)	0.035 (0.08)	0.08 (0.12)	0.08	0.12	≥0.2
Weathered to fragmented chalk	>5	60	80	60	80	0.12 (0.15)	0.08 (0.12)	0.12 (0.15)	0.12	0.15	≥0.2
Compact to very compact sand and gravel	>12	150	300	150	200	0.12 (0.15)	0.08 (0.12)	0.12 (0.15)	0.12	0.15	≥0.2

1. Plain bored piles; mud bored piles; hollow auger bored piles; micropiles (grouted under low pressure); cast screwed piles; piers; barrettes.

2. Cased bored piles; driven cast piles.

3. Driven precast piles; prestressed tubular piles; jacket concrete piles.

4. Driven metal piles; jacket metal piles.

5. Driven grouted piles; driven rammed piles.

6. High pressure grouted piles of large diameter 250 mm; micropiles (grouted under high pressure).

*Note: maximum limit unit skin friction, r_s: bracket values apply to careful execution and minimum disturbance of soil due to construction.

2.3.4 KTRI Method, Takesue et al. (1998)

The Kajima Technical Research Institute (KTRI) method is based on the results of 6 pile load tests in clay, silts, sands, and mixed soil conditions (Niazi, 2013). The unit toe resistance (r_t) in clay soils is found by a means similar to the UniCone method. In sands, the unit toe resistance is found by the following relationship (Chung et al., 2019):

$$r_t = 0.1q_t \tag{14}$$

Where q_t is the cone tip resistance corrected for pore pressure effects.

The unit shaft resistance (r_s) is a function of the local sleeve friction (f_s) and the measured pore water pressure (Niazi, 2013; Saftner et al., 2018, Chung et al., 2019):

$$r_s = \frac{\Delta u + 950}{1250} f_s \; if \; \Delta u < 300 \; kPa \tag{15}$$

$$r_s = \frac{\Delta u - 100}{200} f_s \; if \; 300 \; kPa < \Delta u < 1250 \; kPa \tag{16}$$

$$\Delta u = u_2 - u_o \tag{17}$$

Where Δu is the change in porewater pressure, u_2 is the CPTu porewater pressure reading, and u_o is the hydrostatic porewater pressure.

2.3.5 Togliani Method (2008)

Originally developed for displacement piles, the Togliani method (2008) can be adjusted to provide capacity estimates for non-displacement and CFA piles. The pile unit side friction is determined as:

$$r_s = \sqrt{k_1 q_c} \tag{18}$$

$$k_1 = [1.2\left(0.8 + \left(R_f/8\right)\right)]\beta \; if \; R_f < 1 \tag{19}$$

$$k_1 = \left[1.1\left(0.4 + Ln\left(R_f\right)\right)\right]\beta \; if \; R_f \geq 1 \tag{20}$$

$$Friction\ ratio, R_f = (f_s/q_c) \quad (21)$$

Where q_c is the cone tip resistance, f_s is the sleeve friction, and β is 1 for displacement driven piles, 0.6 for non-displacement piles and CFA, 0.5 for bored piles.

The unit toe capacity is determined as being:

$$r_t = k_3 q_{c_{toe}} \quad (22)$$

$$k_3 = \{\lambda + [0.01(L_{pile}/d_{toe})]\} \quad (23)$$

Where $q_{c_{toe}}$ is the cone resistance measured from $+8d_{toe}$ to $-4d_{toe}$. The value of λ being 0.2 for all driven piles, and 0.1 for all bored piles.

2.3.6 Enhanced UniCone Method, Niazi and Mayne (2015)

The modified UniCone method was developed based on a total of 330 pile load tests which were associated with CPTu data during site investigations (Niazi and Mayne, 2015, 2016). In comparison, the original UniCone method was developed on data from 106 pile load tests (Eslami and Fellenius 1997). The modified approach provides a greater delineation of soil subclassifications. Instead of the original 5-zone normalized soil behavioral types (SBTn), a 9-zone normalized SBTn is ascertained using CPTu data. Additionally, the pile unit side friction and the unit end bearing expressions are expanded to include additional parameters.

The pile unit side friction (r_s) is obtained from the effective tip resistance (q_E) and the CPT material index (I_c) using the following expression at each elevation along the sides of the pile (Saftner et al., 2018):

$$r_s = q_E \theta_{PT} \theta_{TC} \theta_{Rate} 10^{0.732 \cdot I_c - 3.605} \quad (24)$$

Where θ_{PT} is the coefficient for pile type (0.84 for bored piles, 1.02 for jacked piles, and 1.13 for driven piles), θ_{TC} is the coefficient for loading direction (1.11 for compression and 0.85 for tension/uplift), θ_{Rate} is the rate coefficient applied to the soils (1.09 for constant rate of penetration and 0.97 for maintained load test).

The pile end bearing resistance is obtained from the following (Saftner et al., 2018):

$$r_t = q_E 10^{(0.325 I_c - 1.218)} \quad (25)$$

The CPT material index I_c is determined as being an iteration of equations 26 to 29.

$$I_c = \sqrt{(3.47 - logQ_{tn})^2 + (1.22 + logF_r)^2} \quad (26)$$

Where Q_{tn} is the normalized tip resistance and F_r is the normalized friction.

$$Q_{tn} = \frac{(q_t - \sigma_v)/\sigma_{atm}}{(\sigma_v'/\sigma_{atm})^n} \quad (27)$$

$$n = 0.381 I_c + 0.05\left(\frac{\sigma_v'}{\sigma_{atm}}\right) - 0.15 \leq 1.0 \quad (28)$$

$$F_r(\%) = 100\frac{f_s}{(q_t - \sigma_v)} \quad (29)$$

Here $\sigma_{atm}$is the atmospheric pressure, σ_v is the total vertical overburden stress at the mid layer depth, and σ_v' is the effective vertical overburden stress at the mid layer depth.

2.4 STATIC AXIAL LOAD TEST

Static axial load tests are considered to be the most reliable method for evaluating the load-carrying capacity and deflection behavior of deep foundation units such as piles. The test results provide valuable information for the foundation designer to assess the behavior of the pile under load and to determine its suitability for specific loadings (Brown et al., 2018; ASTM, 2020).

In a static axial load test, a load is applied to the top of the pile using hydraulic jacks, and the resulting axial movement is measured using strain gauges, transducers, and load cells. The load is usually applied in increments, and measurements are taken at each increment to monitor the behavior of the pile (ASTM, 2020).

The test results can be used to determine the distribution of side shear resistance along the pile shaft, the amount of end bearing developed at the pile toe, and the long-term deflection behavior. This information is critical for the foundation designer to evaluate the ultimate static capacity of the pile, as well as the pile behavior under service load (Brown et al., 2018; ASTM, 2020).

The required equipment for a static axial load test typically includes hydraulic jacks, reaction frames anchored by reaction piles, strain gauges, displacement transducers, and load cells. The equipment must be carefully calibrated and installed to ensure accurate and reliable test results (ASTM, 2020).

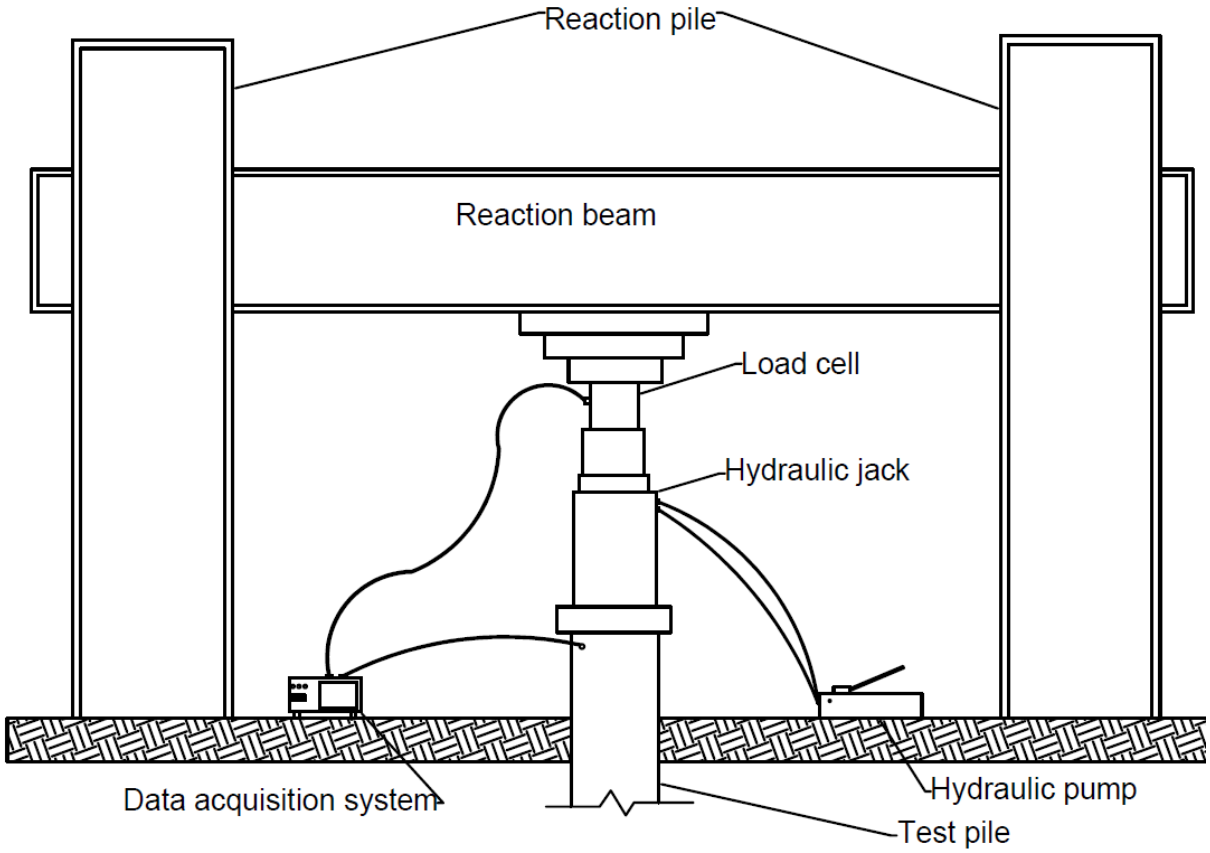

Figure 2.6. Schematic of pile load test setup

Figure 2.7. Hydraulic jack, load cell, steel test plate, test beam, and test pile

Figure 2.8. Anchor piles, load transfer beams, and test beam

2.5 CFA PILE CAPACITY BY INSTRUMENTED STATIC AXIAL LOAD TEST

The total resistance of a pile can be evaluated based on the measured force applied to the test pile by the hydraulic jack and the displacements of the pile head. The ultimate load can then be determined by using various criteria, including Chin's Criterion, Van der Veen's Criterion, Ultimate Load Based on 10% Relative Settlement, Davisson's Criterion, and De Beer's Criterion. According to Salgado (2011), the criterion based on the pile head settlement being equal to 10% of the pile diameter is the most appropriate. This criterion applies to large-displacement, small-displacement (partial-displacement), and non-displacement piles and is closely linked to the concepts of serviceability and ultimate limit states.

If the pile is instrumented with strain gauges at soil stratigraphy changes, information on how the load is distributed along the pile can be obtained. Strain gauges allow the measurement of strain, which can then be used to calculate stress using Young's moduli. These Young's moduli (E) can be determined using either the transformed area method or the modified secant modulus method

(Fellenius, 2001). The force (P) acting along the pile cross-section can then be determined using the following equation:

$$P = E_s A_{steel} \varepsilon + E_c A_{concrete} \varepsilon \quad (30)$$

Where P is the load, ε is the measured strain from the gauges, A_{steel} is the cross-sectional area of the reinforcing steel at the plain of the strain gauges, $A_{concrete}$ is the cross-sectional area of the concrete shaft at the plain of the strain gauges, E_s is the Young's modulus of the steel reinforcement at the strain gauges, and E_c is the Young's modulus of the concrete at the strain gauges.

Knowing the loads at discretized points along the pile can allow for a load transfer curve to be produced, and from this load transfer curve pile shaft capacities and the pile toe capacity can be determined.

2.6 CONCLUSIONS

The various CPT/CPTu based methods reviewed may have similar general form, but they typically require different empirical coefficients and correction factors that are specific to the site conditions and the type of pile being used. Therefore, before applying any of these methods to a different site, it is important to calibrate and validate the method using reliable pile capacities determined from static axial loading tests.

Static axial loading tests are commonly used to determine the ultimate capacity of a pile in a particular soil condition. In this test, a load is applied to the pile slowly and progressively until the pile fails. The ultimate capacity of the pile is determined based on the load that causes failure. This test provides a direct measure of the pile capacity and is considered one of the most reliable methods for determining pile capacity.

To validate the results obtained from CPT/CPTu based methods, the pile capacities determined from the static axial loading tests can be compared with the predicted capacities obtained using the CPT/CPTu based methods. This comparison can help in calibrating the CPT/CPTu based method for the specific site conditions and type of pile being used.

In summary, while CPT/CPTu based methods may offer a faster and more cost-effective way of determining pile capacity, the application of these methods should be preceded by the careful

evaluation and calibration of the method using reliable pile capacities determined from static axial loading tests.

CHAPTER 3. METHODOLOGY

3.1 INTRODUCTION

The main aim of this study was to assess the efficiency of various CPT/CPTu-based models for predicting pile capacity and develop a modified method that suits the soil conditions of the site. To achieve this objective, several data were collected from the site, including pile installation records, static axial load test data, soil boring information, and CPTu data. These data were analyzed to determine the axial capacity of the test piles. The shaft capacities were later compared to the predicted shaft capacities from the CPT/CPTu-based methods discussed in the previous chapter. The comparison was evaluated using a rank index (RI) to determine the most effective method.

3.2 TEST SITES

The research site is a vacant piece of farmland located on the northeast limits of the City of Regina. Based on hydrogeological maps of the area, the site overlies the Condie Aquifer. The Condie Aquifer is characterized by its primary composition of sand and gravel deposits, which are interspersed with clay and silt deposits and formed because of glacial activity.

In the Fall of 2021, a preliminary geotechnical investigation was conducted on the job site which involved the drilling of boreholes, soil sampling, monitoring well installation, and CPTu testing at 17 locations. The general soil stratigraphy was understood to consist of two distinct areas: (1) a thin silt/sand aquifer and (2) a thick sand aquifer.

In the thin silt/sand aquifer location, the general subgrade soil conditions consist of 200 to 300 mm of topsoil at the ground surface, followed by clay to a depth of 10.1 to 11.0 m, which was underlain by variable deposits of silt/clay and silt/sand to depths of approximately 13.3 to 16.9 meters below grade (mbg). An extensive deposit of glacial till lies below these depths.

In the thick sand aquifer location, the general subgrade soil conditions consist of 200 to 300 mm of topsoil at ground surface, followed by clay to a depth of 2.3 to 5.0 mbg, which is underlain by a thin layer of clay/silt and/or glacial till to a depth of 5.3 to 7 mbg. An extensive deposit of sand or sand/silt (aquifer deposits) lies below this layer, to depths of about 15.1 to 20 mbg, which is underlain by an extensive deposit of glacial till. The predominant bearing material in this area of the site consists of sand/silt.

In the Fall of 2022, proposed test pile sites were identified, and additional CPTu tests would be done at the center of the proposed sites. Test pile 3 and Test pile 6 would see the actual installations of the test piles being considerably removed from the proposed test sites.

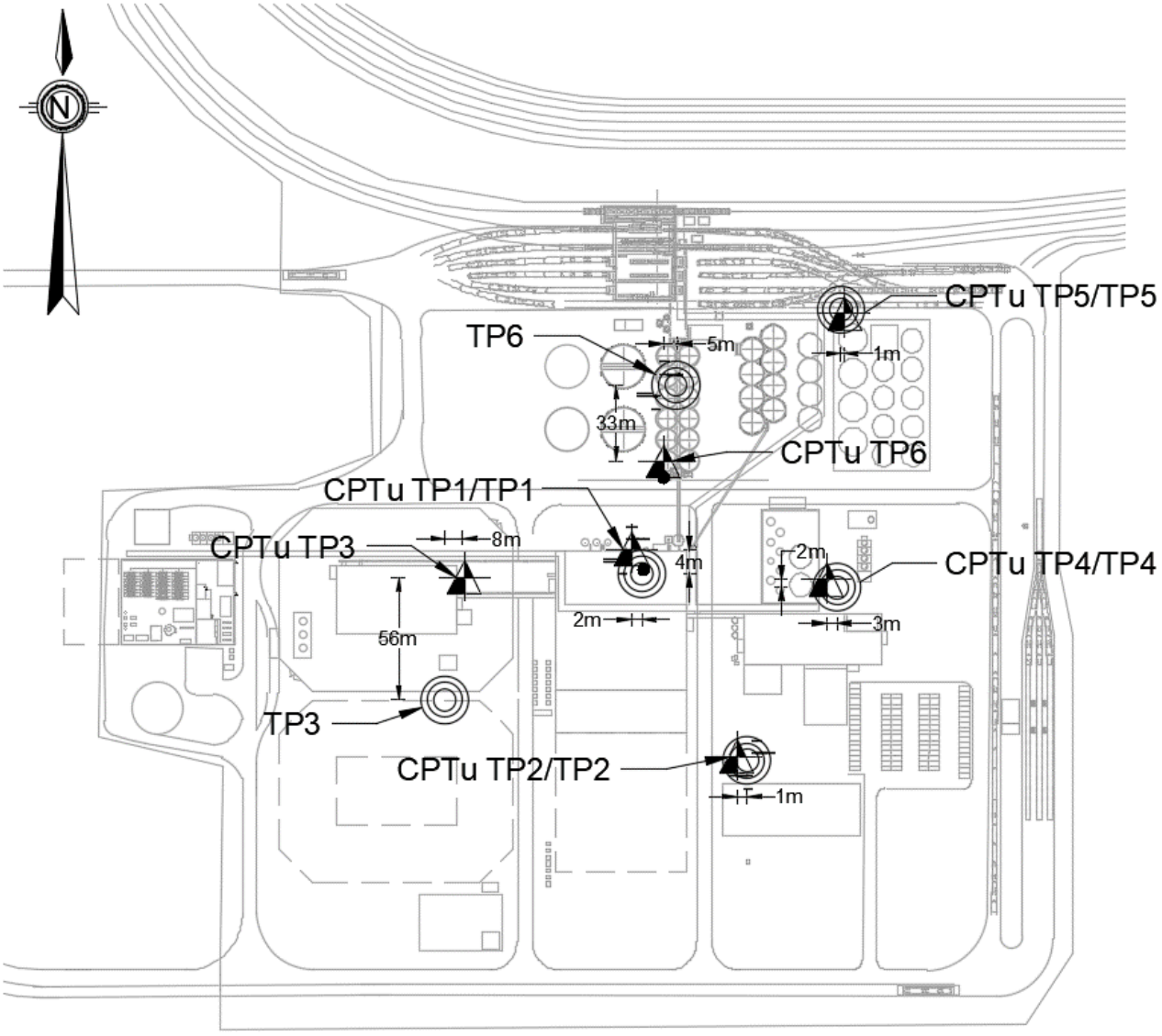

Figure 3.1. Test pile and CPTu layout diagram

3.3 PILES

The test piles for this research were exclusively CFA piles. These piles are installed by drilling a continuous flight, hollow stem auger into the ground, followed by pressure injection of concrete and simultaneous extraction of the hollow stem auger.

Table 3.1. Test pile diameters and drill depths

Test pile	Nominal shaft diameter (mm)	Drilling depth (m)
TP1	450	22.8
TP2	450	15.3
TP3	450	21.8
TP4	450	23.3
TP5	500	22.8
TP6	500	21.8

Test piles 1 to 4 were installed with vertical reinforcement of 7-25M x 9m rebar cages plus 1-35M center rebar to full length. Test piles 5 and 6 were installed with vertical reinforcement of 6-25M x 9m rebar cages plus 1-35M center rebar to full length. For all test piles, a concrete mix with 7-day strength of 50 MPa was used, and a summary of the concrete compressive strength is provided in Table 3.2.

Table 3.2. Summary of concrete strength testing

Test Pile	Compressive Strength (MPa)		
	Day 3	Day 5	Day 7
TP1	47.2	61.4	-
TP2	44.0	57.9	62.2
TP3	44.3	54.5	56.9
TP4	43.4	50.5	54.4
TP5	41.7	53.5	55.0
TP6	38.8	52.4	55.7

Along the full length center rebar, vibrating wire strain gauges were installed at depths where there were changes in soil stratigraphy.

Table 3.3. Strain gauge depths for test piles

Test pile	Strain gauge depths (m)
TP1	1.5, 4, 8, 15, 22.2
TP2	1.5, 5, 10, 14.7
TP3	1.5, 4, 6.5, 15, 19, 21.2
TP4	1.5, 6, 10, 16, 22.7
TP5	1.5, 6, 12, 18, 22.2
TP6	1.5, 5, 11, 18, 21.2

Figure 3.2. CFA piling rig featuring concrete truck and pump

Figure 3.3 CFA piling rig during boring

Figure 3.4. Center rebar instrumented with vibrating wire strain gauges

3.4 CPTu DATA

The data obtained from the CPTu was in [*.csv] format and extracted from the logging software. The log information included various parameters such as cone depth, inclination, average tip resistance (q_c), average sleeve friction (f_s), and average dynamic pore pressure (u_2).

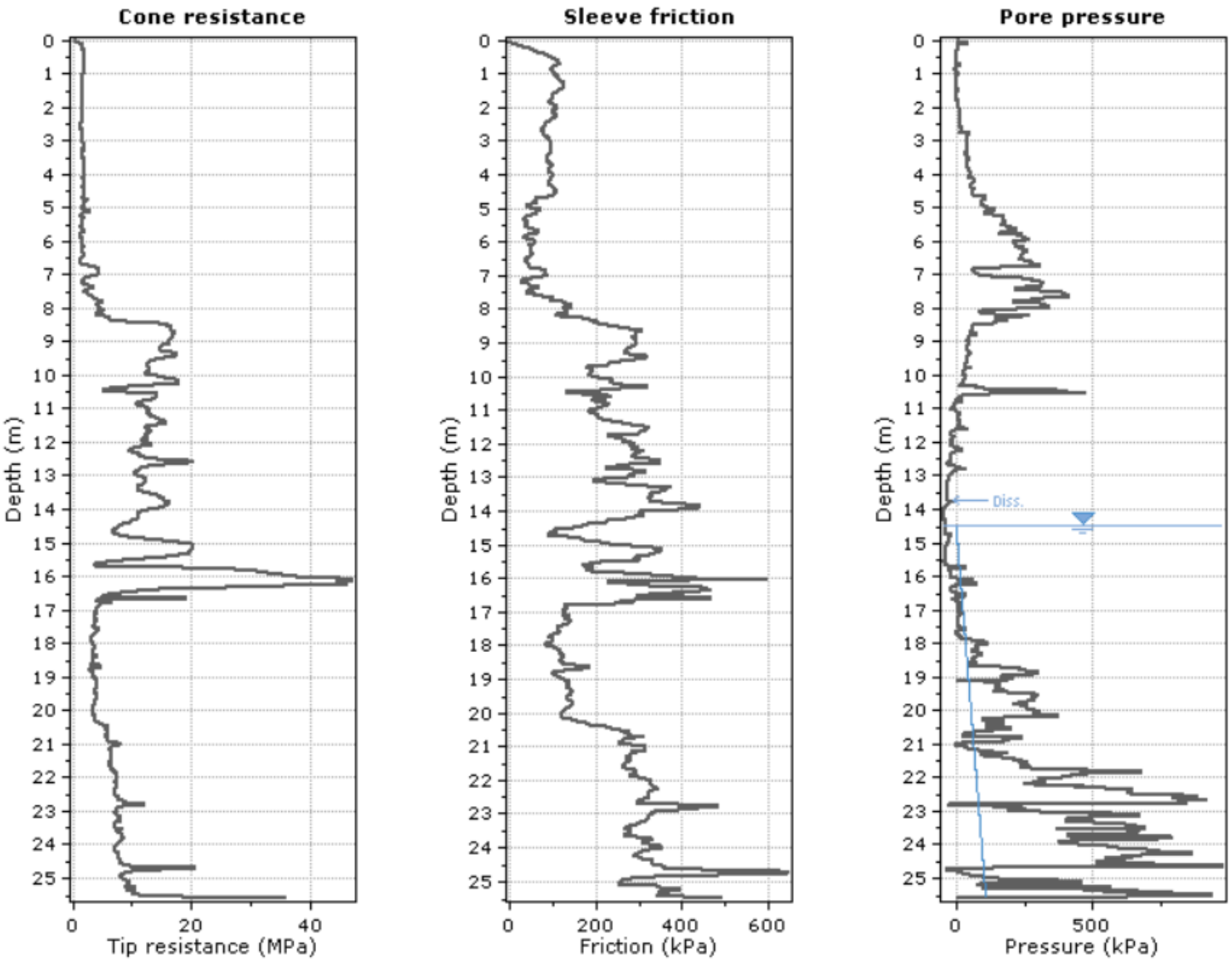

Figure 3.5. In-situ CPTu data for TP1

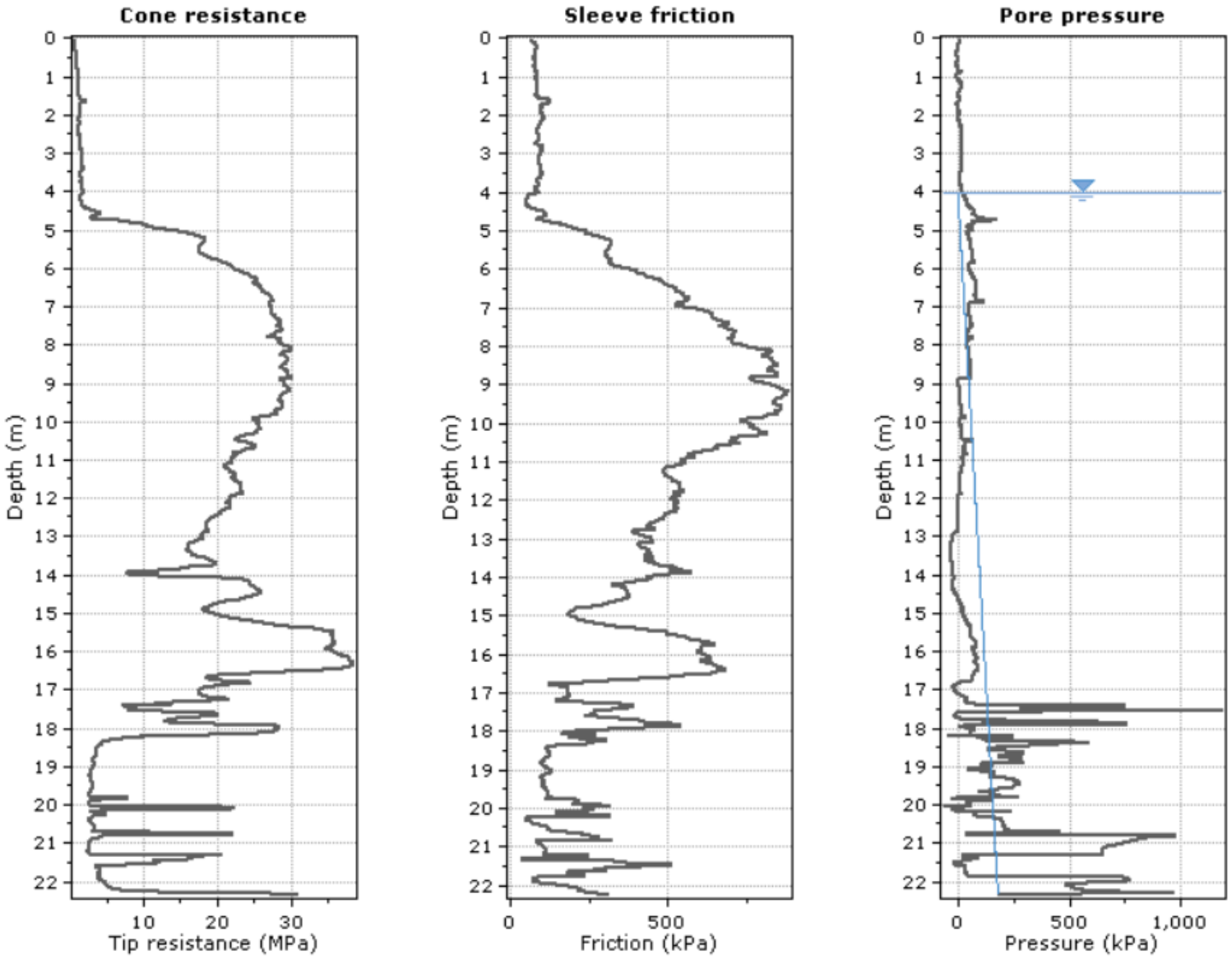

Figure 3.6. In-situ CPTu data for TP2

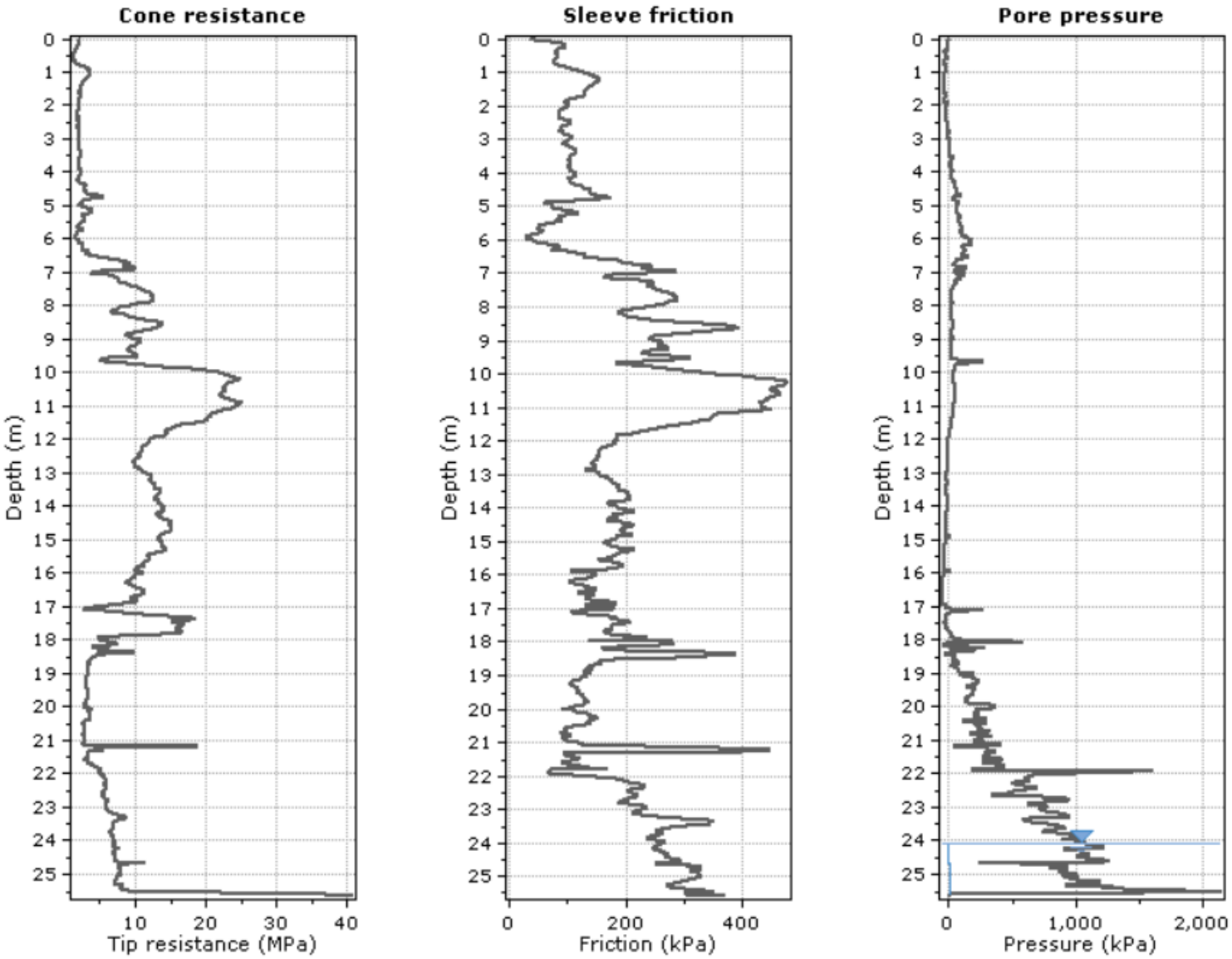

Figure 3.7. In-situ CPTu data for TP3

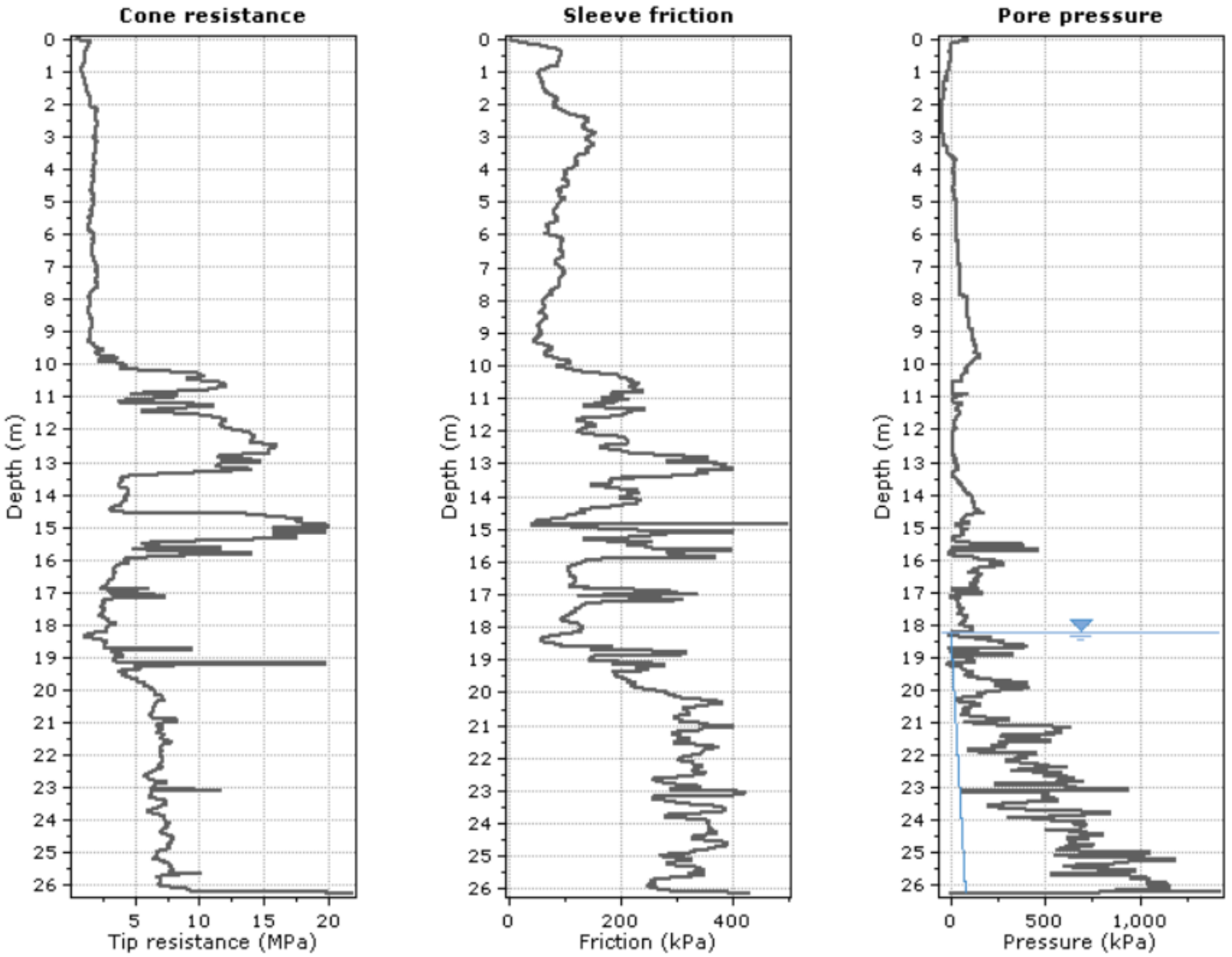

Figure 3.8. In-situ CPTu data for TP4

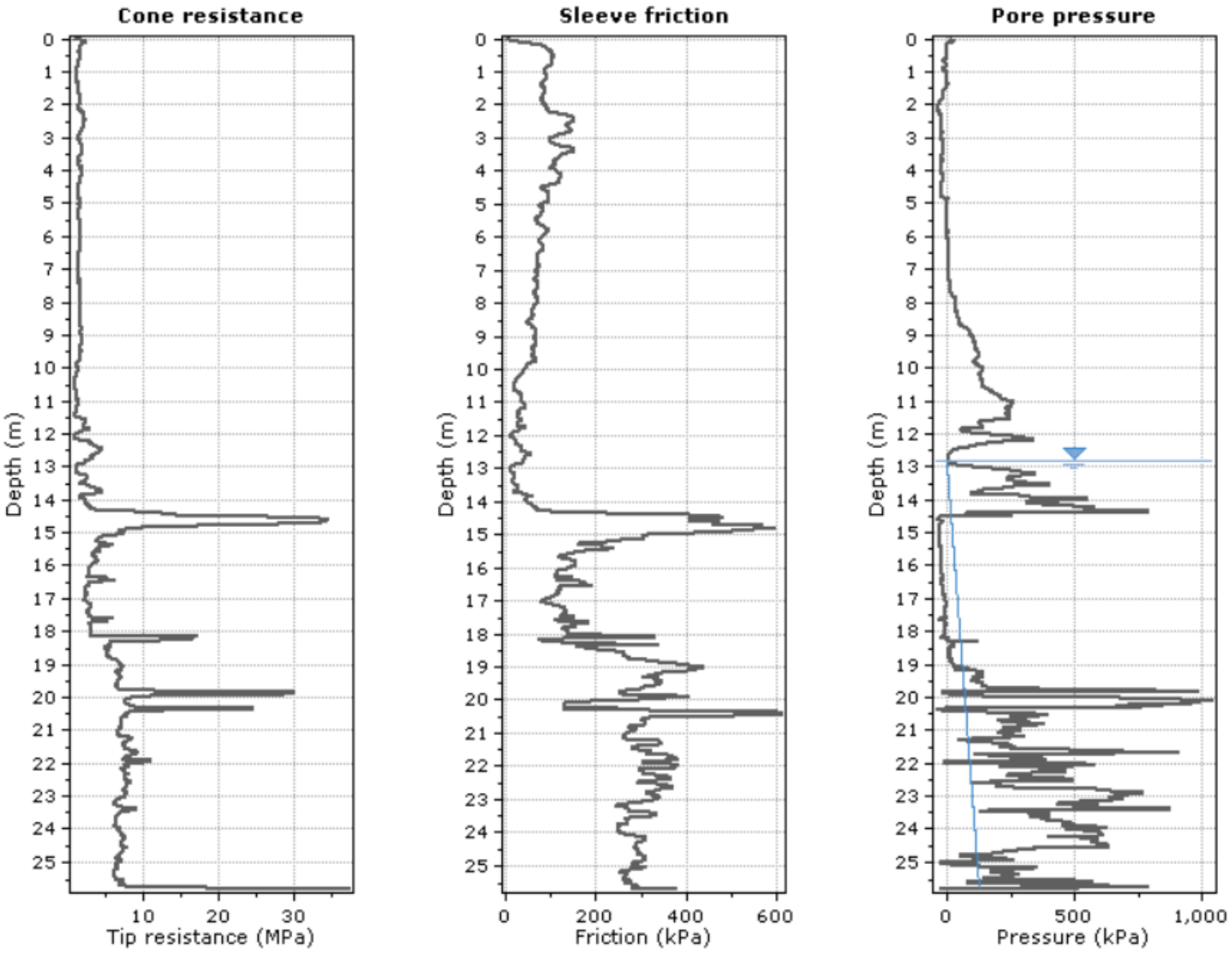

Figure 3.9. In-situ CPTu data for TP5

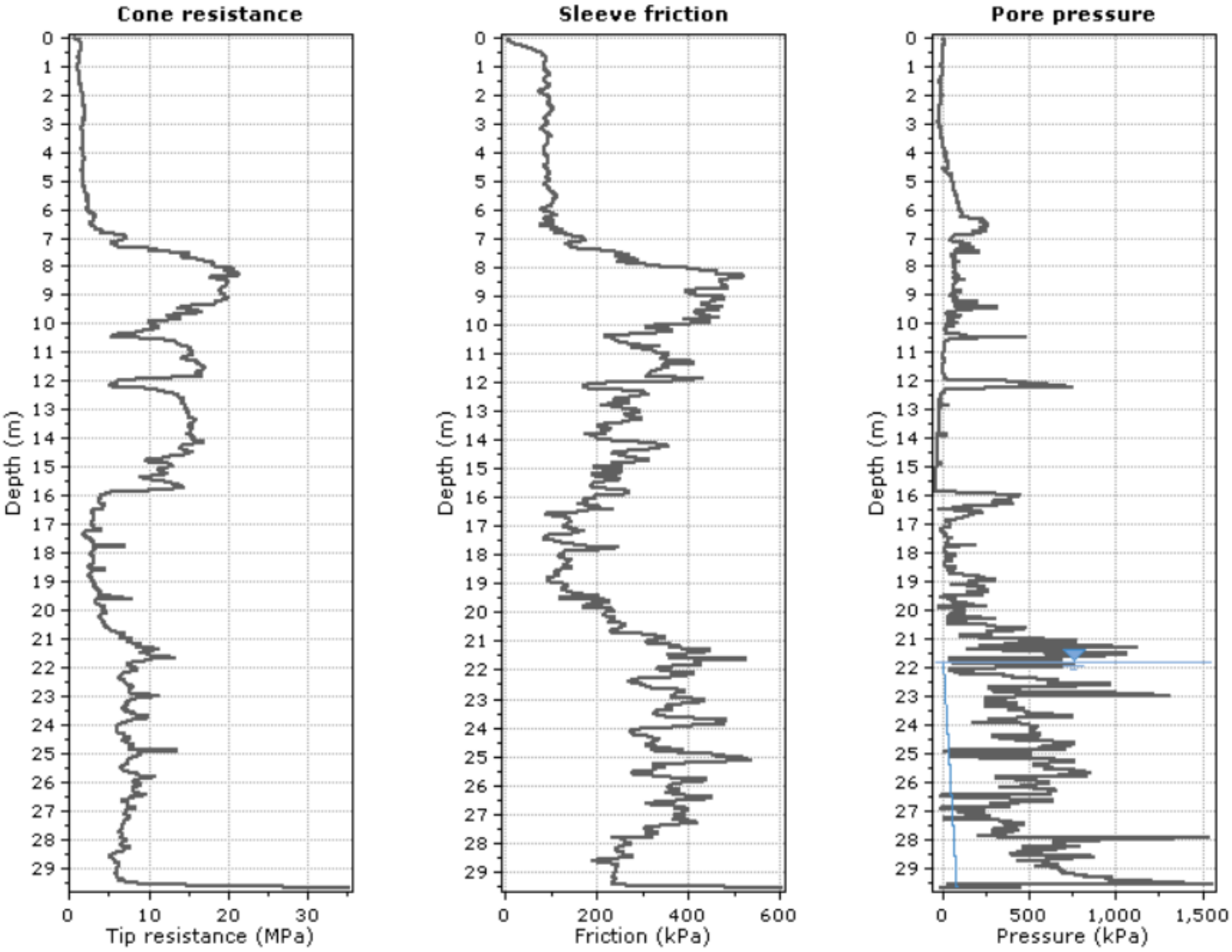

Figure 3.10. In-situ CPTu data for TP6

3.5 SOIL CLASSIFICATION

The classification of soil type through CPT/CPTu is commonly accomplished using soil behavioral type charts (SBT), which are based on measures such as q_c, f_s, and/or u_2, and rely on empirical relationships. While there exist over 25 different sets of charts available (e.g. Hegazy, 1998; Valsson, 2016; Eslami et al., 2017), one of the most popular and widely used is the 9-zone SBT system that employs two normalized cone readings (Saftner et al., 2018): Normalized tip resistance using a variable stress ratio exponent based on soil behavior type index (Q_{tn}), and Normalized friction ratio (F_r). This classification system is referred to as the SBT Q_{tn} and is plotted on charts as Q_{tn} vs. F_r. The normalized tip resistance using a variable stress ratio exponent can be calculated as following according to Robertson (2009):

$$Q_{tn} = \frac{(q_t - \sigma_v)/P_a}{(P_a/\sigma_v')^n} \tag{31}$$

Where P_a is atmospheric pressure (100 kPa), q_t is the average tip resistance corrected for porewater pressure, σ_v is the total vertical overburden stress, and σ'_v is the effective vertical overburden stress. The stress ratio exponent (n) is found by the following (Robertson, 2009):

$$n = 0.0381(I_c) + 0.05(\sigma_v'/P_a) - 0.15 \tag{32}$$

The soil behavior type index (I_c) is based on the variable stress ratio exponent (n), which itself is based on I_c (Robertson, 2009). As a result, an iterative calculation is required to determine I_c and the corresponding n.

$$I_c = \sqrt{(3.47 - log_{10}Q_{tn})^2 + (1.22 + log_{10}F_r)^2} \tag{33}$$

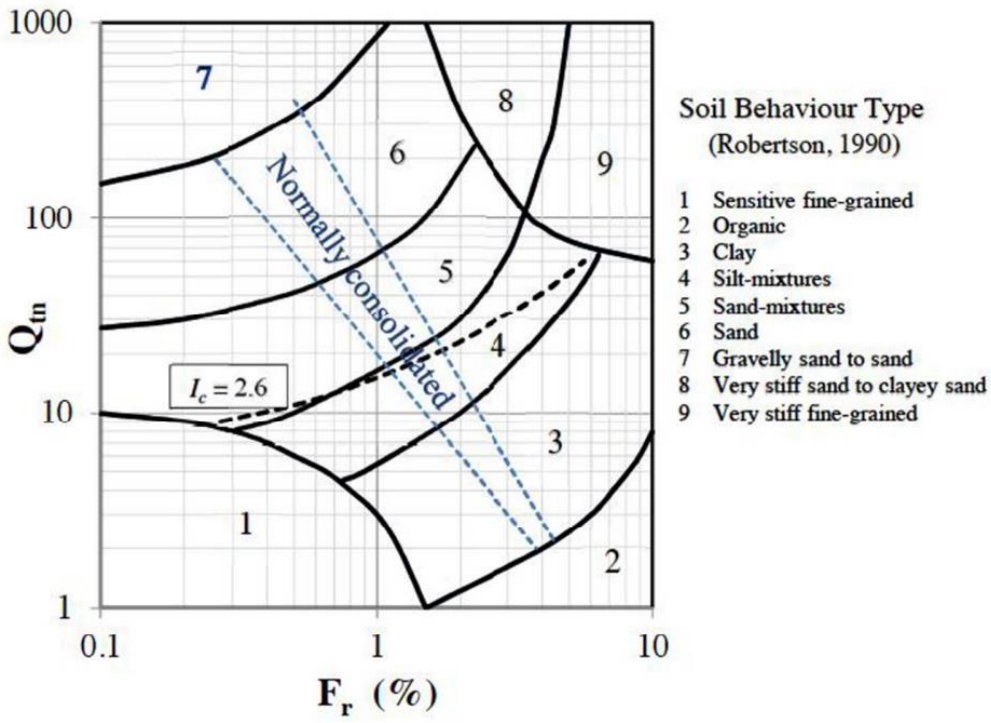

Figure 3.11. Normalized soil behavior type classification chart (SBT Q_{tn}) from Robertson 1990 and updated from Robertson 2009

Based on the CPTu data, soil classification could be based upon the Robertson (Robertson, 2009) normalized soil behavioral type chart (SBT Q_{tn}). Soil classification by this method was necessary to determine the appropriate values for the empirical coefficients used in the CPT/CPTu based methods.

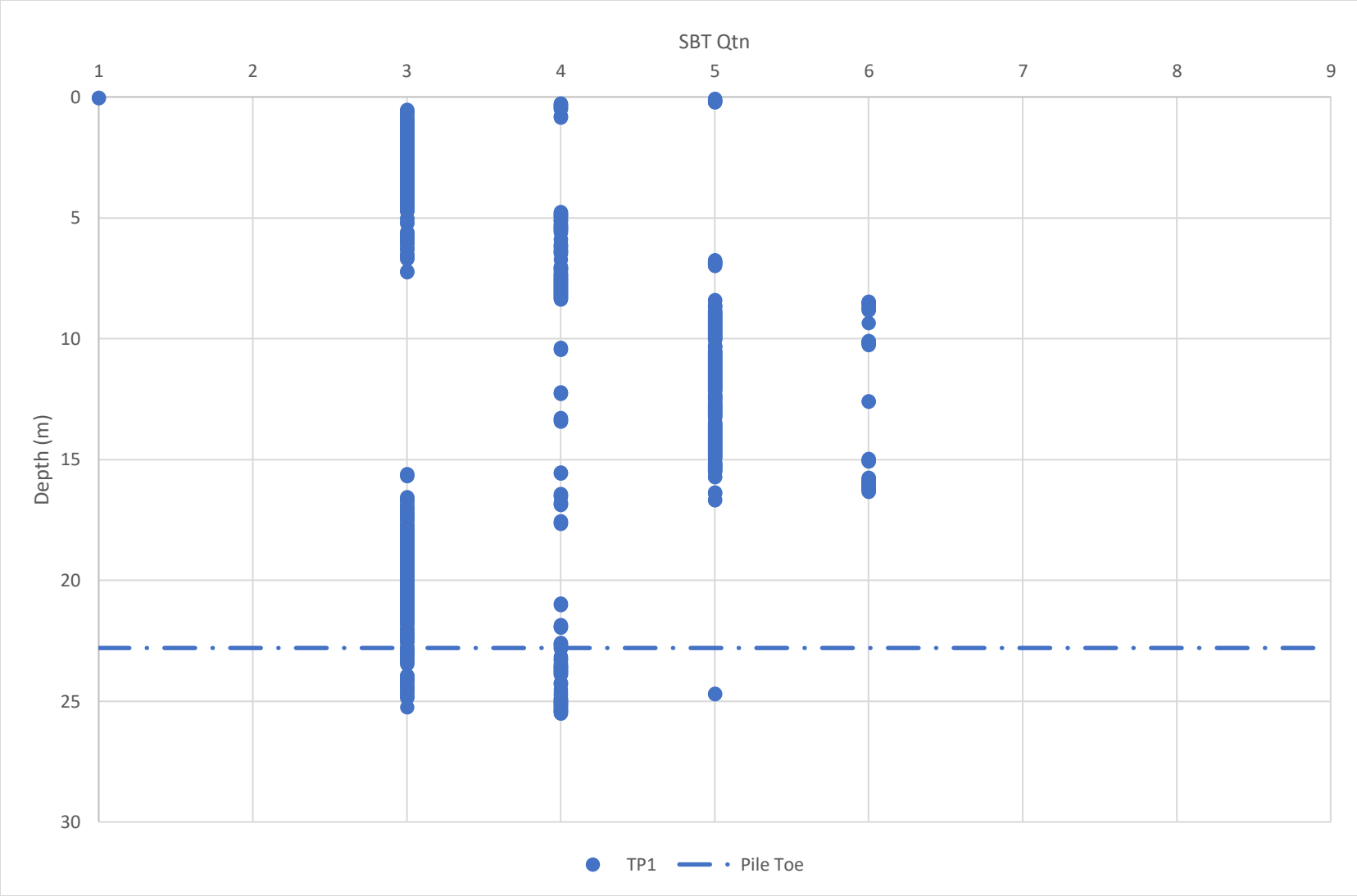

Figure 3.12. TP1 CPTu soil classification based on SBT Q_{tn}

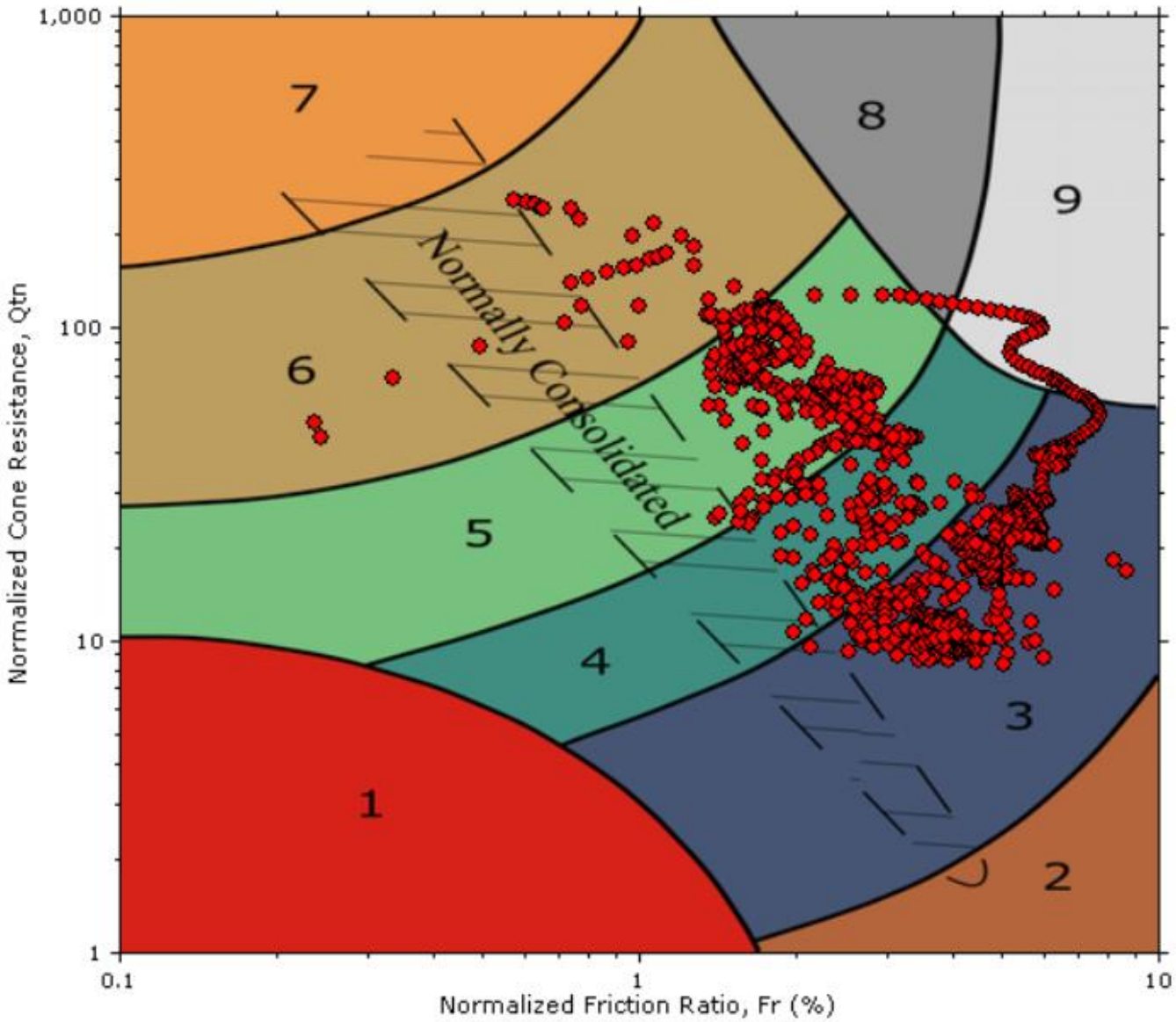

Figure 3.13. SBT Qtn plot for TP1 pile depth (0 to 22.8 m)

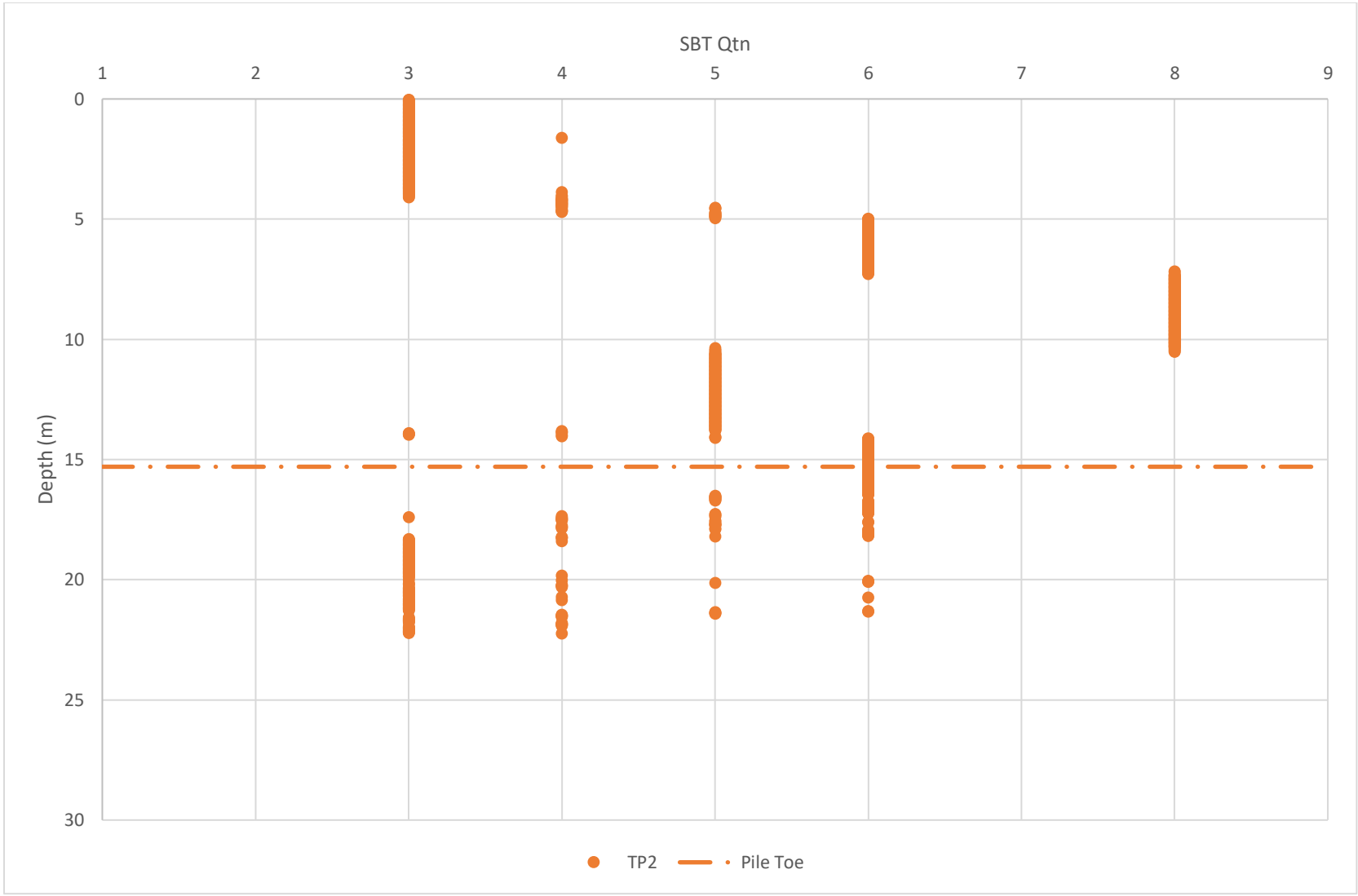

Figure 3.14. TP2 CPTu soil classification based on SBT Qtn

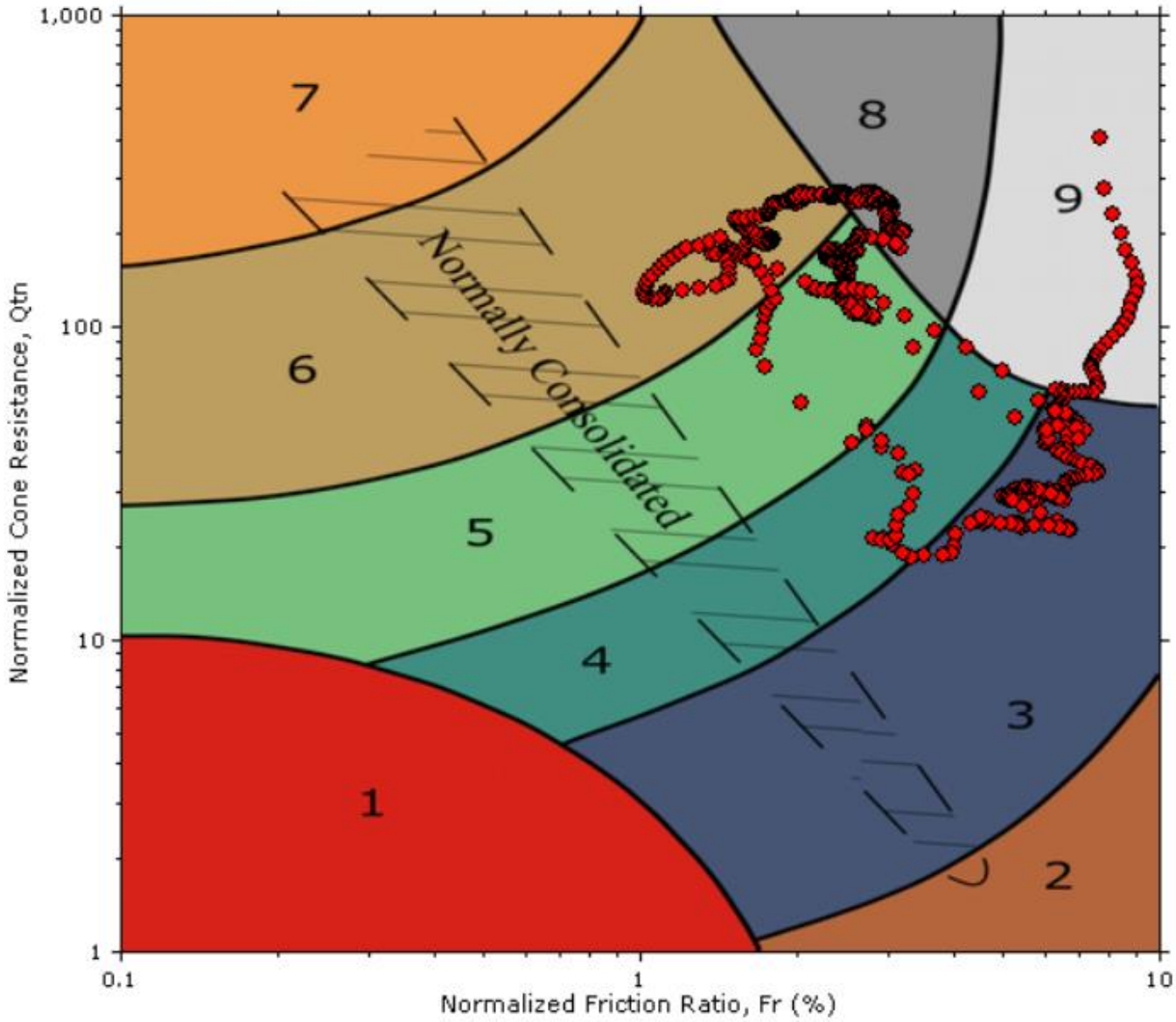

Figure 3.15. SBT Qtn plot for TP2 pile depth (0 to 15.3 m)

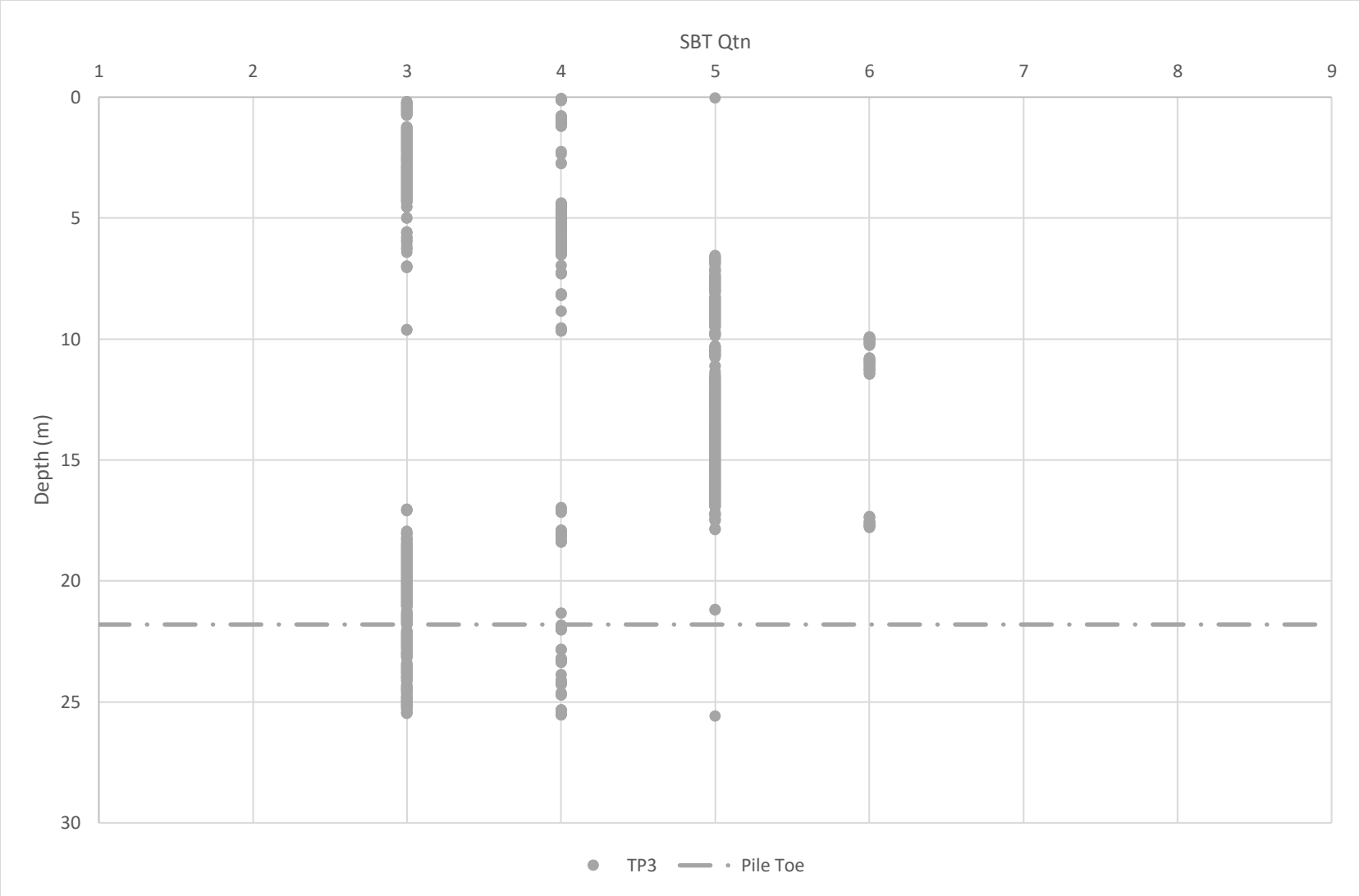

Figure 3.16. TP3 CPTu soil classification based on SBT Qtn

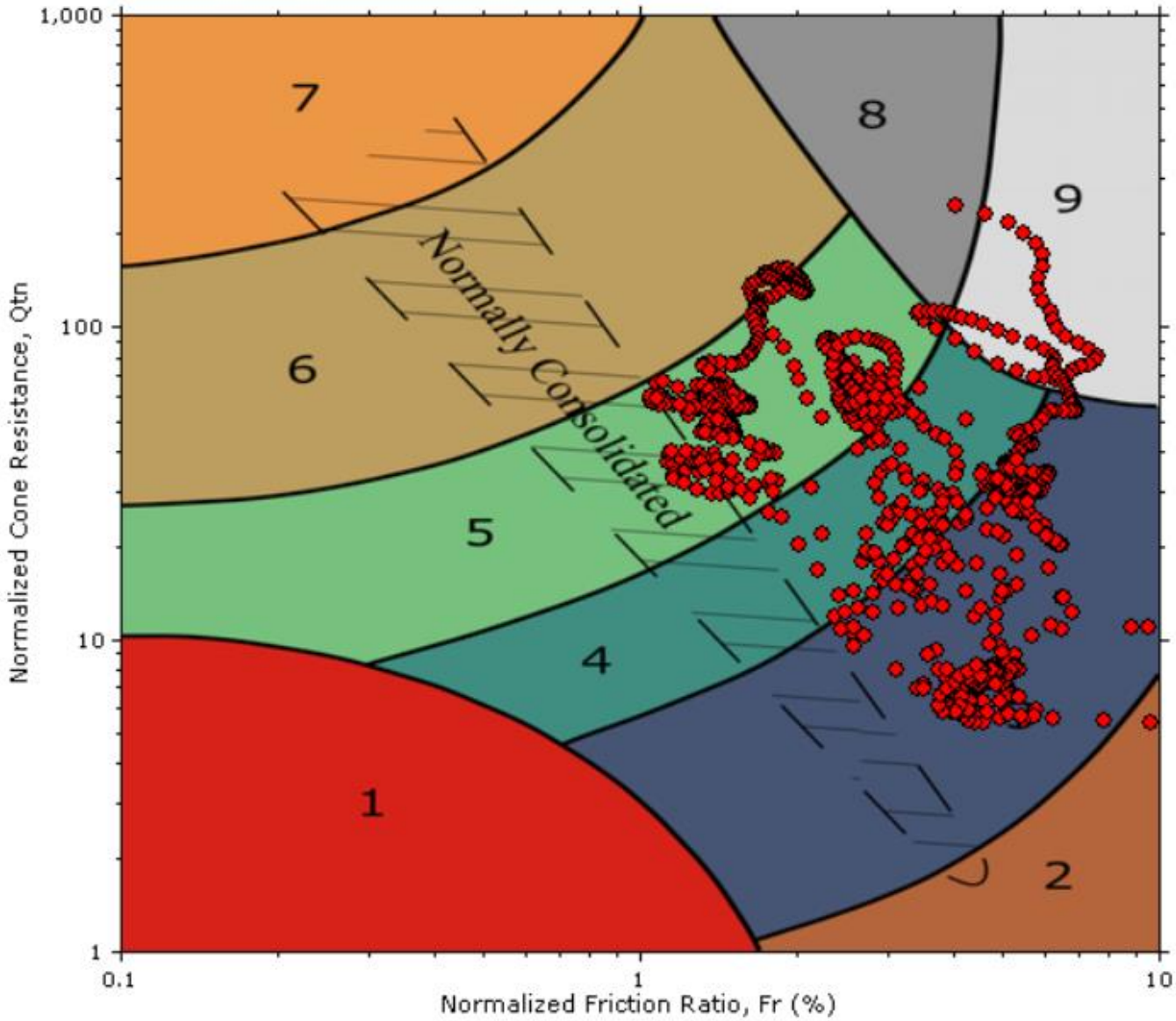

Figure 3.17. SBT Qtn plot for TP3 pile depth (0 to 21.8 m)

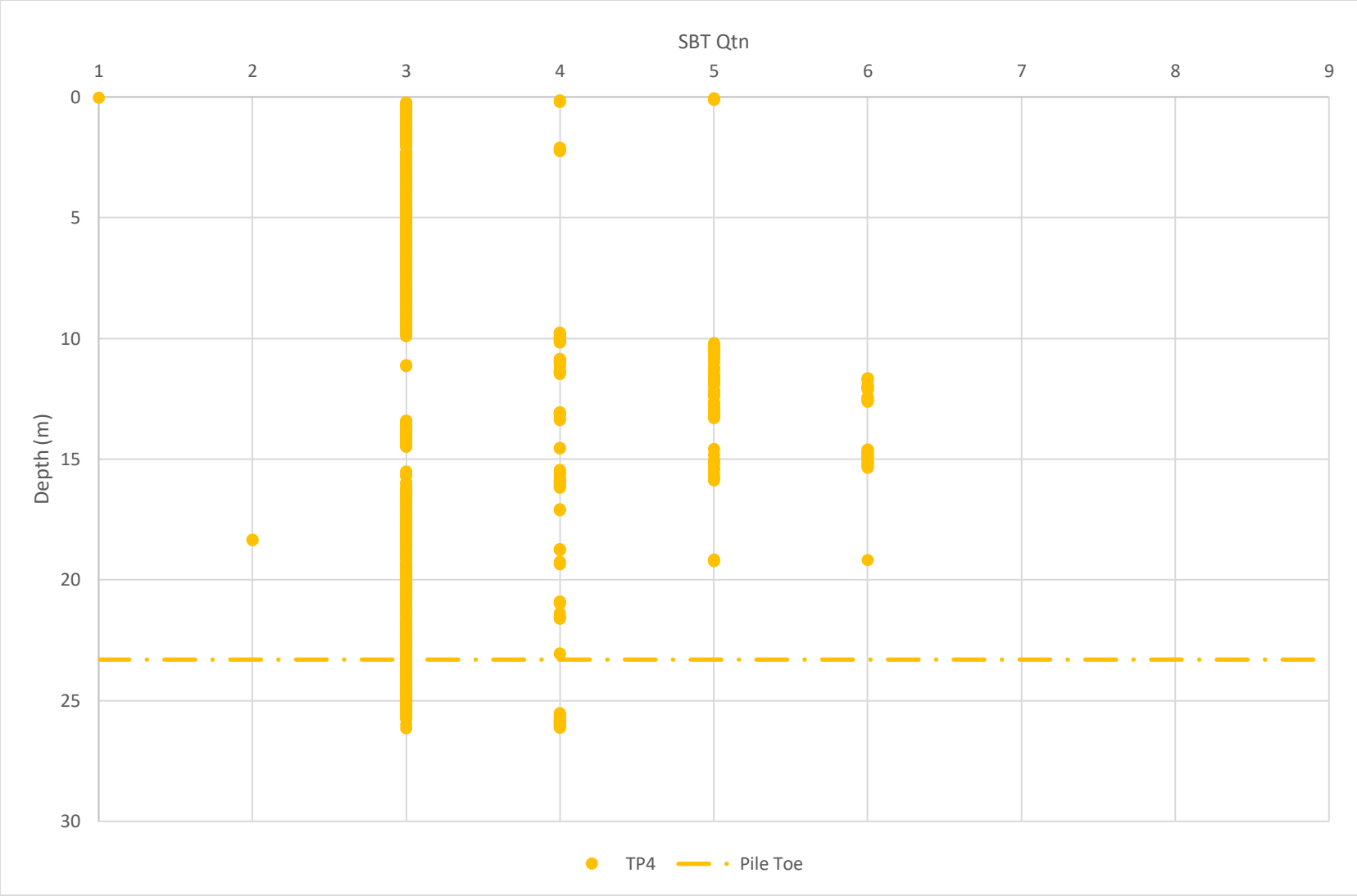

Figure 3.18. TP4 CPTu soil classification based on SBT Qtn

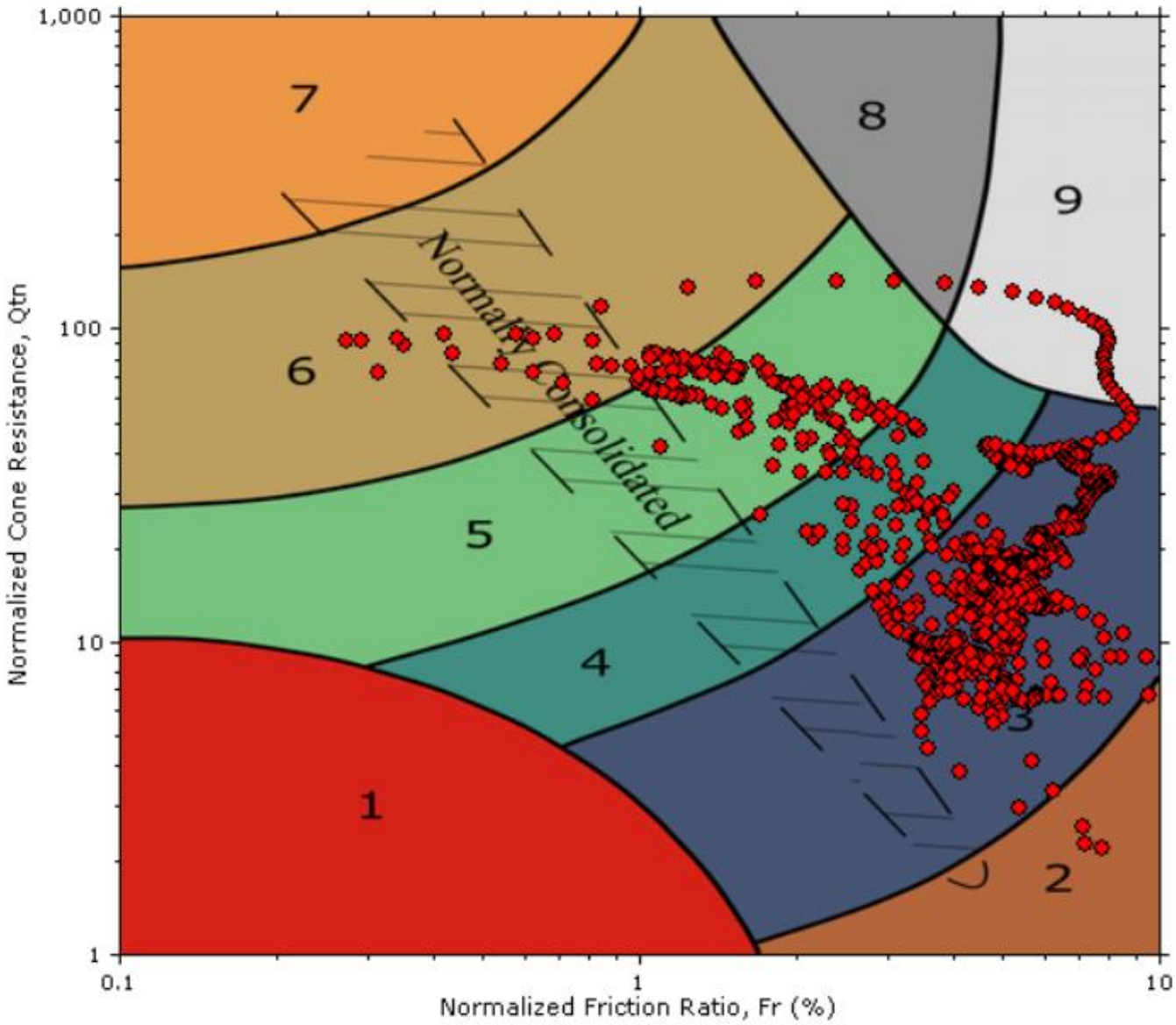

Figure 3.19. SBT Qtn plot for TP4 pile depth (0 to 23.3 m)

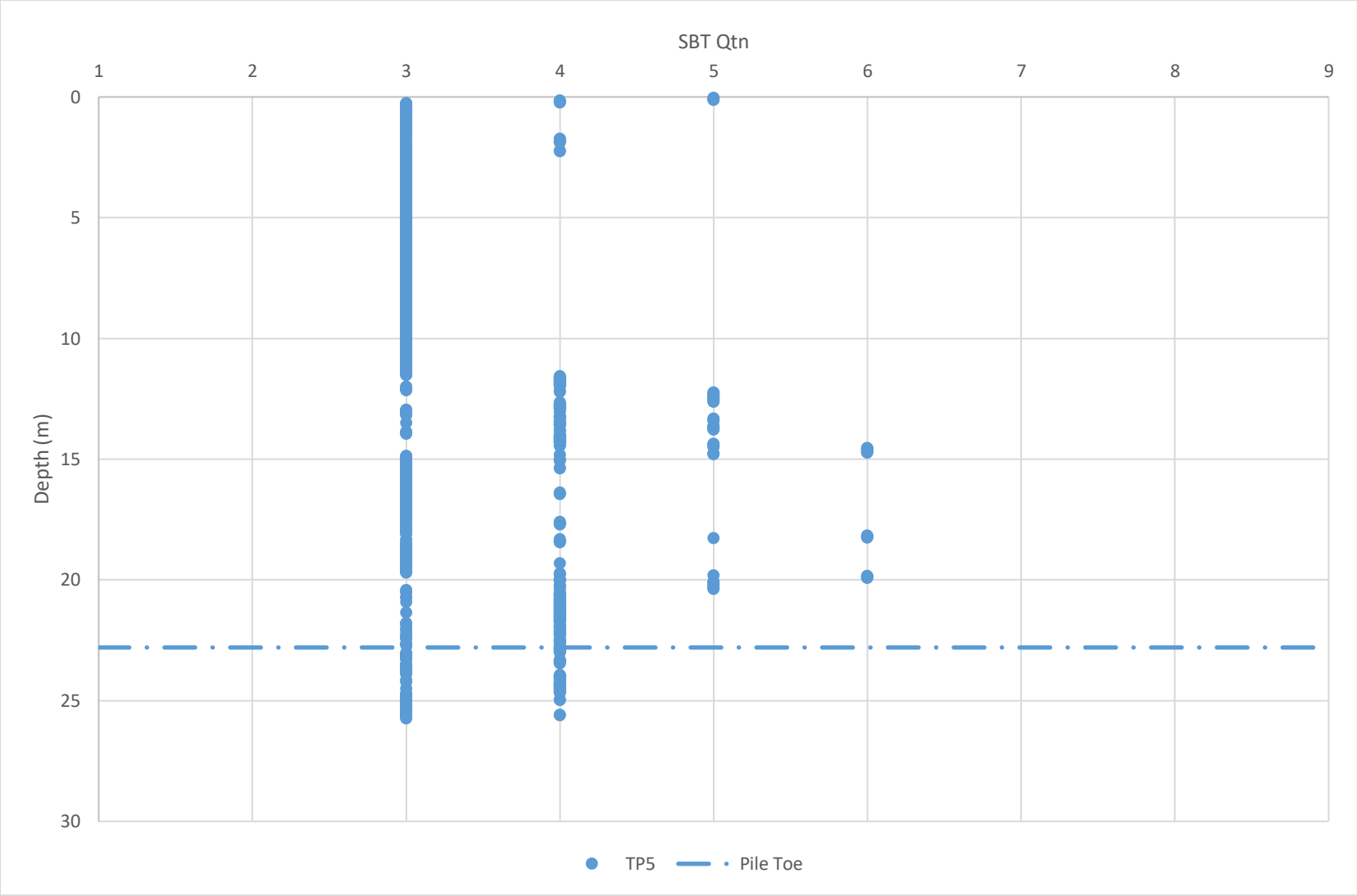

Figure 3.20. TP5 CPTu soil classification based on SBT Qtn

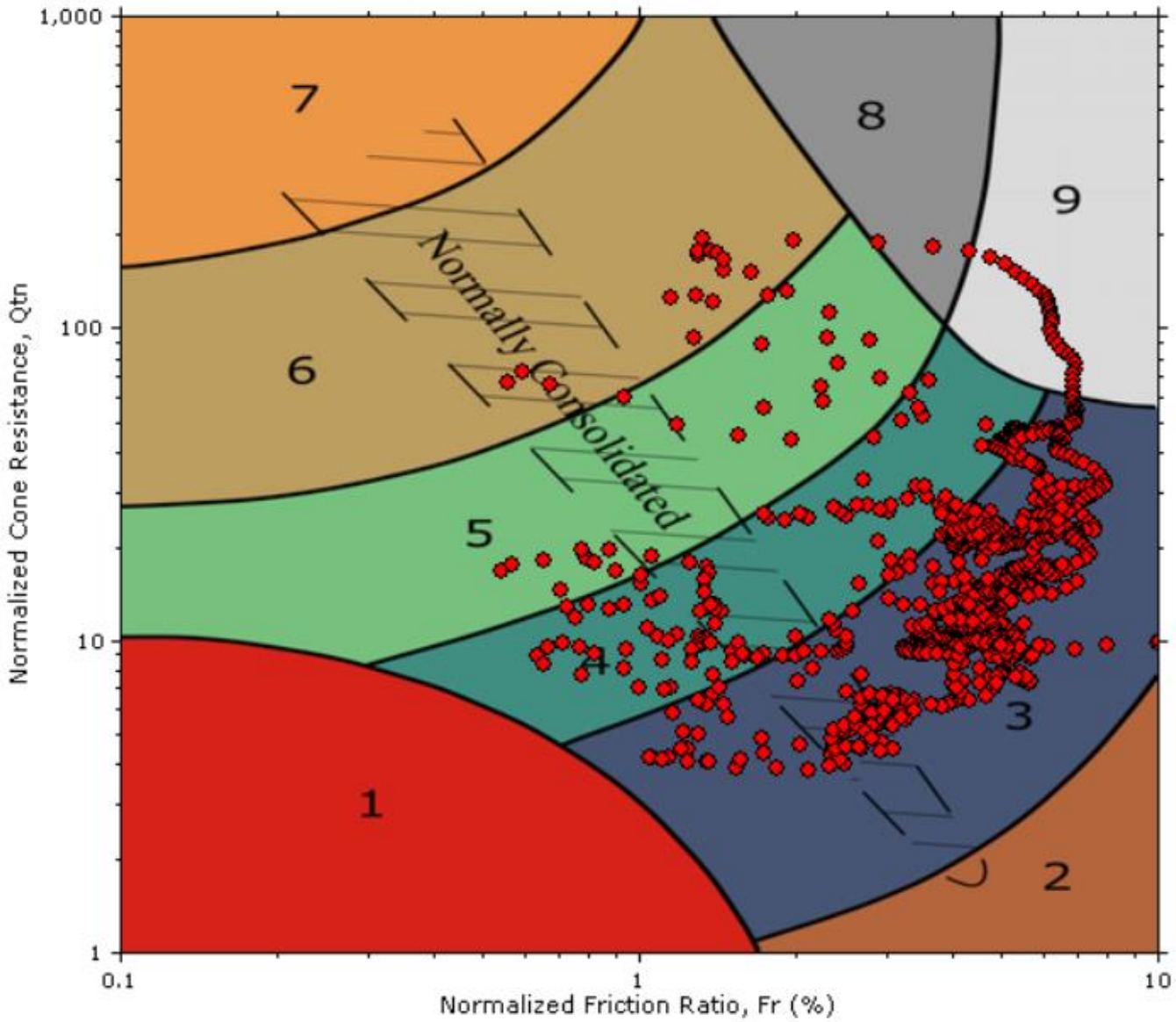

Figure 3.21. SBT Qtn plot for TP4 pile depth (0 to 22.8 m)

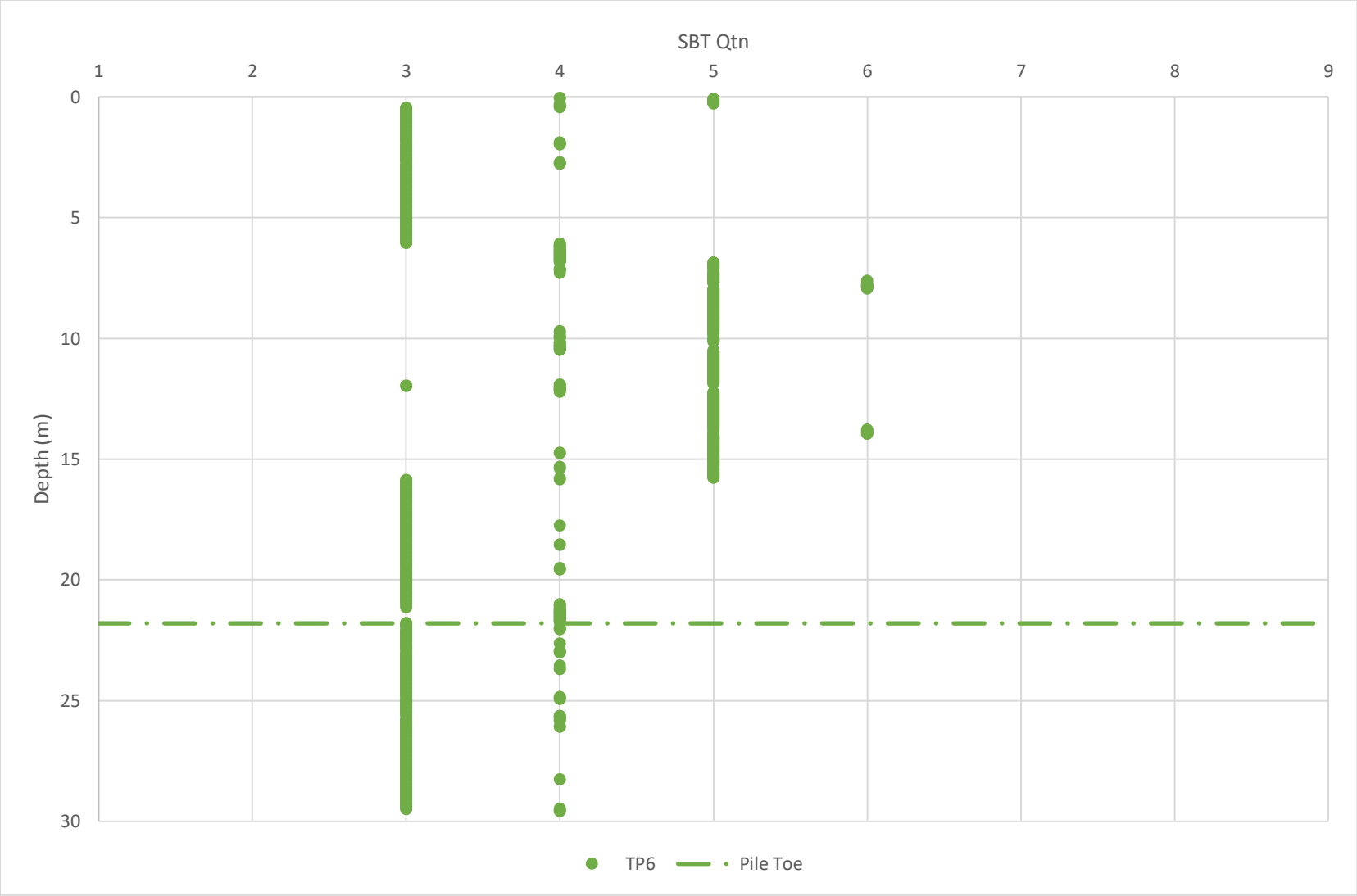

Figure 3.22. TP6 CPTu soil classification based on SBT Qtn

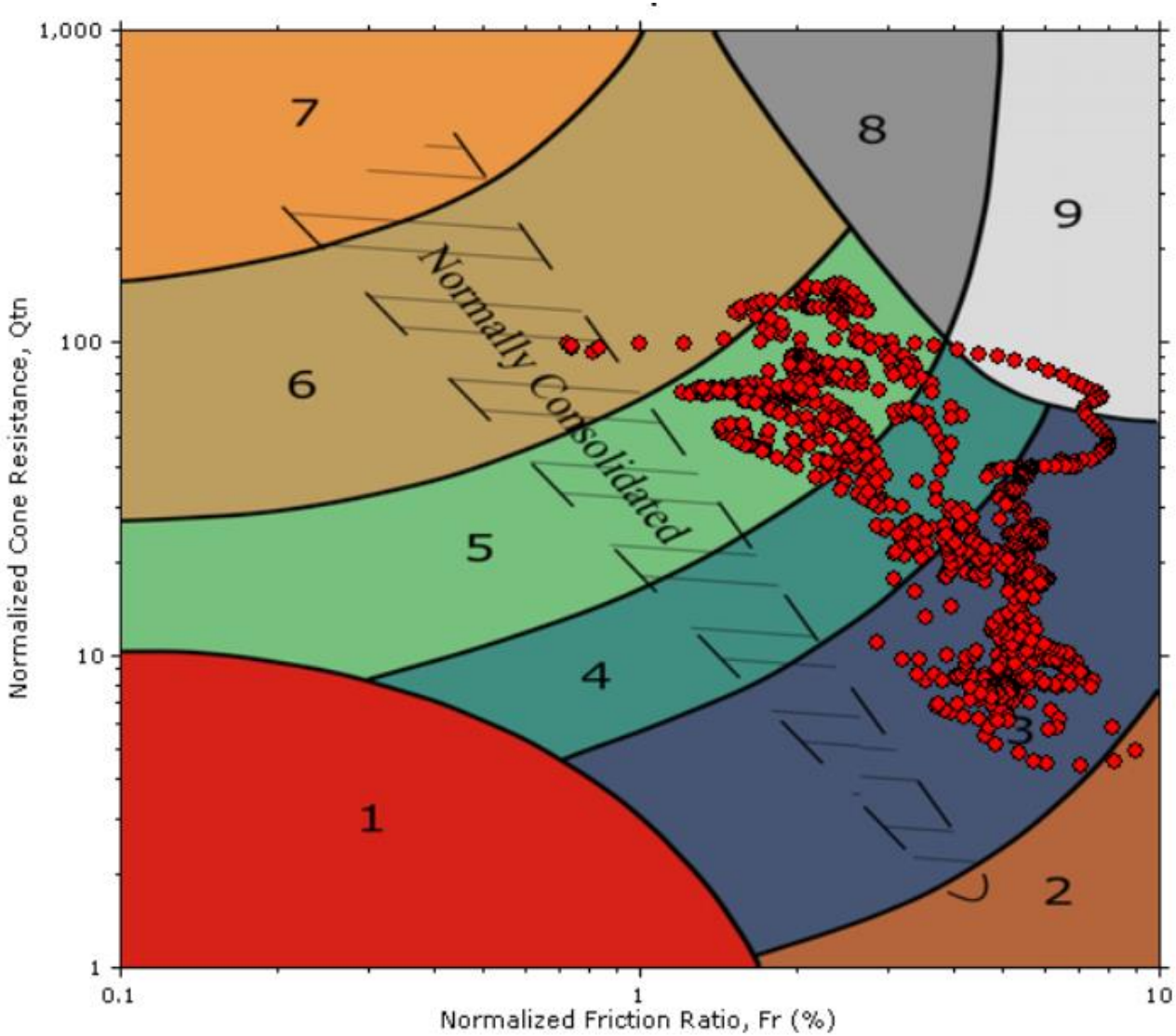

Figure 3.23. SBT Qtn plot for TP4 pile depth (0 to 21.8 m)

3.6 STATIC AXIAL LOAD TEST DATA

The reference capacities of the test piles were determined using static axial load test data. To apply a static load to the shaft, a hydraulic jack was used with a pump to apply hydraulic pressure. The jack was calibrated to ensure that the applied pressure corresponded to the known load during the test. A load cell, an elastic steel element with calibrated strain gauges, was used to measure the load applied to the pile head. Displacement measurements were made using four linear variable differential transformers (LVDT) as load was applied to the pile head. Figure 3.24 shows the plots for displacement vs. load for each test piles, for clarity the unloading of the test piles are not shown).

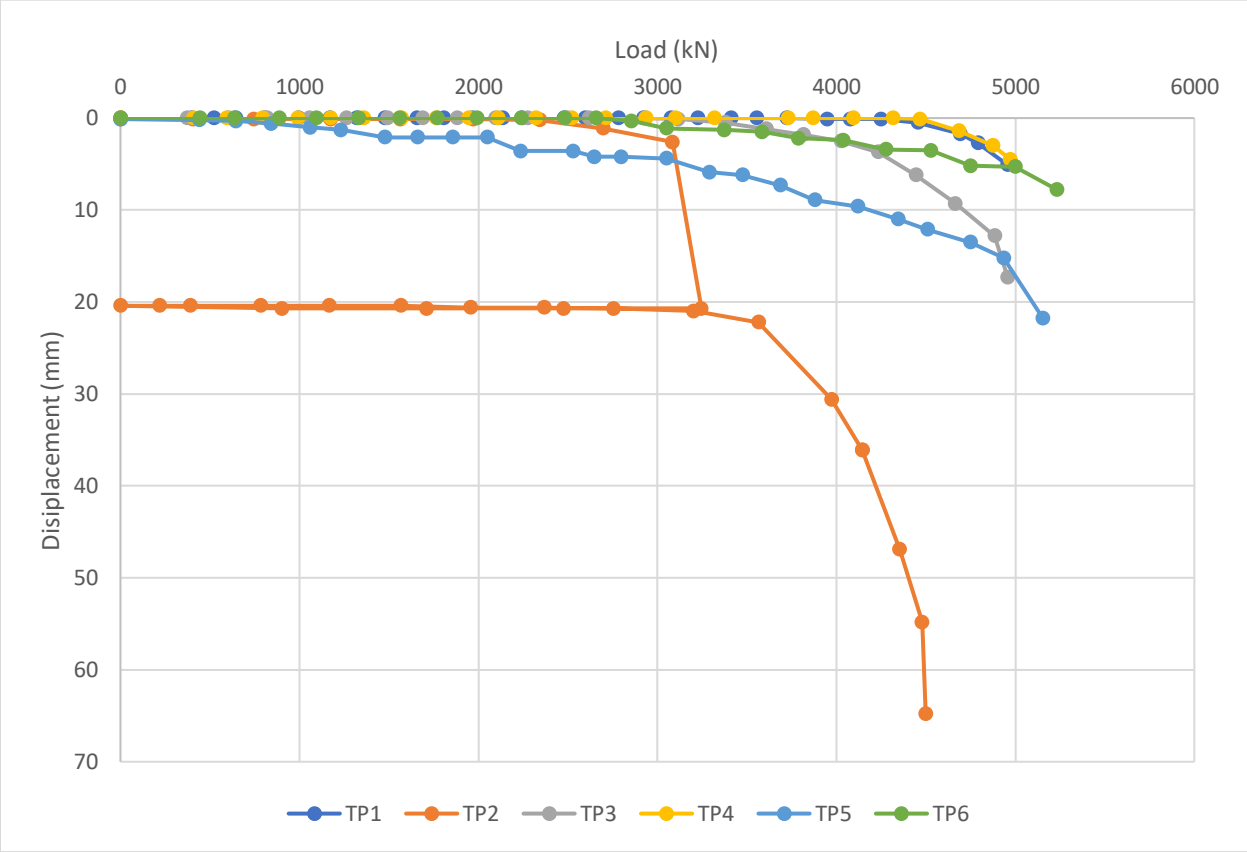

Figure 3.24. Plot of displacements vs. load for all test piles (note that TP2 was unloaded/reloaded)

Vibrating wire strain gauges mounted on a steel rebar running through the entire length of the pile were used to measure the strains developing within the pile, allowing for the determination of axial force in the shaft at each measurement point, so that the load transfer to the soil between measurement points could be calculated using Eq. 30.

Once the force at each strain measurement elevation was determined, force vs. depth plots were created as shown in Figures 3.25, 3.28, 3.31, 3.34, 3.37, and 3.40. Each curve in the plot represents a measurement for a specific load atop the shaft at the top displacement, as indicated in the legend. The topmost point in the curve is the load cell measurement, while the remaining points below grade are interpreted from the strain measurements. The difference between the force at each measurement elevation represents the load transferred to the soil over the length of that segment.

Figures 3.26, 3.29, 3.32, 3.38, and 3.41 plot the mobilized shaft resistances against the pile head displacements. While Figures 3.27, 3.30, 3.33, 3.39, and 3.42 plot the mobilized end bearing resistances against the pile head displacements.

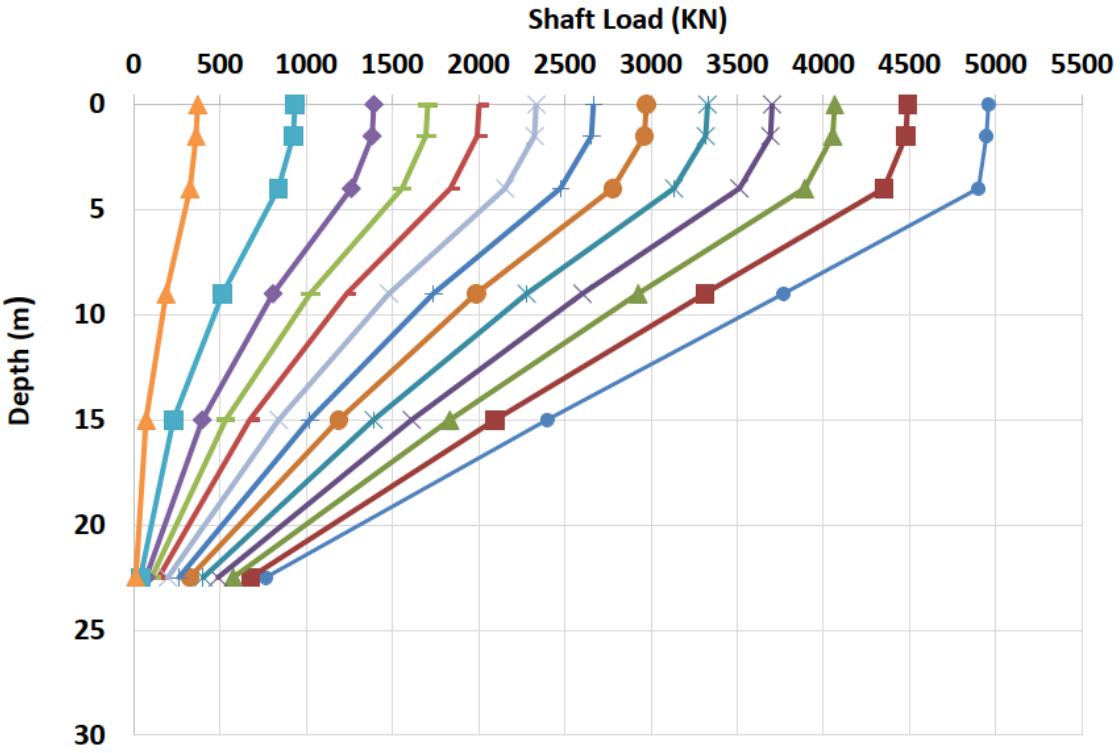

Figure 3.25. TP1 force vs. depth plot from static axial load test

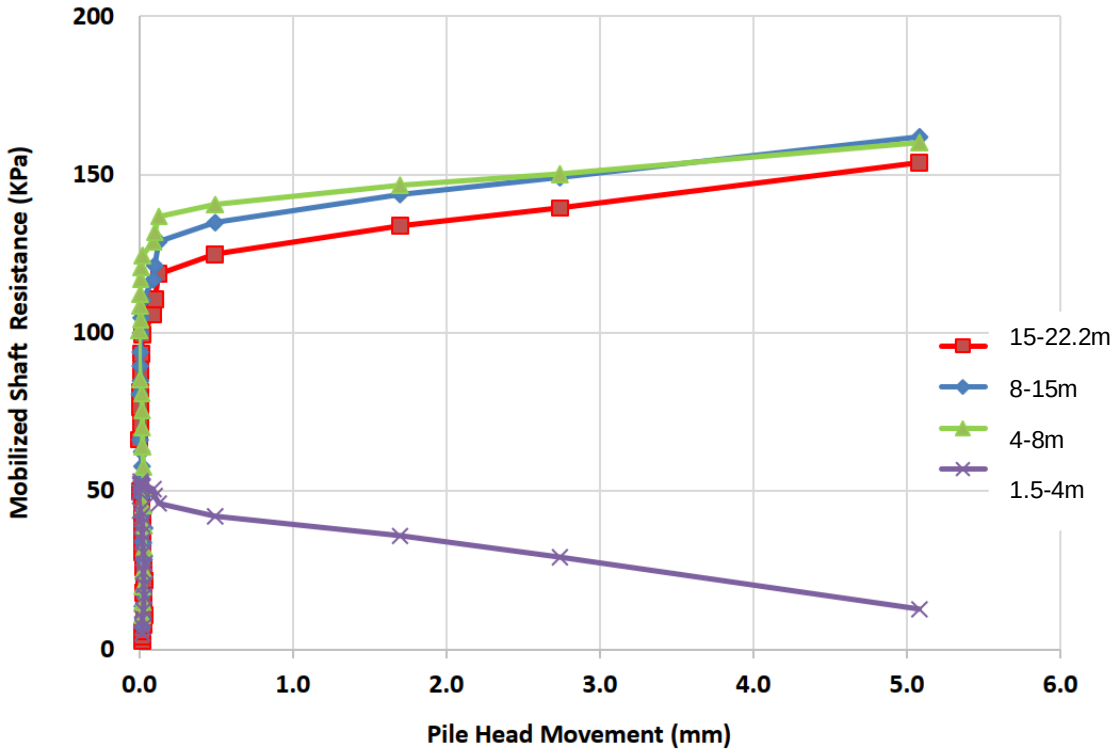

Figure 3.26. TP1 mobilized shaft resistance vs. pile head movement

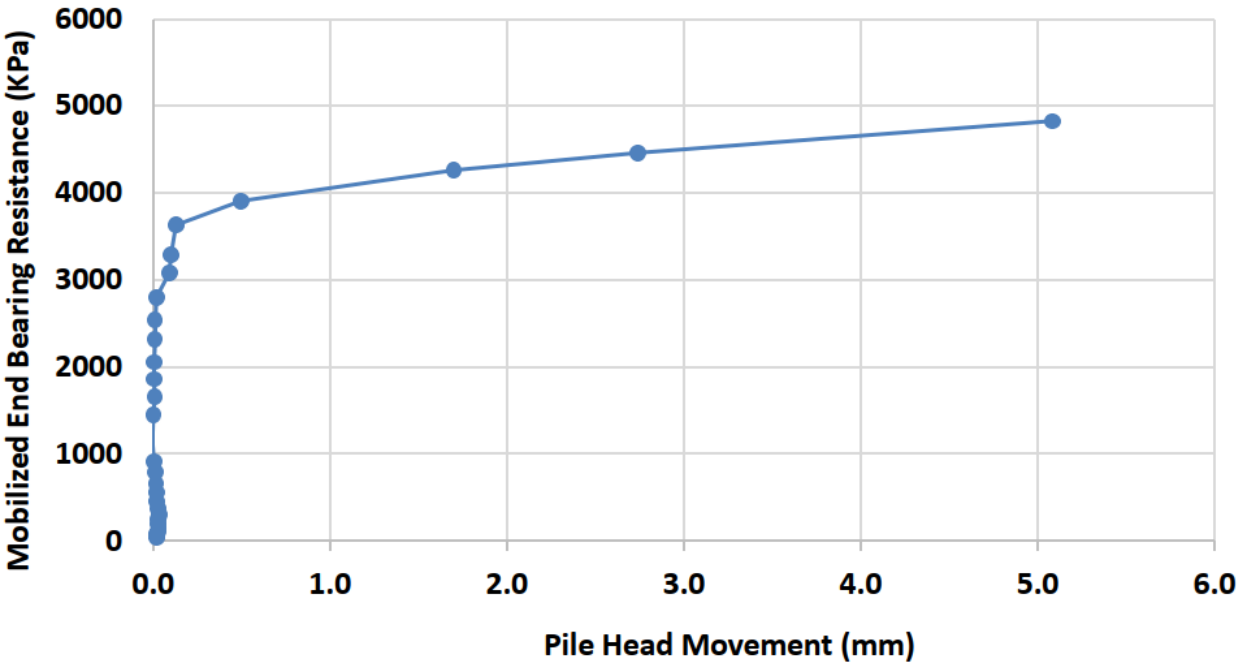

Figure 3.27. TP1 mobilized end bearing resistance vs. pile head movement

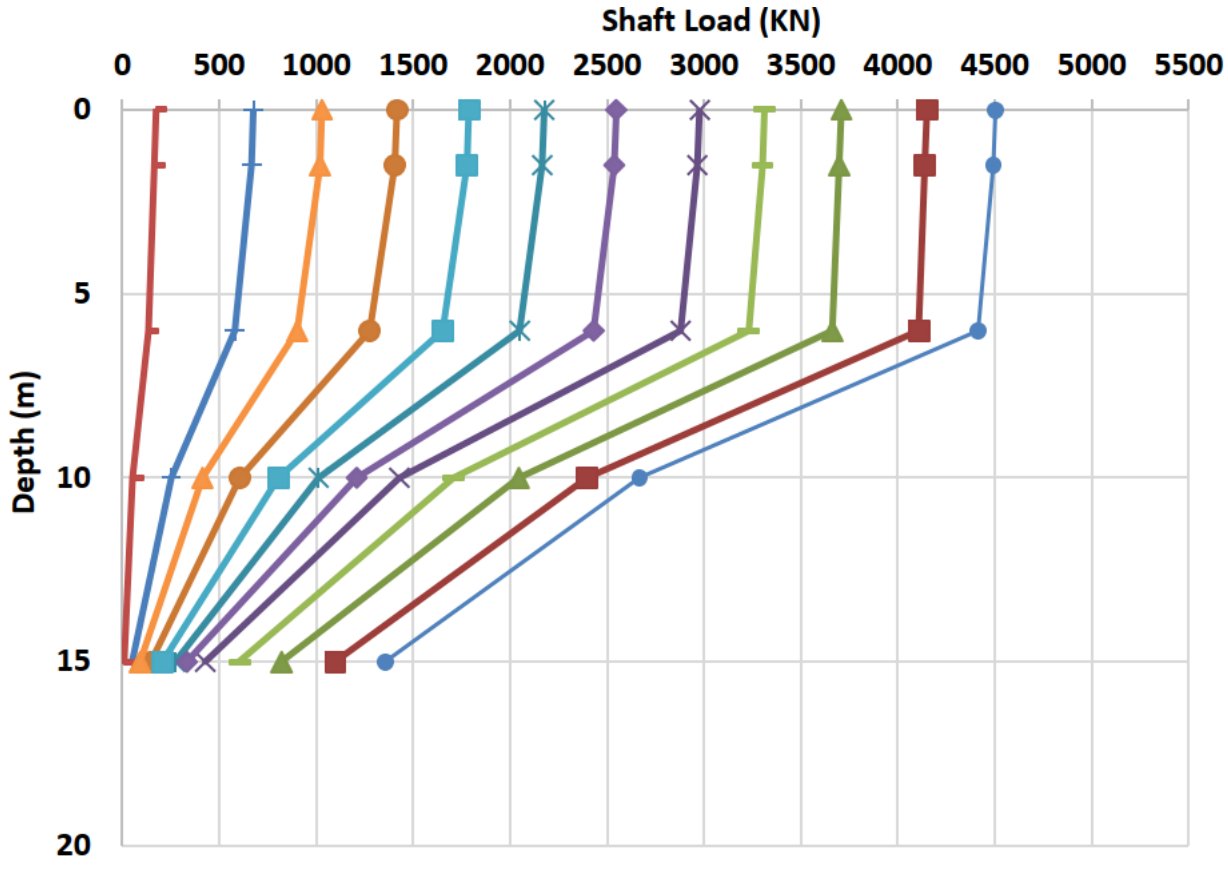

Figure 3.28. TP2 force vs. depth plot from static axial load test

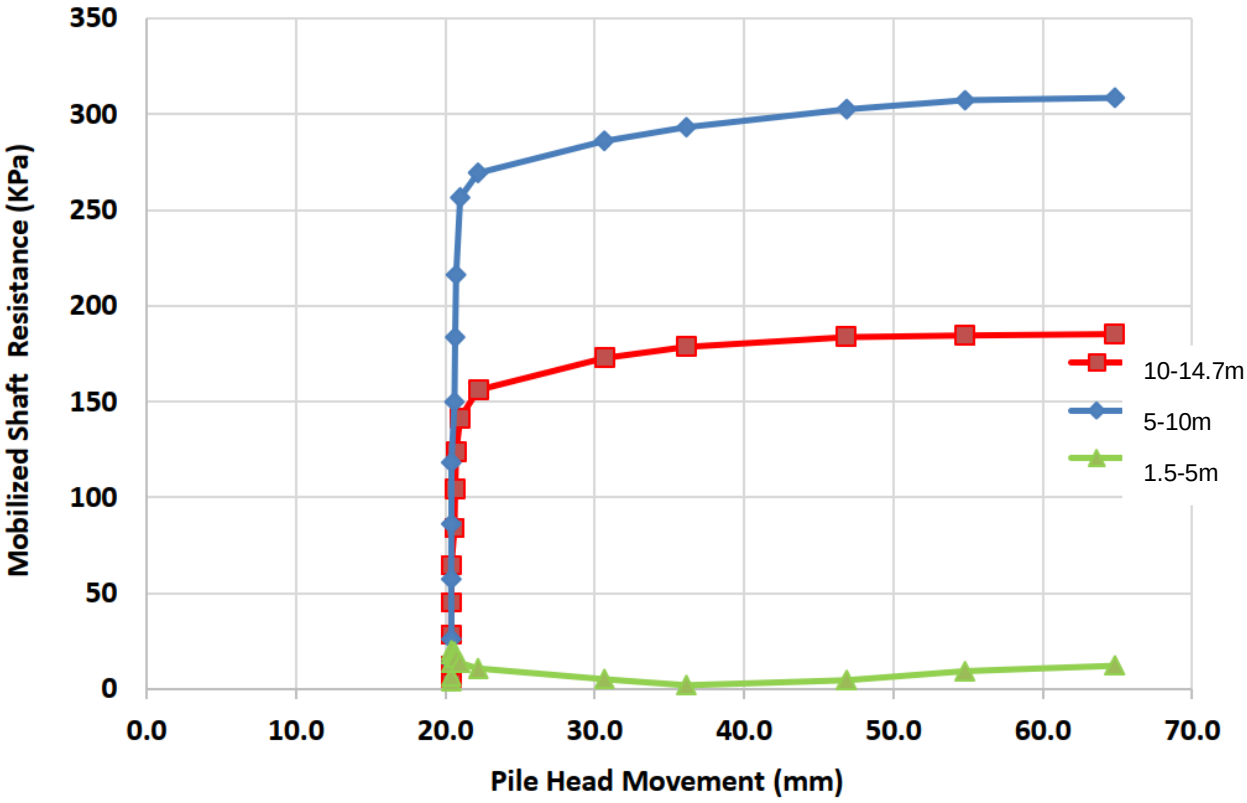

Figure 3.29. TP2 mobilized shaft resistance vs. pile head movement

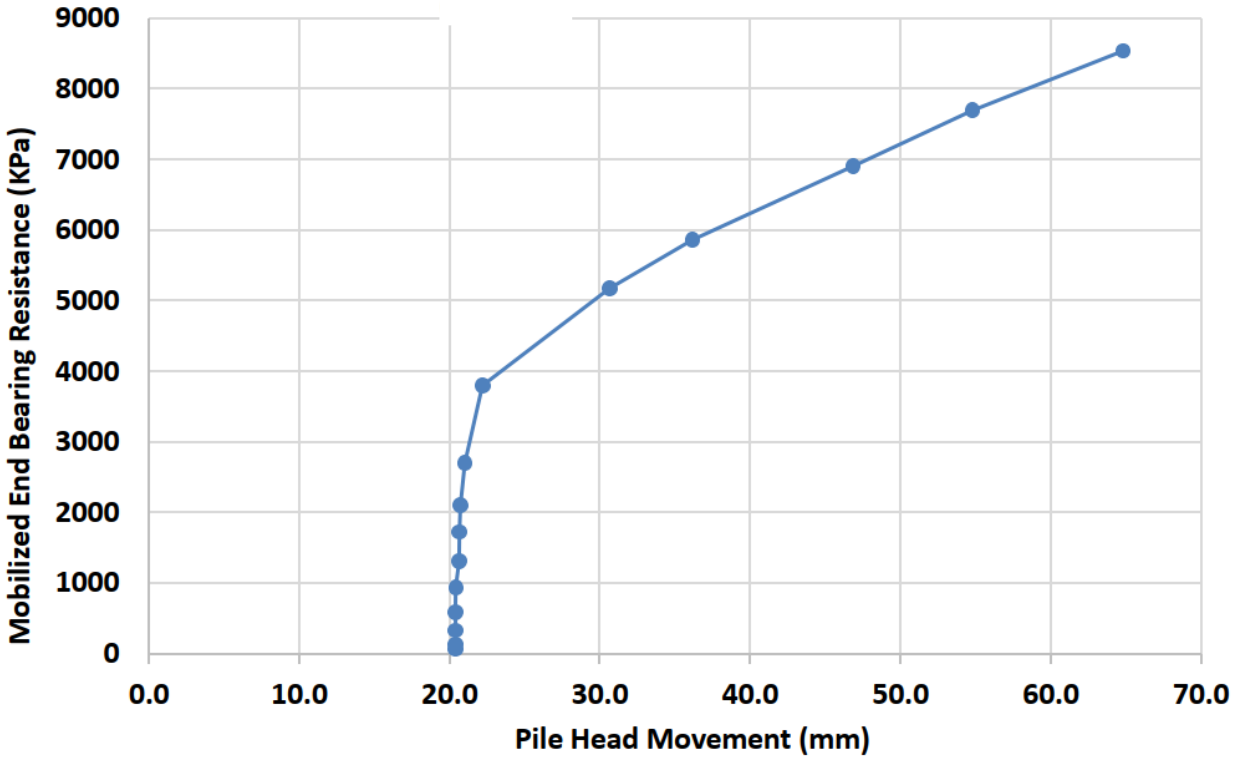

Figure 3.30. TP2 mobilized end bearing resistance vs. pile head movement

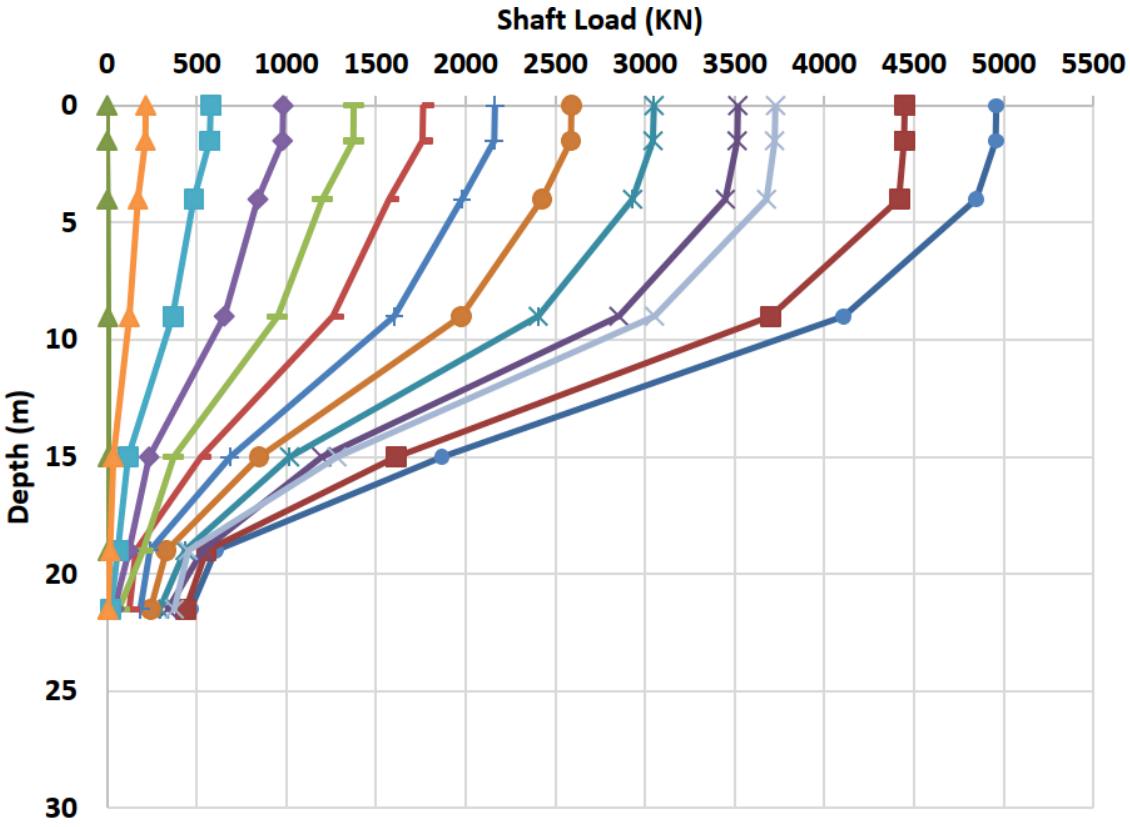

Figure 3.31. TP3 force vs. depth plot from static axial load test

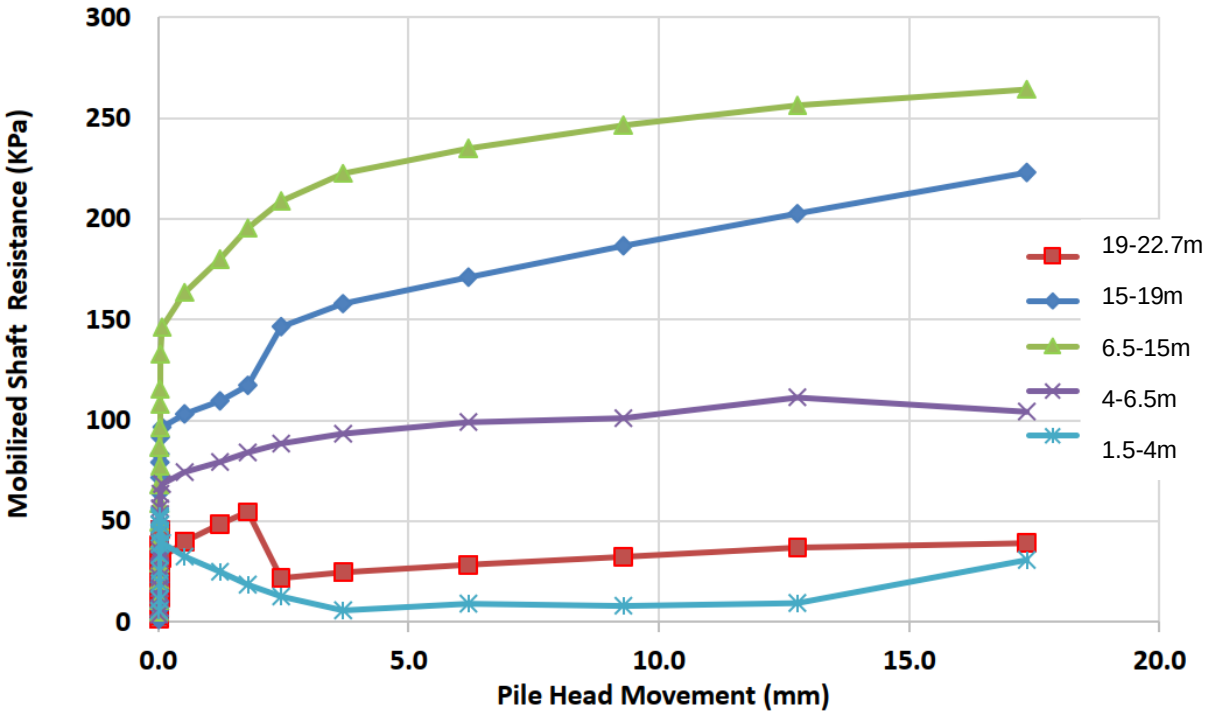

Figure 3.32. TP3 mobilized shaft resistance vs. pile head movement

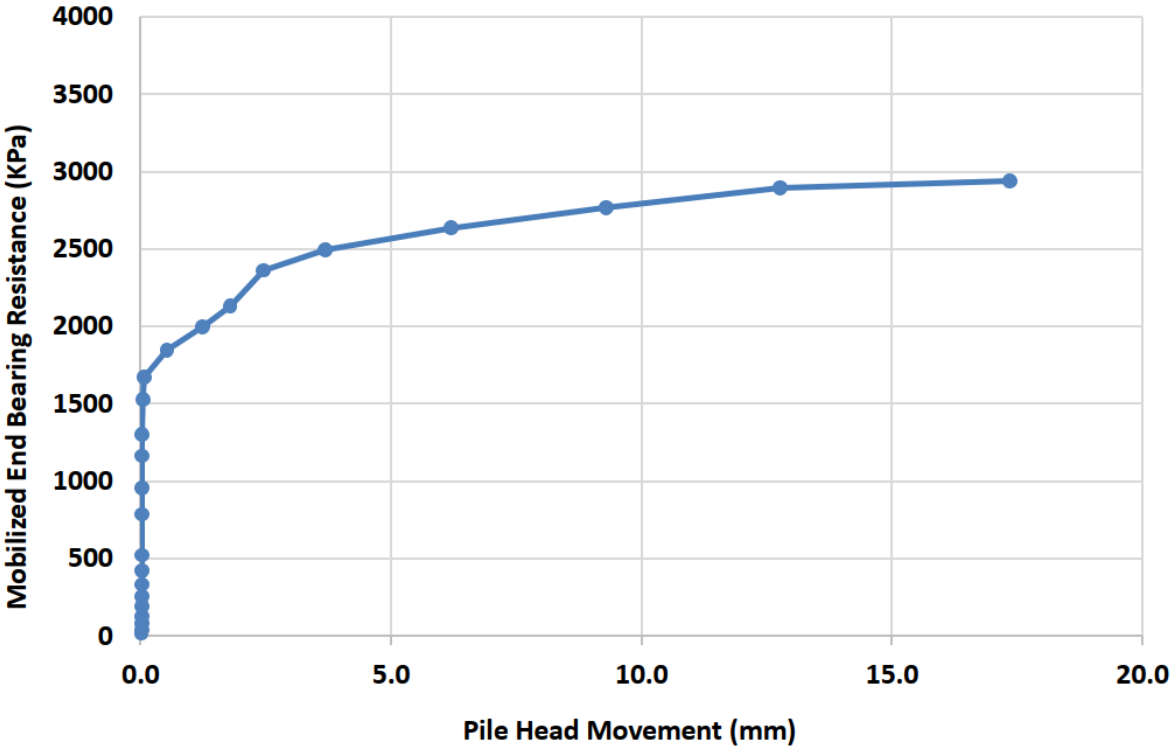

Figure 3.33. TP3 mobilized end bearing resistance vs. pile head movement

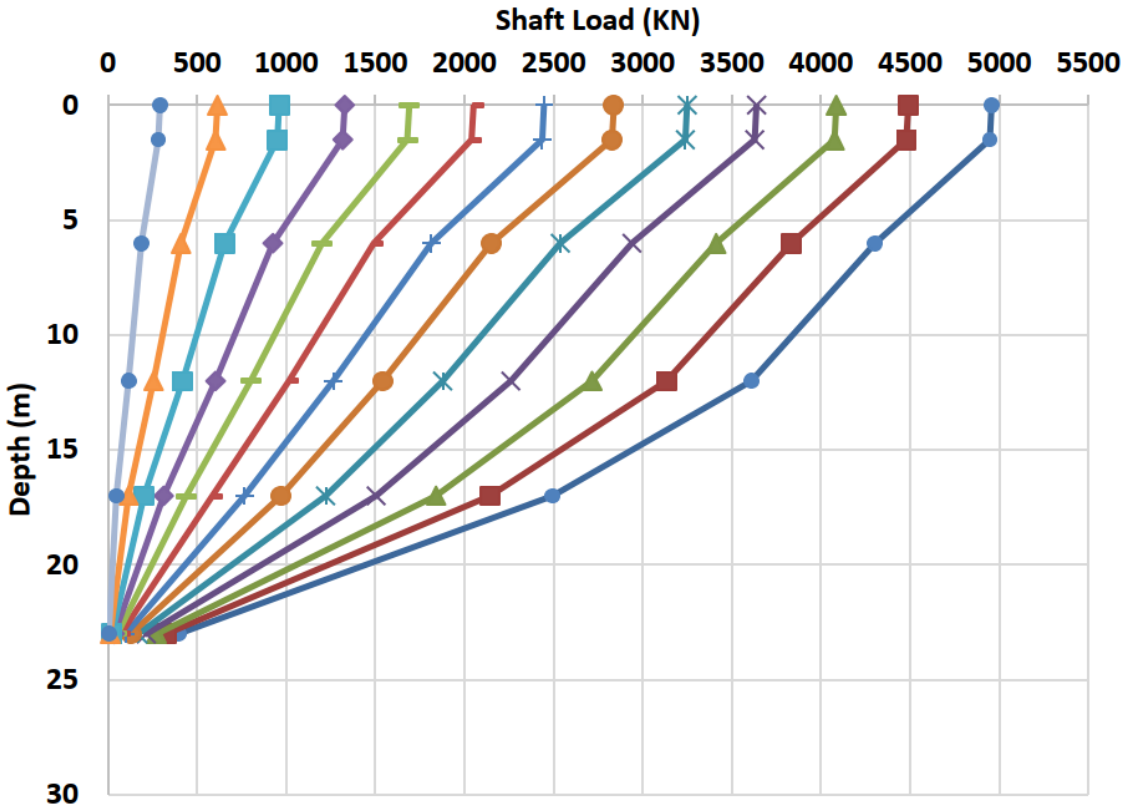

Figure 3.34. TP4 force vs. depth plot from static axial load test

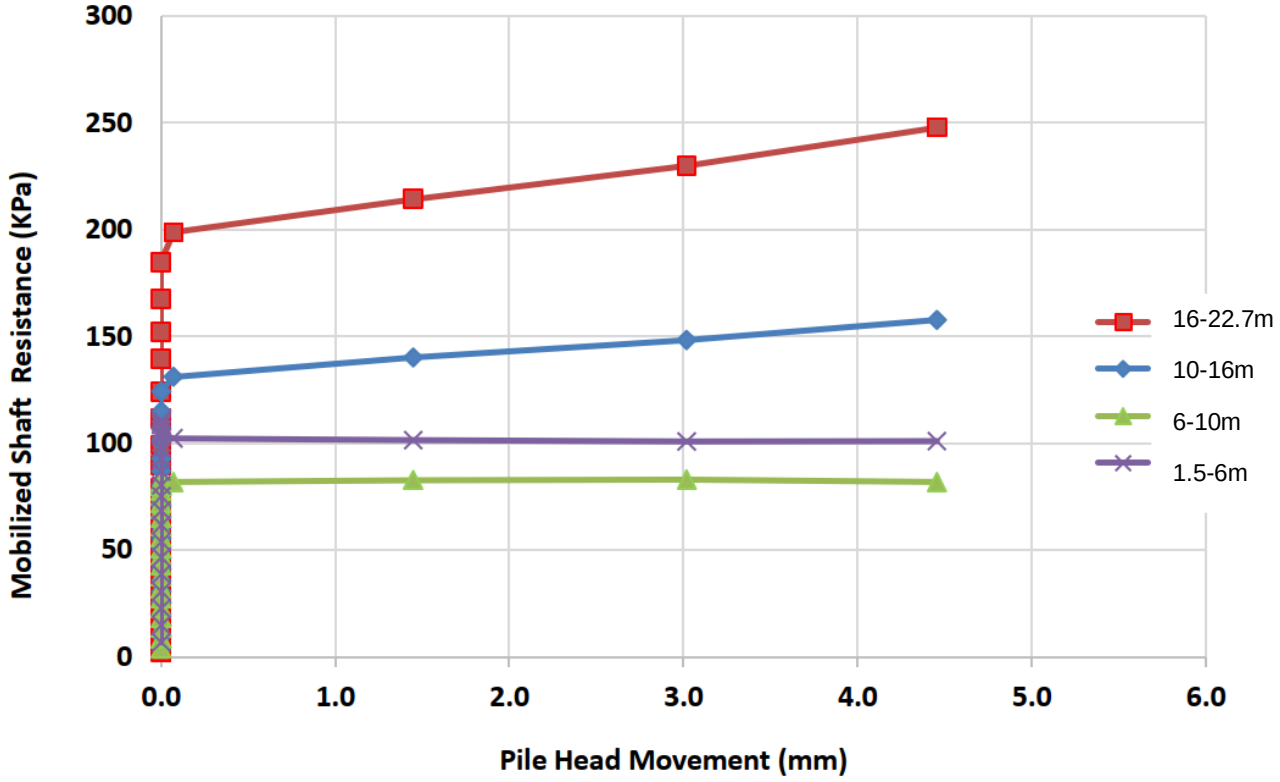

Figure 3.35. TP4 mobilized shaft resistance vs. pile head movement

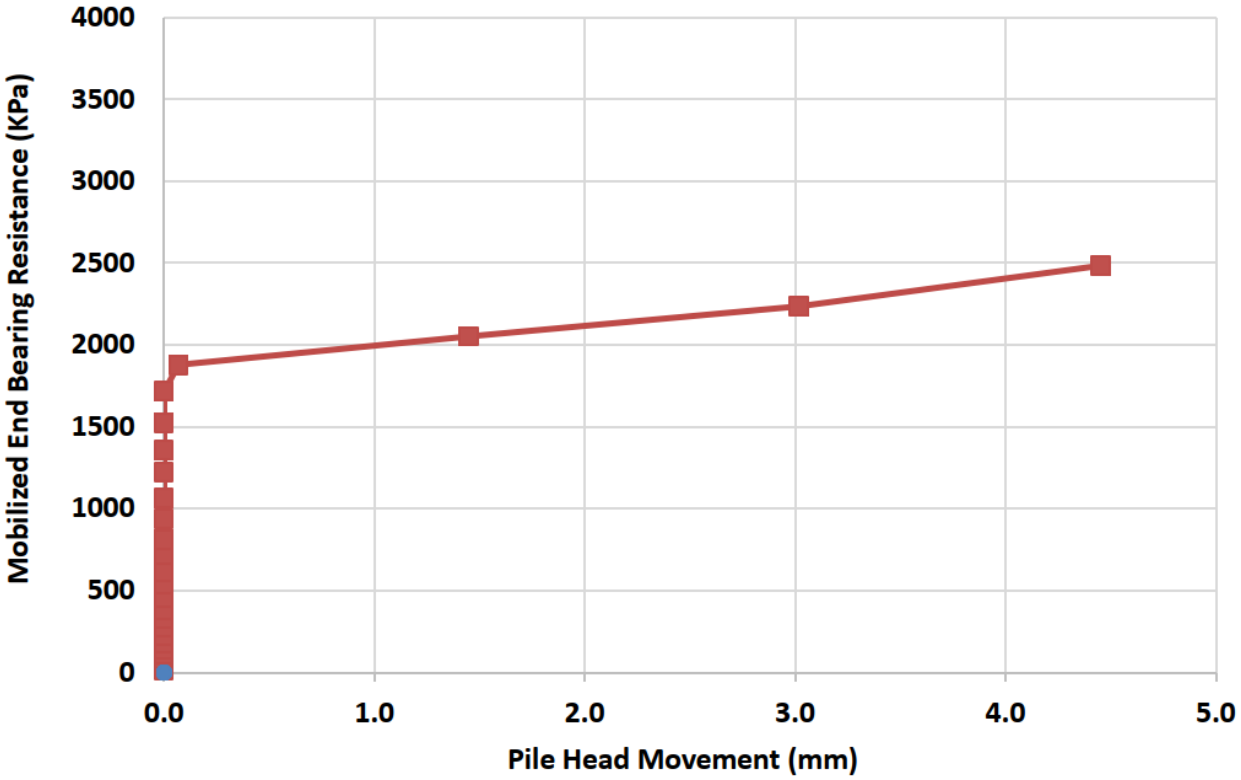

Figure 3.36. TP4 mobilized end bearing resistance vs. pile head movement

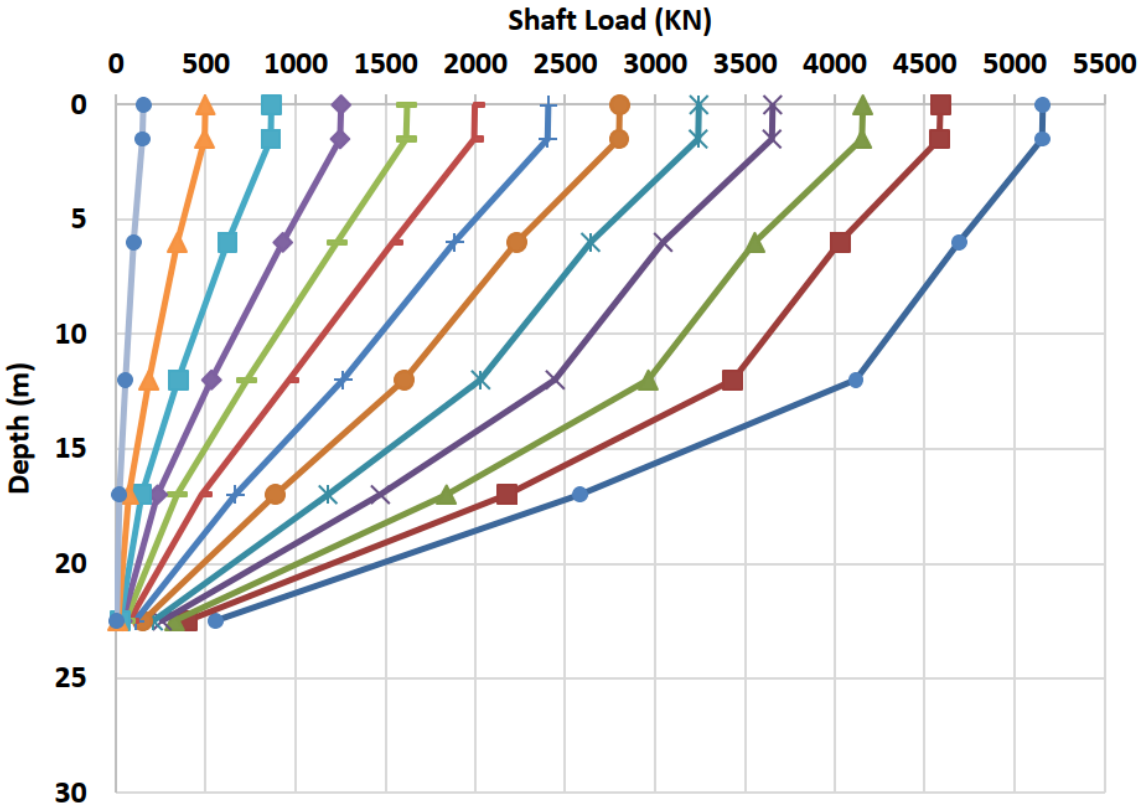

Figure 3.37. TP5 force vs. depth plot from static axial load test

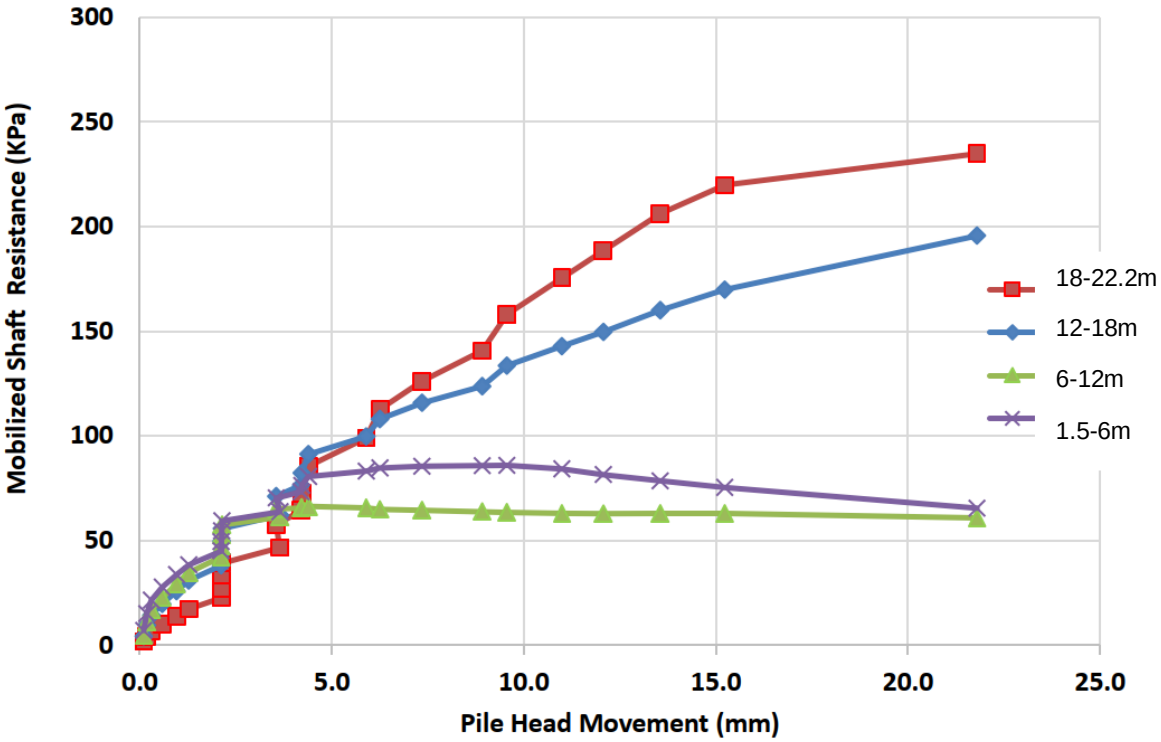

Figure 3.38. TP5 mobilized shaft resistance vs. pile head movement

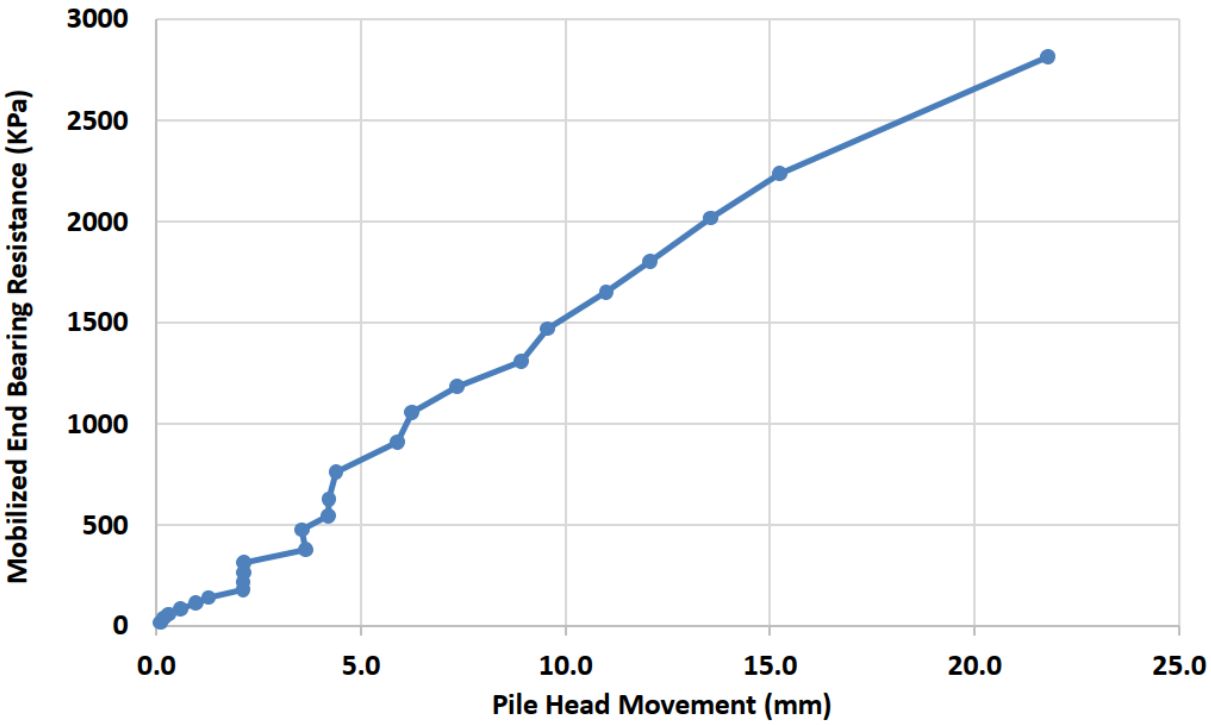

Figure 3.39. TP5 mobilized end bearing resistance vs. pile head movement

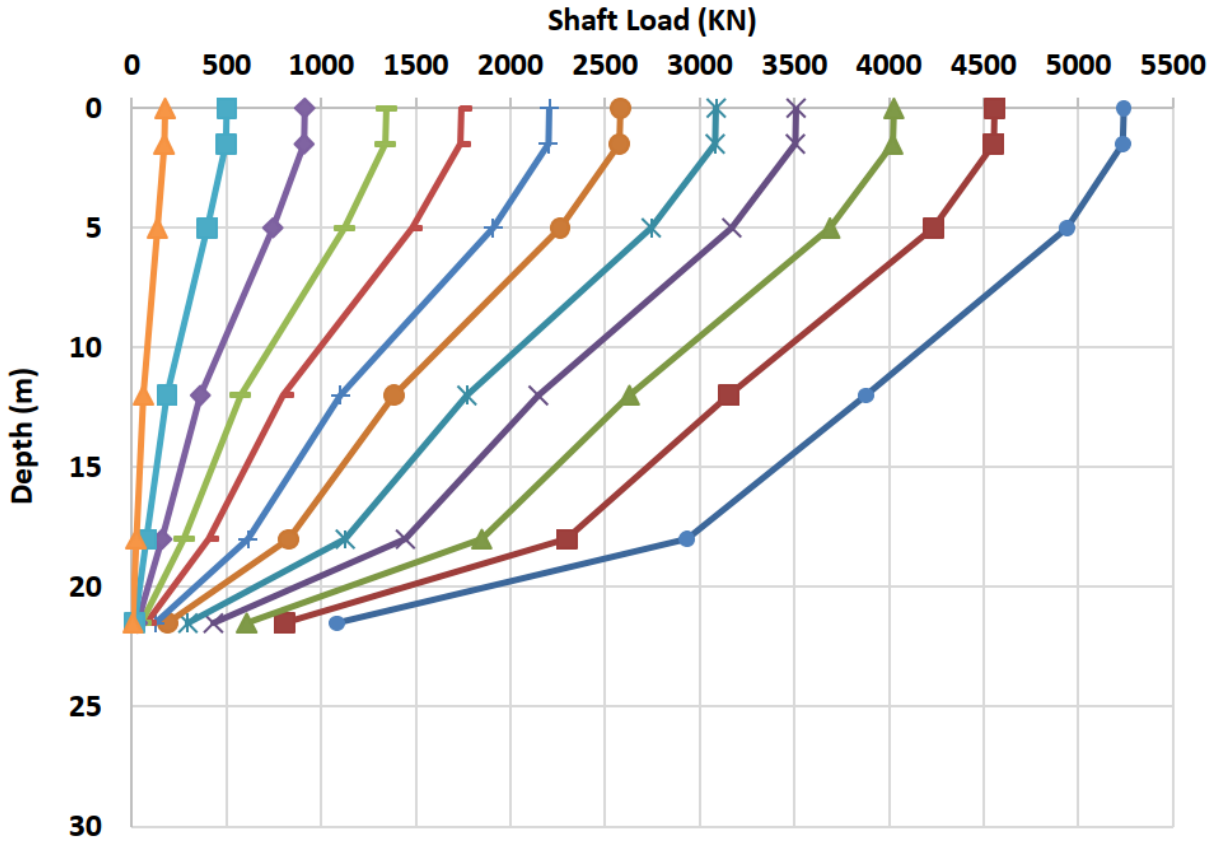

Figure 3.40. TP6 force vs. depth plot from static axial load test

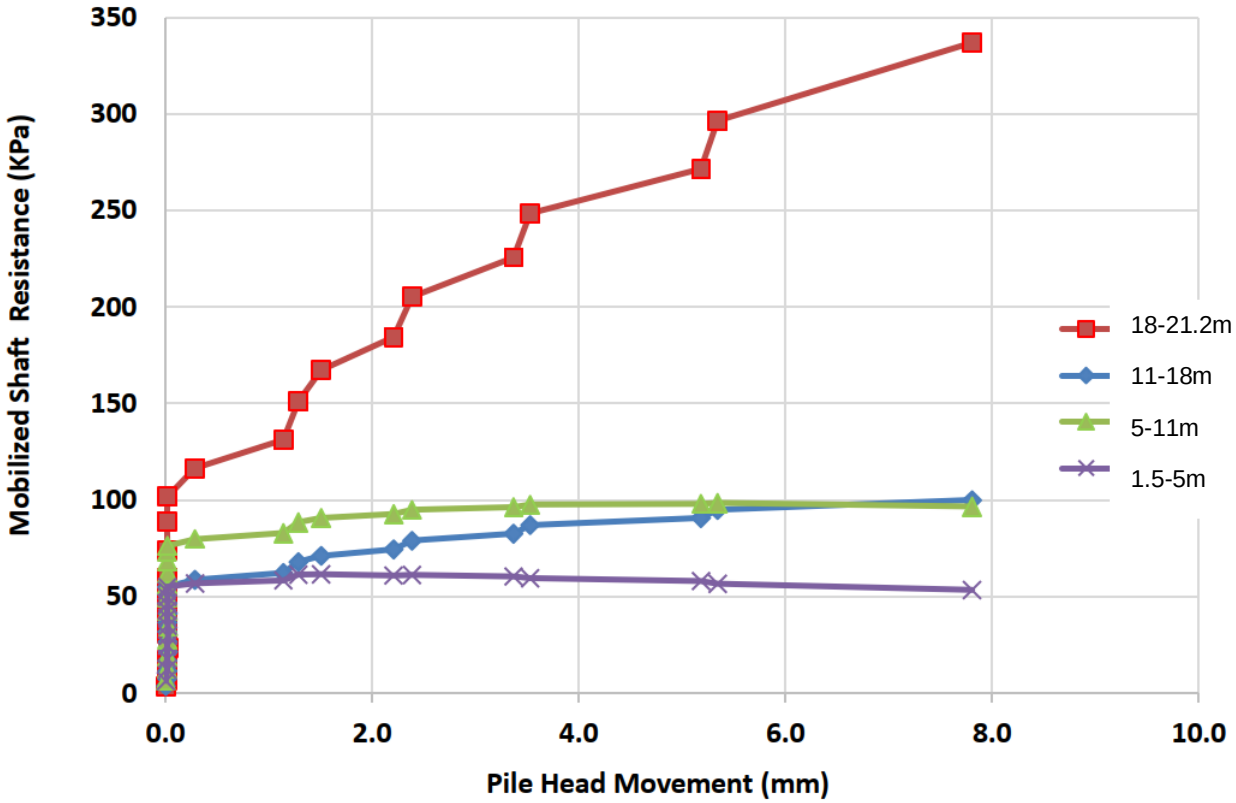

Figure 3.41. TP6 mobilized shaft resistance vs. pile head movement

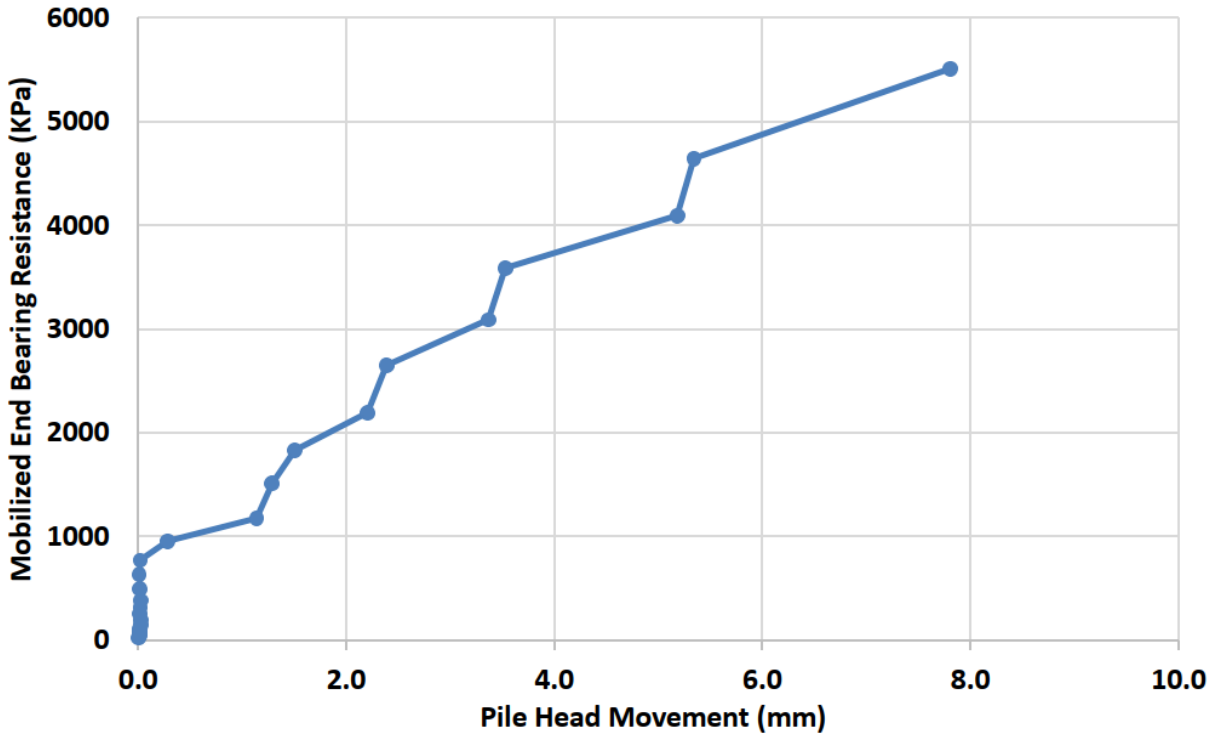

Figure 3.42. TP6 mobilized end bearing resistance vs. pile head movement

The unit load transfer is determined by dividing the difference in load between two points compromising a segment of the test shaft by the surface area of that segment of the pile shaft.

3.7 EVALUATION METHODOLOGY

The evaluation of the effectiveness of CPT/CPTu-based methods involved both statistical and non-statistical analyses. Previous studies have employed similar techniques to evaluate these methods, including researchers such as Briaud and Tucker (1998), Long and Wysockey (1999), Abu-Farsakh and Titi (2004), Cai et al. (2009), Nguyen et al. (2016), and Chung et al. (2019). However, relying solely on statistical analyses may yield misleading results, as pointed out by Briaud and Tucker (1998) and later Chung et al. (2019). Therefore, it is recommended to examine the predicted versus measured pile capacity plots in addition to statistical analyses before making any conclusions regarding the effectiveness of a method.

Before carrying out the evaluation of the methods it was understood from that the capacities would primarily be made up from the shaft resistances of the piles. This in combination with five out of six of the piles not meeting failure criteria meant that the evaluation would consist entirely of evaluating shaft capacities. To add, the test piles would be categorized and evaluated in two distinct groups – the test pile which met failure criteria and the five test piles which did not meet failure criteria. With the category of test piles that met failure criteria only having one pile, it was decided that the pile shaft capacities should be discretized and evaluated at the strain gauge intervals.

In this report, pile shaft capacities obtained from the static axial load test will be referred to as $Q_{s(m)}$, while the predicted capacities from the CPT/CPTu-based methods will be called $Q_{s(p)}$. A $Q_{s(p)}/Q_{s(m)}$ ratio of 1 indicates a perfect prediction. To evaluate the accuracy and precision of the CPT/CPTu-based methods, various statistical and plot-based evaluation schemes were used. The mean and standard deviation of the $Q_{s(p)}/Q_{s(m)}$ ratio indicate the accuracy and precision of the prediction, respectively. The evaluation process considered statistical criteria as well as non-statistical measures that showed the quality of the $Q_{s(p)}$ vs. $Q_{s(m)}$ plots. The adopted evaluation scheme included three criteria:

(1) the slope of the best fit line between the $Q_{s(p)}$ vs. $Q_{s(m)}$ and the square root of the residual sum of squares ($\sqrt{RSS}$) between prediction ($Q_{s(p)}$) and measured ($Q_{s(m)}$).
(2) the coefficient of variation (COV) of $Q_{s(p)}/Q_{s(m)}$.
(3) the 50% (P50) and 90% (P90) cumulative probabilities of the $Q_{s(p)}/Q_{s(m)}$ ratio.

A rank (R_i) was used to determine the performance of a method for each criterion, and these ranks were then summed to determine the rank index (RI) which evaluated the overall performance. The method with the lowest RI was the best performing method. The following subsections provide details on the three criteria.

3.7.1 Criterion I

The first criterion consists of two sub-criteria. The initial sub-criterion compares the slope of the best-fit line passing through the origin of the $Q_{predicted}$ vs. $Q_{measured}$ plot. This evaluation criterion assesses the tendency of a method to overestimate or underestimate the measured pile capacity. The best method is considered to be the one with a slope closer to 1. The second sub-criterion evaluates the method by calculating the square root of the residual sum of squares (√RSS) between the measured and predicted shaft capacity. This sub-criterion demonstrates the accumulated deviation of a method from an ideal scenario. The method's performance is lower if the √RSS is higher, and vice versa.

$$\sqrt{RSS} = \sqrt{\sum_{i=1}^{n} \left(Q_{p(ideal)_i} - Q_{m_i}\right)^2} \tag{34}$$

The rank for this criterion was determined by summing the sub-ranks corresponding to each sub-criterion.

3.7.2 Criterion II

The second criterion evaluates the method by calculating the coefficient of variation (COV). To obtain the COV, the standard deviation is normalized by the mean for the Q_p/Q_m data set, as shown in Eq. 35. This statistical measure indicates the extent of data scattering relative to the mean and is considered indicative of the precision of the predictive methods. A lower COV indicates better performance of the method.

$$COV = \frac{\sigma}{\mu} \tag{35}$$

Where σ is the standard deviation of $Q_{s(p)}/Q_{s(m)}$, and μ is the mean of $Q_{s(p)}/Q_{s(m)}$.

3.7.3 Criterion III

The third criterion was based on the 50% (P50) and 90% (P90) cumulative probabilities. These statistical measures were computed by arranging $Q_{s(p)}/Q_{s(m)}$ ratios in ascending order, using Eq. 36 (Long and Wysockey, 1999), where i is the order number, and n is the total number of $Q_{s(p)}/Q_{s(m)}$ ratios.

$$P = \frac{i}{n+1} \tag{36}$$

Criterion three consisted of two sub-criteria. The first sub-criterion evaluated the magnitude of the P50. This evaluation showed the $Q_{s(p)}/Q_{s(m)}$ value halfway through the data and depicted the method's tendency to overestimate or underestimate the pile capacity. This measure was advantageous over simply computing the mean because the mean was often biased by the largest and smallest $Q_{s(p)}/Q_{s(m)}$ values. The better the method's performance, the closer the P50 value was to 1. The second sub-criterion evaluated the difference between the P90 and the P50. A smaller difference indicated better method performance because it showed reduced scatter of the $Q_{s(p)}/Q_{s(m)}$ values above the P50 value. The rank for criterion three was obtained similarly to criterion one, by summing the sub-ranks corresponding to each sub-criterion.

3.8 CALIBRATION METHODOLOGY

Upon evaluating all the CPT/CPTu based methods, it was discovered that certain methods demonstrated better precision but weaker accuracy. As previously mentioned, these methods are empirical and specific to a particular site. To improve their predictive accuracy, a calibration was performed. The calibration process involved minimizing the square root residual sum of squares between the measured and predicted pile shaft capacities, with the aim of enhancing the accuracy of the methods. The following procedure was employed for calibrating the CPT/CPTu-based methods:

$$\text{Minimum} \Rightarrow \sqrt{RSS} = \sum_{i=1}^{n} Q_{m_i} - \left(\theta Q_{s_i}\right)^2 \tag{37}$$

Here, θ represents a calibration factor. The calibration process was carried out using the MS-Excel application.

CHAPTER 4. RESULTS AND DISCUSSION

4.1 INTRODUCTION

This chapter presents an evaluation of the performance of CPT/CPTu based pile design methods based on the criteria discussed in the previous chapter. The shaft capacities of the piles were analyzed by the positions of the strain gauges, with the piles divided into two groups. Group one includes the shaft capacities of Test Pile 2 (TP2), which met failure criteria, while group two includes the remaining test pile shaft capacities, which did not meet this requirement.

This chapter is organized into two main sections. Firstly, an evaluation of the original CPT/CPTu based methods is presented. Secondly, the best-performing methods were calibrated to improve their performance.

4.2 INITIAL EVALUATION

4.2.1 Criterion I

The first sub-criterion in this category pertains to the slope of the best-fit line between $Q_{s(p)}$ and $Q_{s(m)}$, while the second sub-criterion evaluates the √RSS. The summary of the sub-ranks for these sub-criterions are presented in Table 4.1, while Figure 4.1 to 4.10 exhibit the $Q_{s(p)}$ and $Q_{s(m)}$ plots of the CPT/CPTu methods. In Table 4.1, the sub-ranks for the slope of the best-fit line and √RSS criteria are denoted as R_1^* and R_2^*, respectively. In the failure group, the pile shaft capacities were overestimated using the KTRI method. Conversely, in all other groups and their respective methods, the shaft capacities were underestimated. It should be noted that all methods overestimated the shaft capacities in the upper 1.5 m of the piles. One such possibility for this is offered by Bartz and Blatz (2020). The decreased shaft capacity during the static axial load test can be attributed to shrinkage occurring within the silty clays above the water table.

Table 4.1. The slope of the best-fit line between $Q_{s(p)}$ and $Q_{s(m)}$ and $\sqrt{RSS}$

	CPT/CPTu Based Method	$Q_{s(p)}$ vs. $Q_{s(m)}$ slope	sqrt RSS	R_1^* (for slope)	R_2^* (for sqrt RSS)	$\sum R^*$	R
Failure group	Modified Unicone	0.626	906.17	1	1	2	1
	Togliani	0.469	1202.78	2	2	4	2
	LCPC	0.412	1402.28	3	4	7	3
	KTRI	1.714	2059.27	5	5	10	5
	Penpile	0.390	1399.49	4	3	7	4
Underestimated group	Modified Unicone	0.688	2094.15	2	2	4	2
	Togliani	0.340	3710.35	4	4	8	4
	LCPC	0.285	4260.86	5	5	10	5
	KTRI	0.866	1242.56	1	1	2	1
	Penpile	0.402	3428.24	3	3	6	3

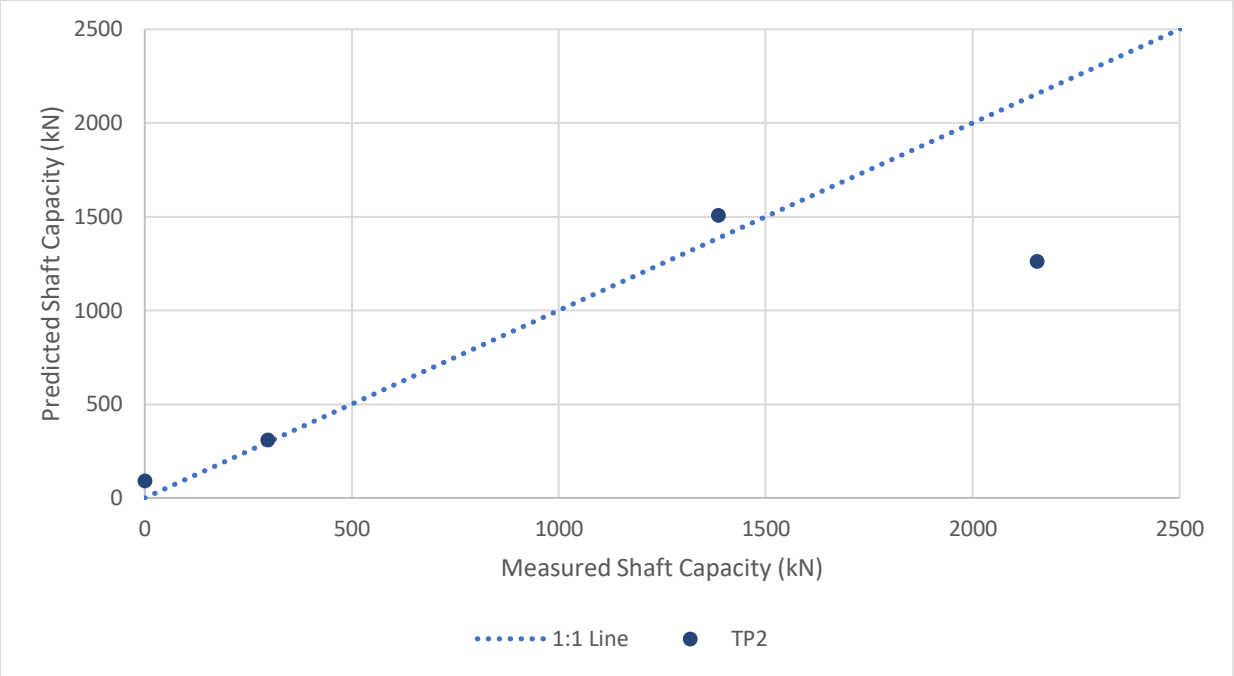

Figure 4.1. Modified Unicone predicted vs. measured shaft capacities (failure group)

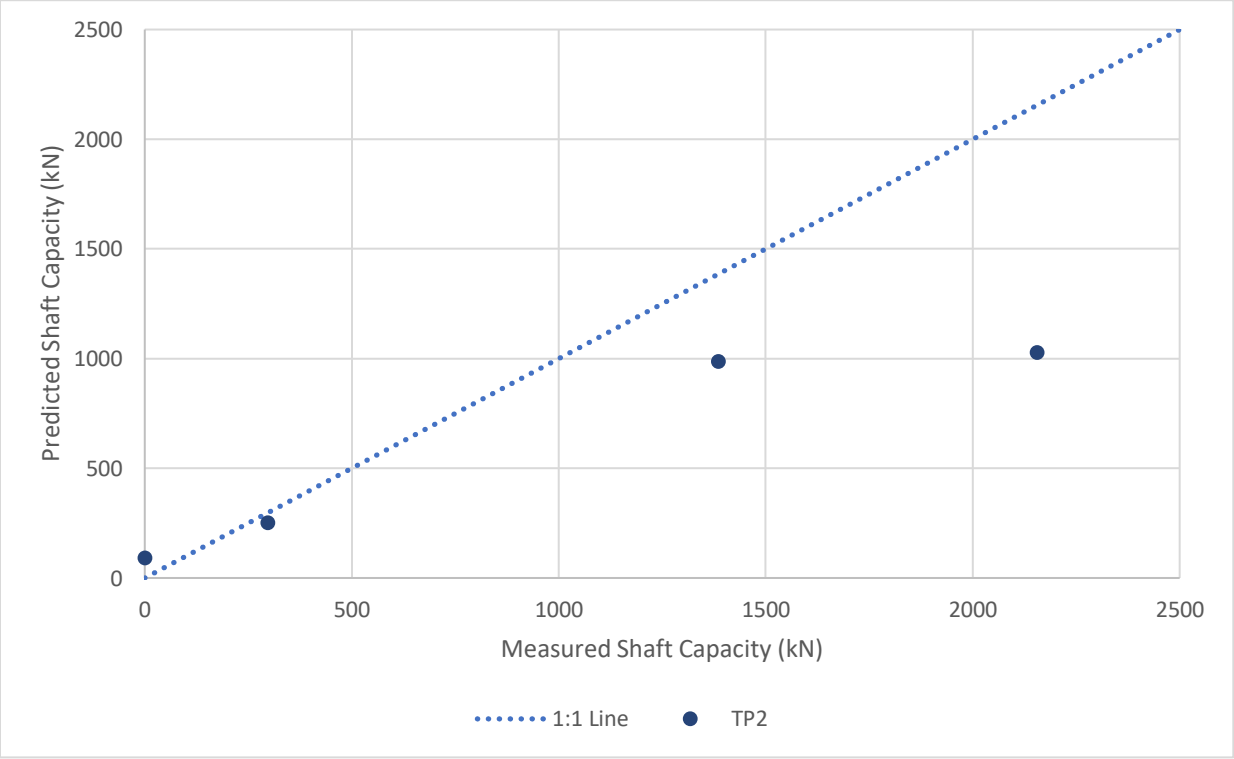

Figure 4.2. Togliani predicted vs. measured shaft capacities (failure group)

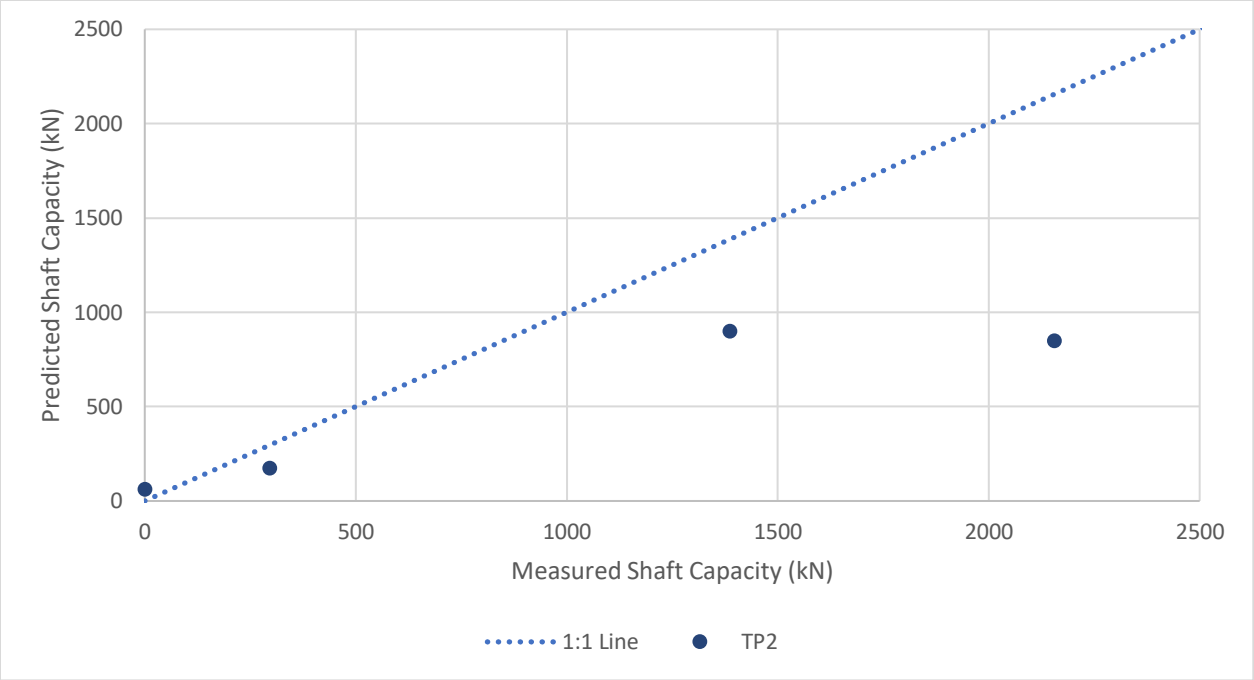

Figure 4.3. LCPC predicted vs. measured shaft capacities (failure group)

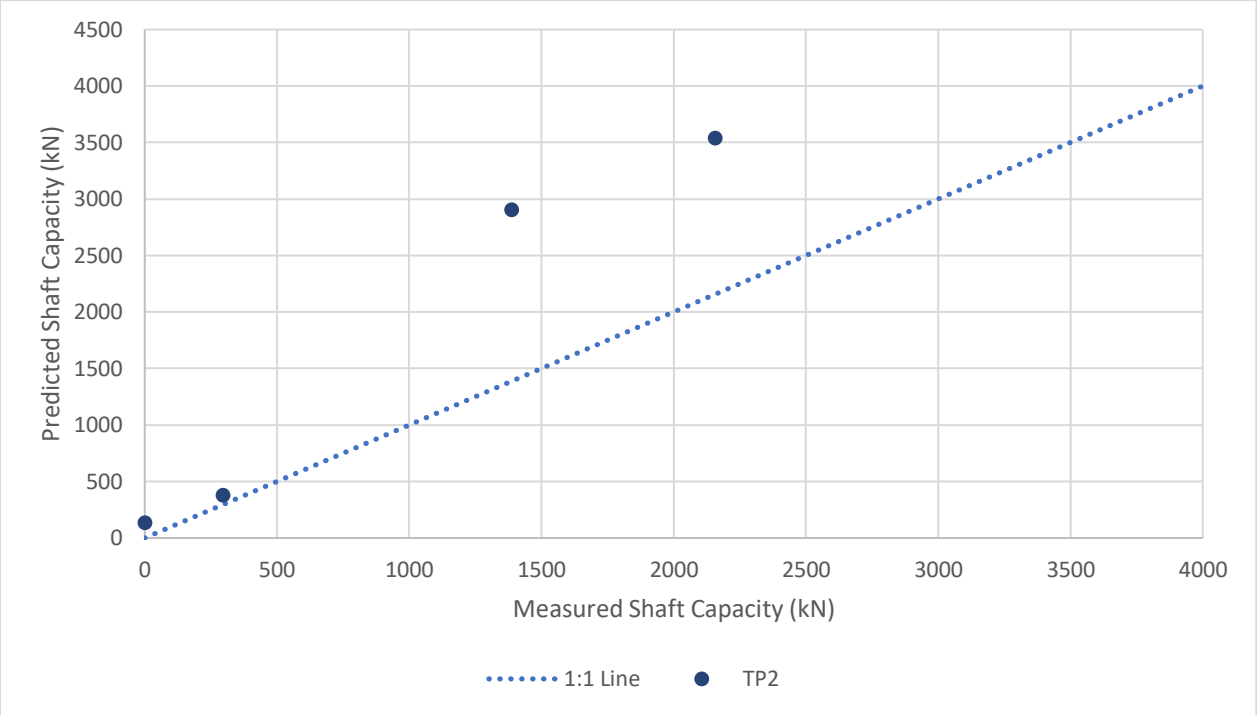

Figure 4.4. KTRI predicted vs. measured shaft capacities (failure group)

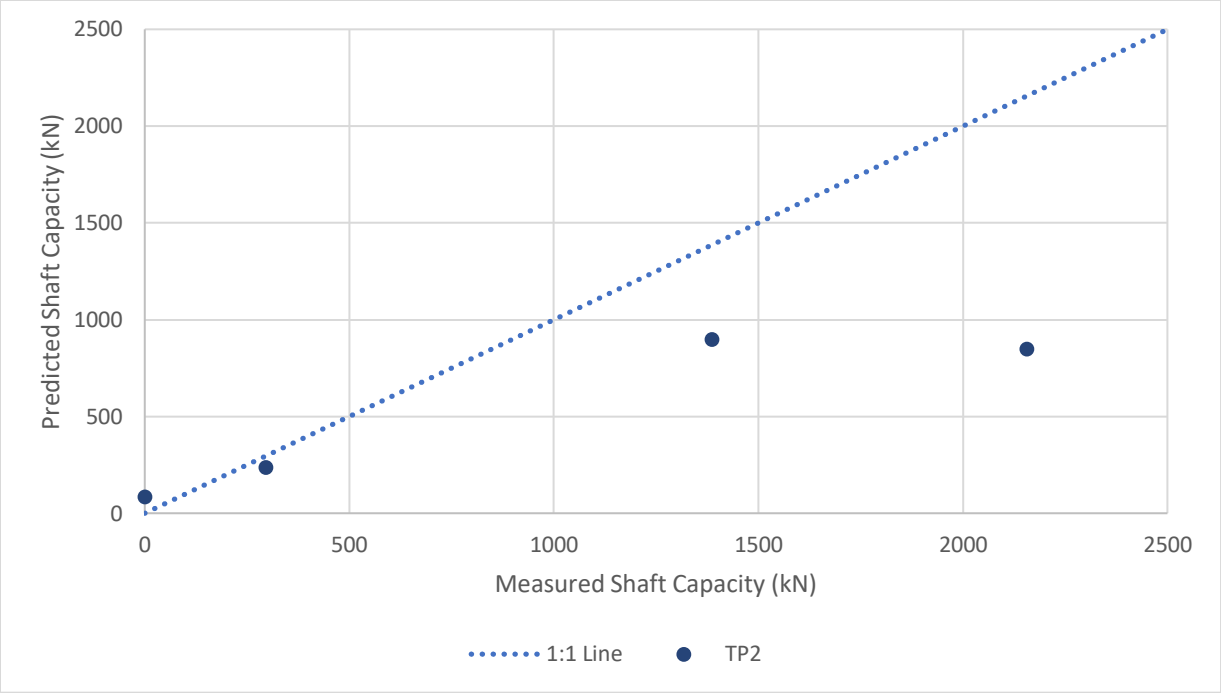

Figure 4.5. Penpile predicted vs. measured shaft capacities (failure group)

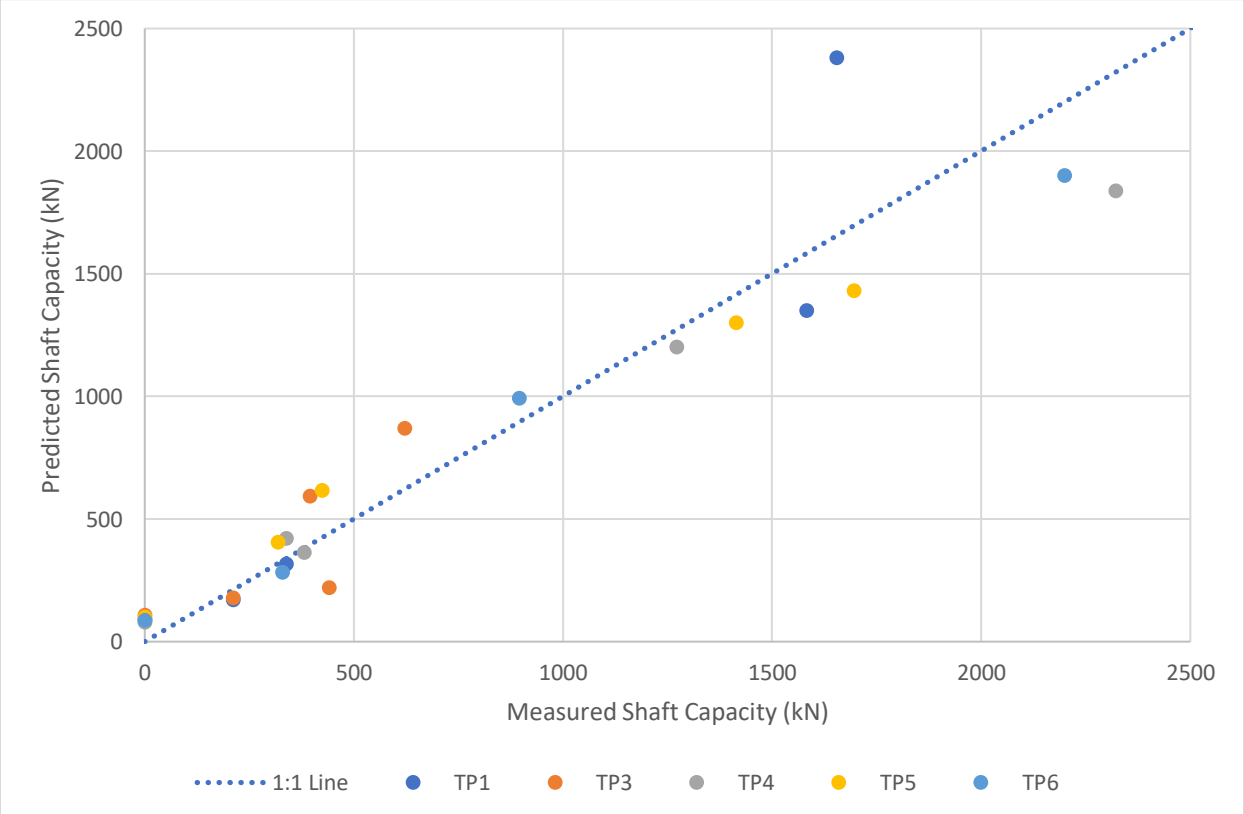

Figure 4.6. Modified Unicone predicted vs. measured shaft capacities (underestimated group)

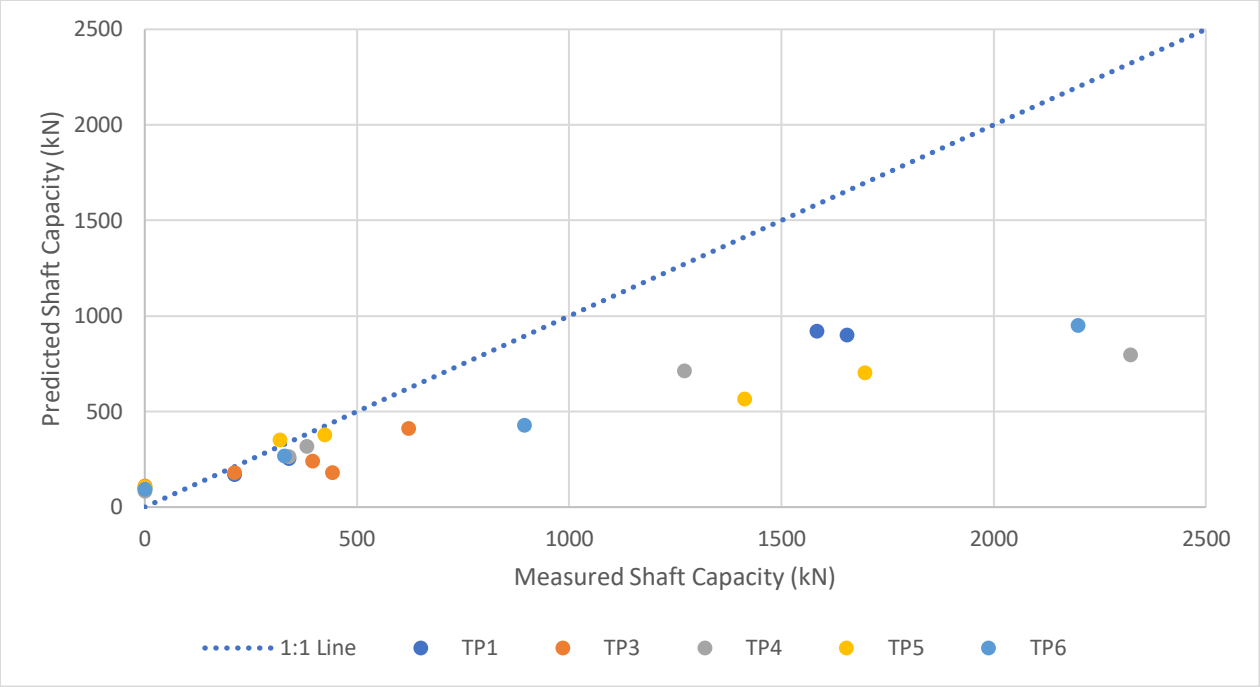

Figure 4.7. Togliani predicted vs. measured shaft capacities (underestimated group)

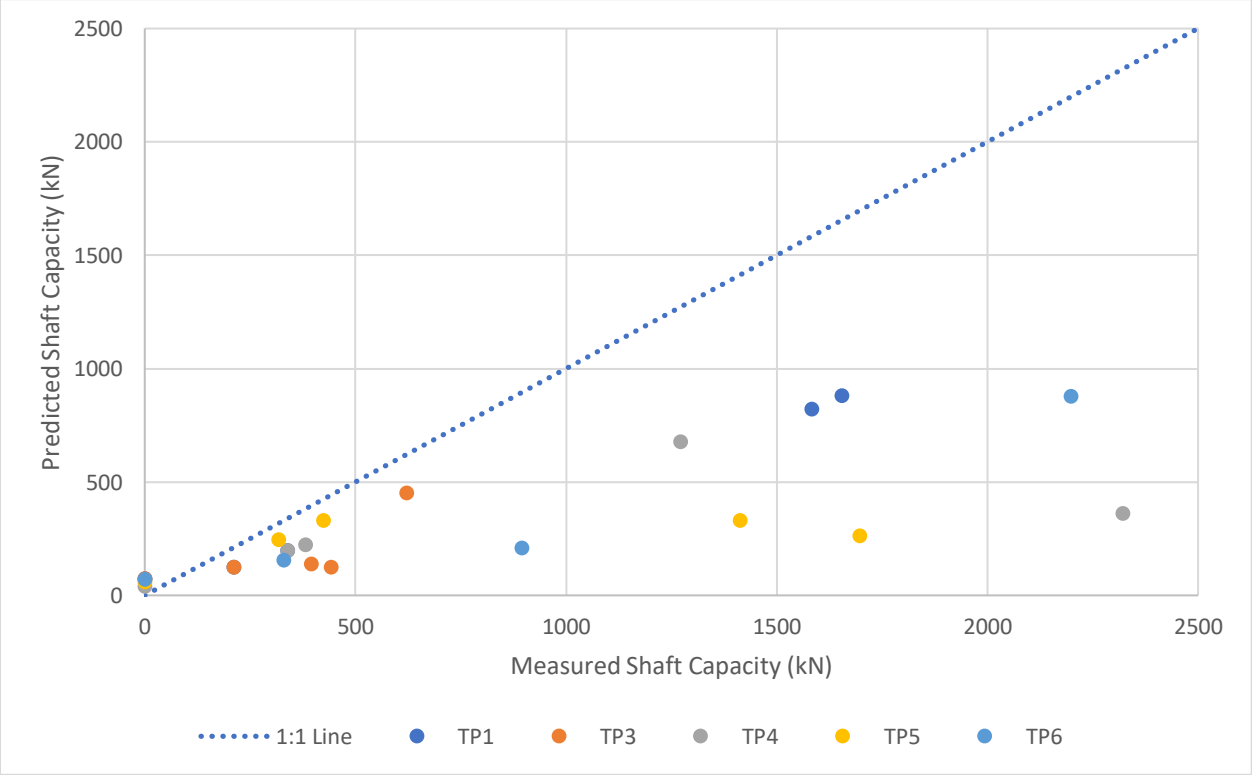

Figure 4.8. LCPC predicted vs. measured shaft capacities (underestimated group)

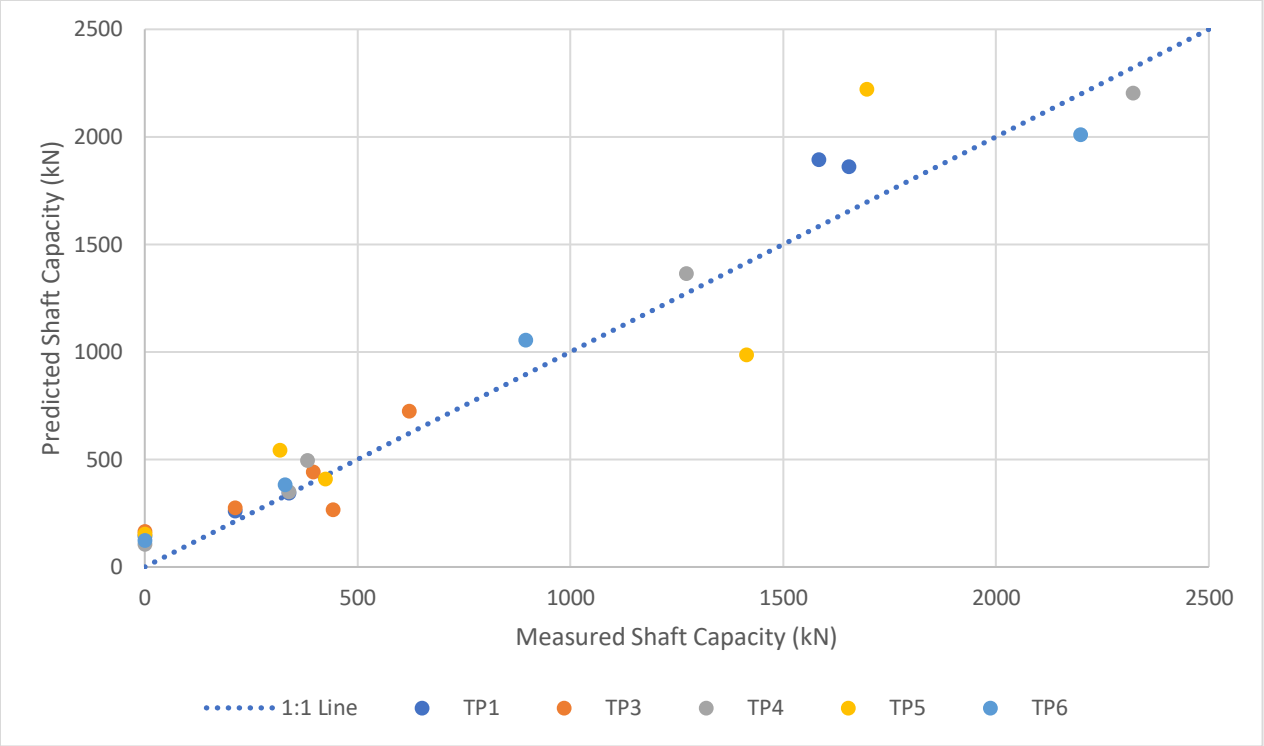

Figure 4.9. KTRI predicted vs. measured shaft capacities (underestimated group)

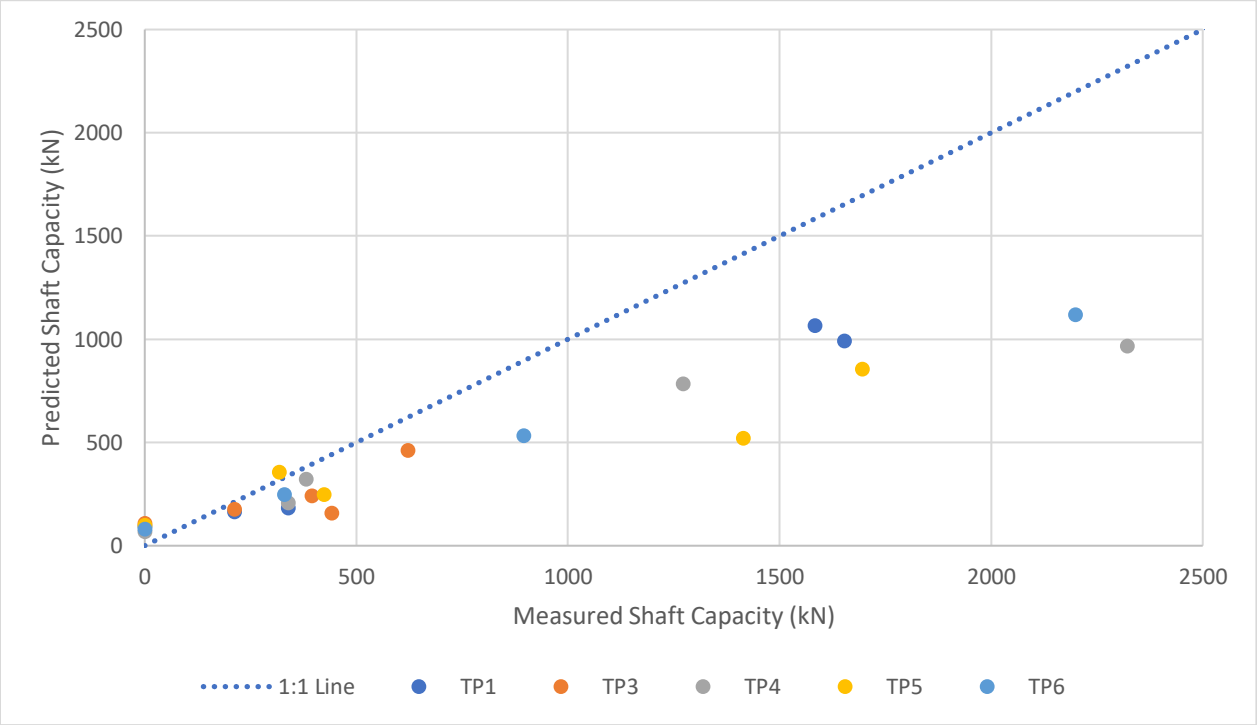

Figure 4.10. Penpile predicted vs. measured shaft capacities (underestimated group)

4.2.2 Criterion II

This criterion evaluated the precision of the CPT/CPTu-based methods, and Table 4.2 presents a summary of the results. Within the failure group, the LCPC method demonstrated the best precision, while in the underestimate group, it was the KTRI method that showed the best precision. In the failure group, the range of coefficient of variation (COV) between the first and last ranks was within 0.071, indicating that the methods exhibited similar levels of precision. However, within the larger population of the underestimated group, the COV range was within 0.188. Within both groups, the LCPC method displayed a substantially low mean value of $Q_{s(p)}/Q_{s(m)}$, suggesting that it consistently underestimated the pile capacity. On the other hand, the Modified Unicone method approached unity in both groups, indicating that it was able to predict the capacities within a high degree of accuracy.

Table 4.2. COV in the ratio of $Q_{s(p)}$ and $Q_{s(m)}$

	CPT/CPTu Based Method	σ	μ	COV	R
Failure group	Modified Unicone	0.226	0.90	0.250	4
	Togliani	0.153	0.68	0.226	3
	LCPC	0.108	0.54	0.200	1
	KTRI	0.337	1.67	0.202	2
	Penpile	0.166	0.61	0.271	5
Underestimated group	Modified Unicone	0.293	0.98	0.299	2
	Togliani	0.212	0.62	0.343	4
	LCPC	0.188	0.46	0.406	5
	KTRI	0.235	1.08	0.218	1
	Penpile	0.186	0.61	0.305	3

4.2.3 Criterion III

To evaluate this criterion, ranks were obtained by comparing the 50% (P_{50}) and 90% (P_{90}) cumulative probabilities, and the results are summarized in Table 4.3. The Modified Unicone method emerged as the top performer in both groups based on the first sub-criterion, which prioritizes having a P_{50} closer to unity. With such a P_{50}, the predictions of this method exhibit a balance of over- and under- predictions. However, the same method was ranked the worst performer in the unfailed group by the second sub-criterion (P_{90}-P_{50}). This indicates that the scattering of points was higher compared to that of the other methods.

Table 4.3. 50% and 90% cumulative probabilities in the ratio of $Q_{s(p)}$ and $Q_{s(m)}$

	CPT/CPTu Based Method	P50	P90	P90-P50	R1*	R2*	∑R*	R
Failure group	Modified Unicone	1.039	1.077	0.04	1	1	2	1
	Togliani	0.711	0.820	0.11	2	3	5	2
	LCPC	0.583	0.636	0.05	4	2	6	3
	KTRI	1.642	2.004	0.36	5	5	10	5
	Penpile	0.649	0.765	0.12	3	4	7	4
Underestimated group	Modified Unicone	0.919	1.439	0.52	1	5	6	2
	Togliani	0.581	0.847	0.27	4	4	8	5
	LCPC	0.520	0.727	0.21	5	2	7	4
	KTRI	1.115	1.299	0.18	2	1	3	1
	Penpile	0.599	0.835	0.24	3	3	6	3

4.2.4 Rank Index

To compute the overall rank of all the CPT/CPTu-based methods, a rank index (RI) was determined as the sum of all ranks from each criterion (1-3). Table 4.4 presents the summary of the RI and overall ranks for predicting shaft capacities. Based on this method, the Modified Unicone method ranked first in the failure group and second in the underestimated group. Although the KTRI method performed well in the underestimated group, it had poor performance within the failure group. Specifically, within the failure group, the KTRI method significantly overpredicted the shaft capacities for the CFA piles. However, in both groups, the KTRI method demonstrated the best cumulative precision (criterion 2). Given that the Modified Unicone method only marginally underperformed compared to the KTRI method in the underestimated group, it is evident that the former is the best performing method. Both the Modified Unicone method and the KTRI method were selected for improvement via calibration.

Table 4.4. Rank index (RI) and overall ranks of each CPT/CPTu-based methods

	CPT/CPTu Based Method	Criterion 1	Criterion 2	Criterion 3	RI	Rank
Failure group	Modified Unicone	1	4	1	6	1
	Togliani	2	3	2	7	2
	LCPC	3	1	3	7	3
	KTRI	5	2	5	12	4
	Penpile	4	5	4	13	5
Underestimated group	Modified Unicone	2	2	2	6	2
	Togliani	4	4	5	13	4
	LCPC	5	5	4	14	5
	KTRI	1	1	1	3	1
	Penpile	3	3	3	9	3

4.3 CALIBRATION

Using the calibration method outlined in Section 3, the top two performing CPT/CPTu-based methods were calibrated to enhance their predictive accuracy. An excel application was utilized to solve the optimization problem by determining a calibration factor for the shaft capacity. The calculated factor was subsequently applied to the original method's determined shaft capacities. After obtaining the calibration factors, a re-assessment of the two design methods was carried out, and the findings are presented. Table 4.5 displays the calibration factors for the methods.

Table 4.5. Calibration factors for selected methods

	CPT/CPTu Based Method	Calibration Factor
Failure group	Modified Unicone	0.74
	KTRI	0.57
Underestimated group	Modified Unicone	0.79
	KTRI	0.95

4.4 FINAL EVALUATION

4.4.1 Criterion I

After calibration, it was determined that the KTRI method performed the best according to criterion I, while the calibrated Modified Unicone method performed poorly in comparison. In both groups, the calibrated Modified Unicone $Q_{s(p)}$ and $Q_{s(m)}$ slope as well as the √RSS were lower than those of the uncalibrated method. The values for the $Q_{s(p)}$ and $Q_{s(m)}$ slope and the √RSS are presented in Table 4.6, and Figures 32 to 35 depict a comparison between the uncalibrated and calibrated estimates of the respective methods.

Table 4.6. Calibrated methods slope of the best-fit line between $Q_{s(p)}$ and $Q_{s(m)}$ and √RSS

	CPT/CPTu Based Method	Qs(p) vs. Qs(m) slope	sqrt RSS	R* (for slope)	R* (for sqrt RSS)	∑R*	R
Failure group	Calibrated Modified Unicone	0.461	1261.16	2	2	4	2
	Calibrated KTRI	0.970	319.03	1	1	2	1
Underestimated group	Calibrated Modified Unicone	0.543	2686.62	2	2	4	2
	Calibrated KTRI	0.819	1309.31	1	1	2	1

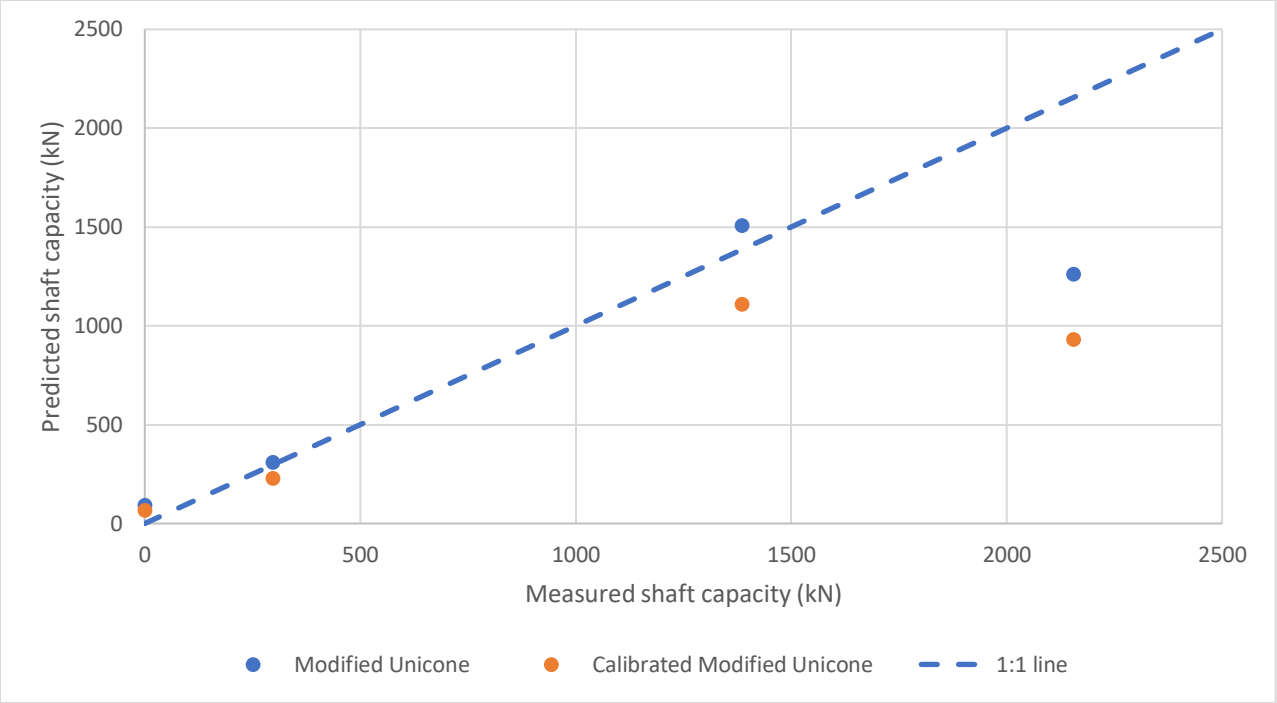

Figure 4.11. Plot of Modified Unicone and Calibrated Modified Unicone Shaft Capacities (Failure Group)

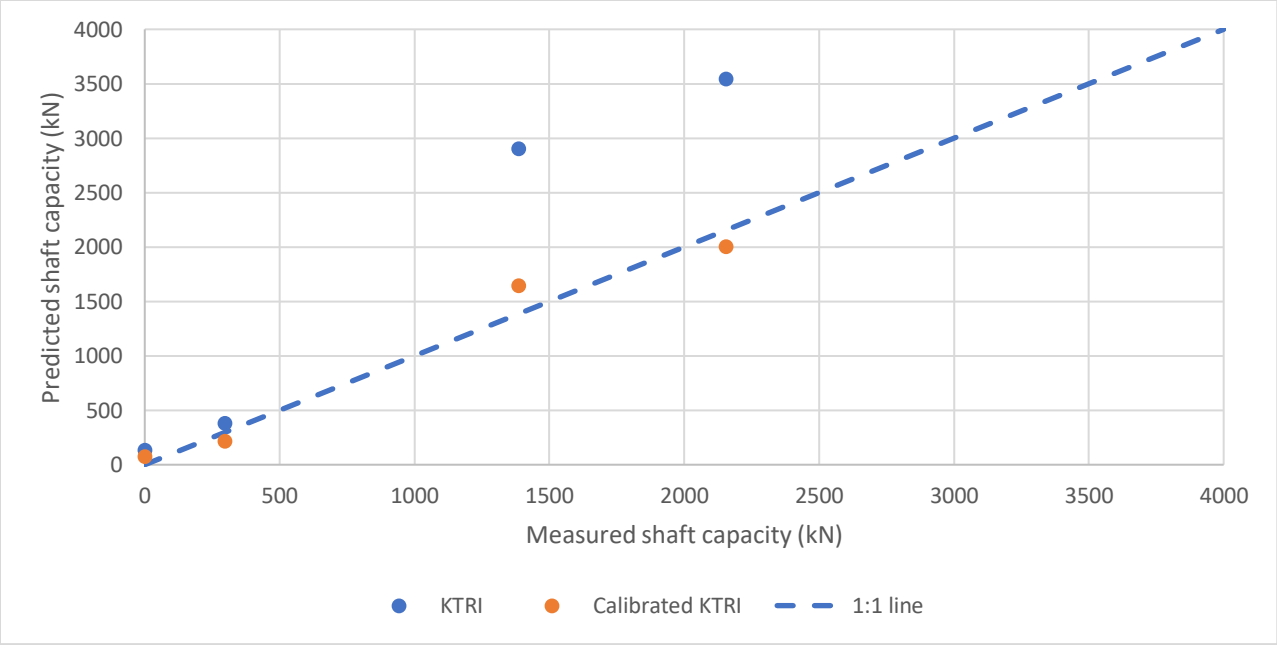

Figure 4.12. Plot of KTRI and Calibrated KTRI Shaft Capacities (Failure Group)

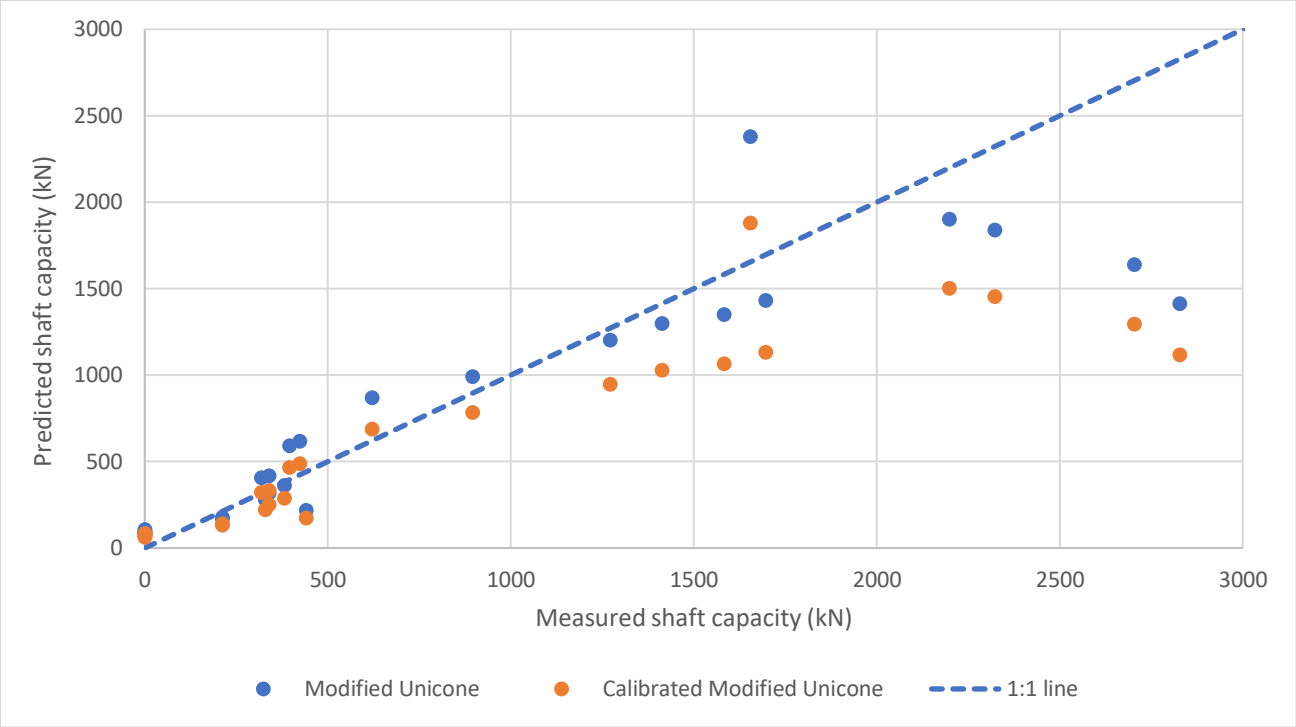

Figure 4.13. Plot of Modified Unicone and Calibrated Modified Unicone Shaft Capacities (Underestimated Group)

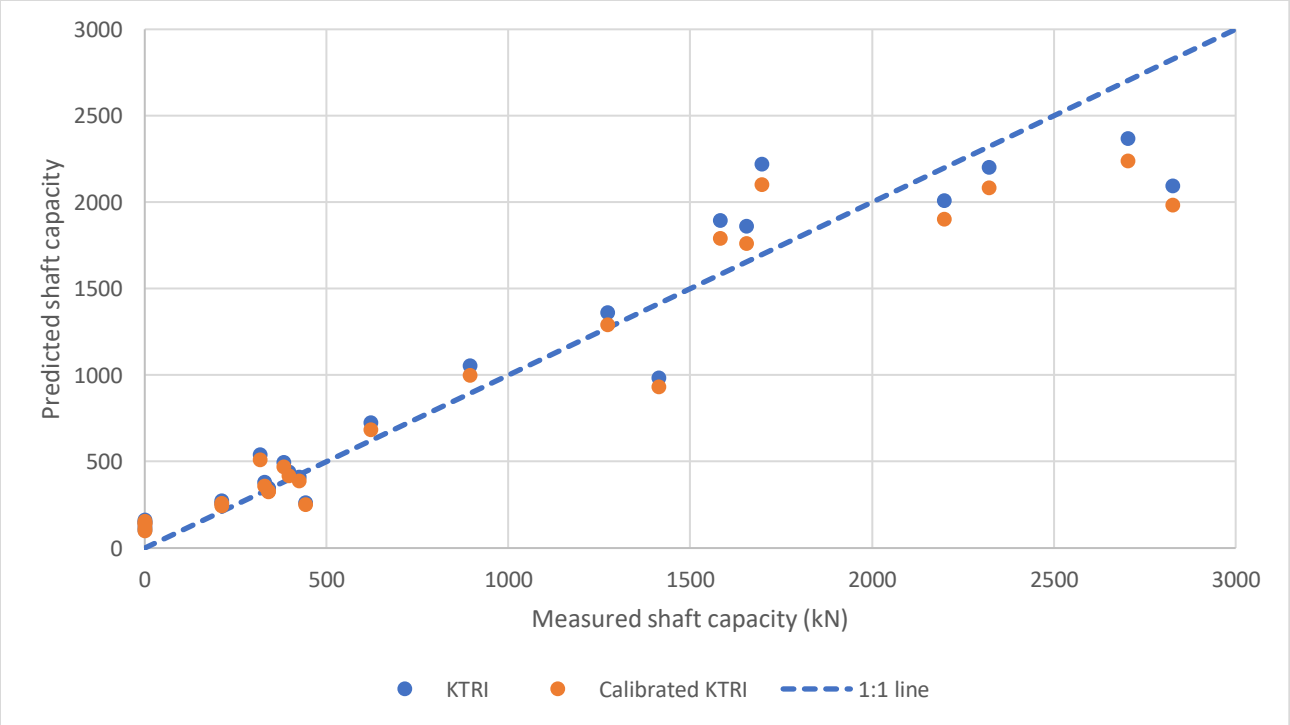

Figure 4.14. Plot of KTRI and Calibrated KTRI Shaft Capacities (Failure Group)

4.4.2 Criterion II

Based on the COV values, the calibration of both methods resulted in either maintained or slightly increased values, with the KTRI method showing slightly underestimated values. Using this criterion, the calibrated KTRI method demonstrated superior performance in both groups.

Table 4.7. Calibrated methods COV in the ratio of $Q_{s(p)}$ and $Q_{s(m)}$

	CPT/CPTu Based Method	σ	μ	COV	R
Failure group	Calibrated Modified Unicone	0.166	0.67	0.250	2
	Calibrated KTRI	0.191	0.94	0.202	1
Underestimated group	Calibrated Modified Unicone	0.232	0.78	0.299	2
	Calibrated KTRI	0.225	1.02	0.222	1

4.4.3 Criterion III

In relation to this criterion, the calibrated Modified Unicone method demonstrated decreased accuracy compared to the original evaluation in both groups. With the calibrated P50 values shifting away from unity. Conversely, the calibrated KTRI method exhibited substantial improvements in accuracy, with the P50 values of both groups approaching unity. Furthermore, the precision of both methods (measured by the difference between P90 and P50) improved within both groups.

Table 4.8. Calibrated 50% and 90% cumulative probabilities in the ratio of $Q_{s(p)}$ and $Q_{s(m)}$

	CPT/CPTu Based Method	P50	P90	P90-P50	R1*	R2*	∑R*	R
Failure group	Calibrated Modified Unicone	0.765	0.79	0.03	2	1	3	1
	Calibrated KTRI	0.929	1.13	0.21	1	2	3	1
Underestimated group	Calibrated Modified Unicone	0.726	1.14	0.41	2	2	4	2
	Calibrated KTRI	1.055	1.23	0.17	1	1	2	1

4.4.4 Rank Index

After calibration was performed, the best performing method in both groups was found to be the KTRI method.

Table 4.9. Calibrated methods rank index and overall rank

	CPT/CPTu Based Method	Criterion 1	Criterion 2	Criterion 3	RI	Rank
Failure group	Calibrated Modified Unicone	2	2	1	5	2
	Calibrated KTRI	1	1	1	3	1
Underestimated group	Calibrated Modified Unicone	2	2	2	6	2
	Calibrated KTRI	1	1	1	3	1

4.5 RISK ANALYSIS

An important comparison was conducted by analyzing $Q_{s(p)}$ and $Q_{s(m)}$ using a risk analysis method proposed by Briaud and Tucker (1998), which assessed the probability of the predicted pile shaft capacity being greater than the measured pile shaft capacity for both CPTu based methods. Equation 38 defines this method as follows:

$$Risk\ (\%) = Probability\left\{\frac{Q_{s(p)}}{Factor\ of\ Safety} > Q_{s(m)}\right\} \tag{38}$$

By this approach, a factor of safety is incorporated into $Q_{s(p)}$ to assess the risk linked with the method shaft capacity estimates. The two calibrated methods were compared using this approach to demonstrate the associated risk. The plots depicting the risk (%) versus the factor of safety for both methods are presented in Figures 36 and 37.

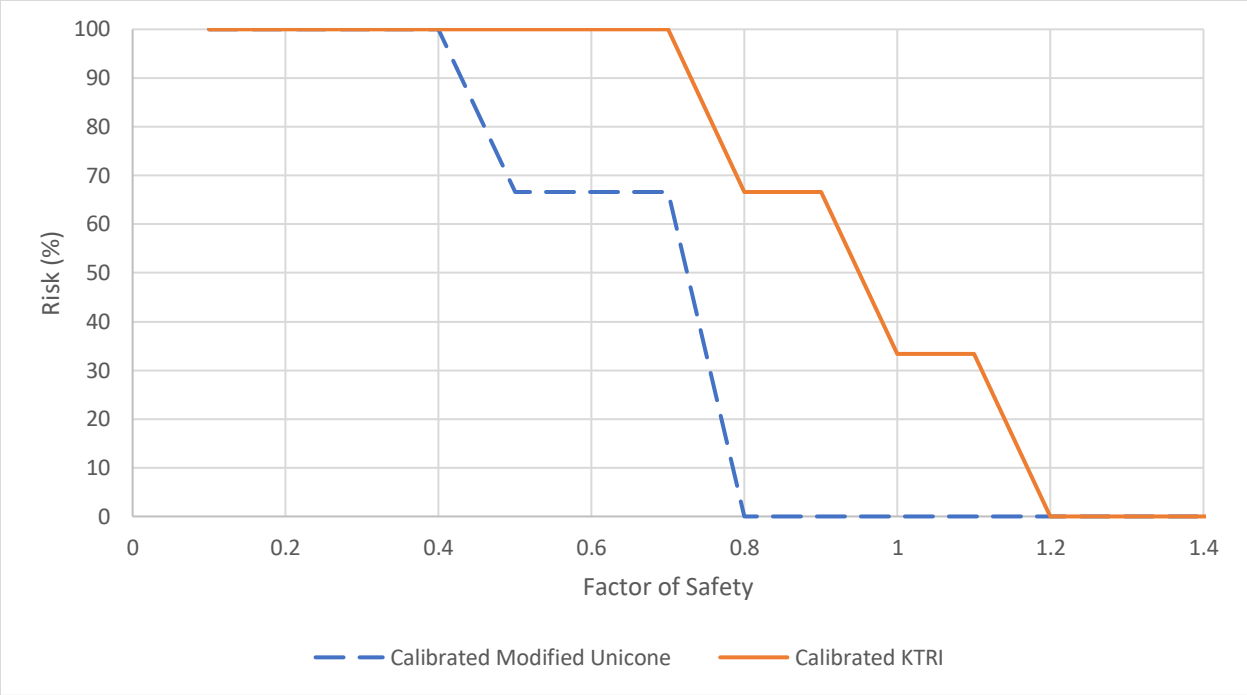

Figure 4.15. Risk vs. factor of safety plot (failure group)

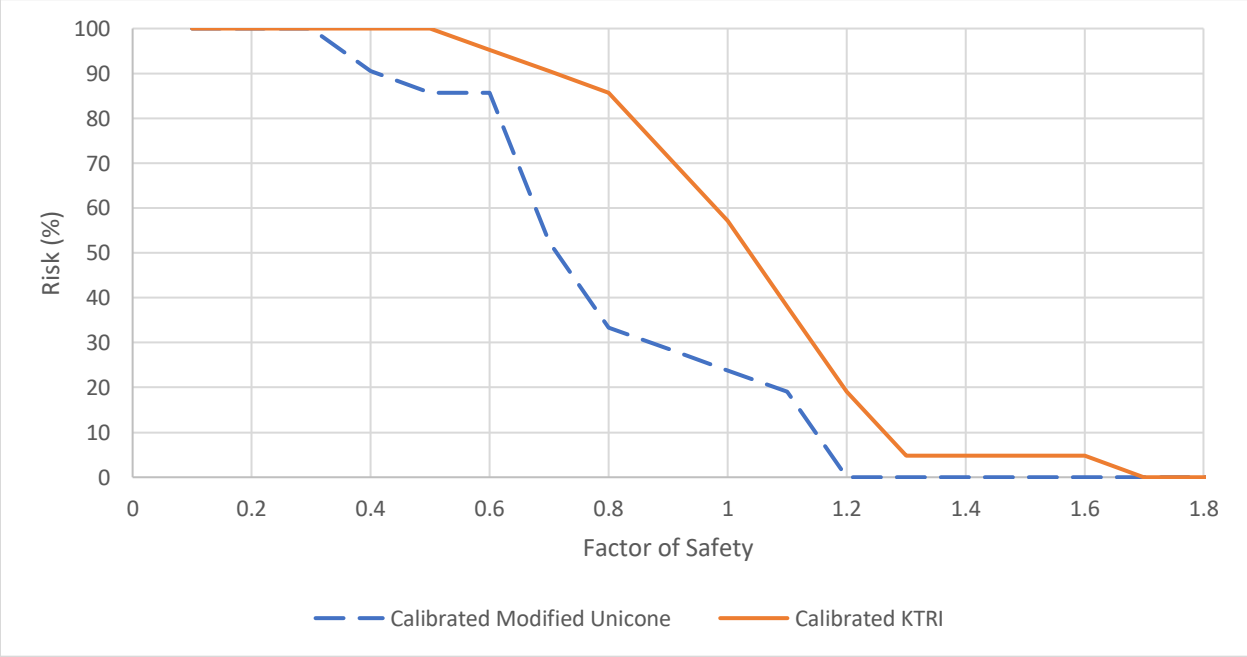

Figure 4.16. Risk vs. factor of safety plot (underestimated group)

Table 4.10 presents the risks associated with the calibrated CPTu based methods when predicting shaft capacities greater than the measured shaft capacity using common factors of safety. Given that the analysis was conducted on a limited number of data sets (especially so with the failure

group), it may not be appropriate to draw firm conclusions about which calibrated CPTu-based method has less associated risk.

Table 4.10. Risk associated to calibrated methods with respective factors of safety

CPT/CPTu Based Method		Risk (%)		
		FoS of 1	FoS of 1.5	FoS of 2
Failure group	Calibrated Modified Unicone	24	0	0
	Calibrated KTRI	57	5	0
Underestimated group	Calibrated Modified Unicone	0	0	0
	Calibrated KTRI	33	0	0

CHAPTER 5. CONCLUSIONS

5.1 THESIS SUMMARY

This research investigates the use of direct CPT/CPTu-based pile design methods for analyzing continuous flight auger piles in soils predominantly composed of silt and sand. Initially, the performance of existing methods was evaluated by comparing the estimated shaft capacities with the shaft capacities determined by static axial load tests. To assess the accuracy and precision of the direct CPT/CPTu methods, appropriate statistical and non-statistical quantitative evaluation criteria were adopted. The top two methods were identified based on these criteria and later calibrated to minimize the square root of the residual sum of squares against load test data. These calibrated methods were then evaluated again using the same criteria employed in the initial evaluation. The KTRI method was found to provide the closest estimates to the actual pile shaft capacities after calibration. On the other hand, the calibrated Modified Unicone method was found to be more conservative, with a significantly lower chance of overestimating pile shaft capacities.

5.2 A NOTE ON PRACTICALITY

The appeal of in-situ sounding tests like Cone Penetration Testing with pore pressure measurements (CPTu) has been consistently growing. However, choosing appropriate methods for site conditions and pile types in pile design remains a challenge. The increasing utilization of CPTu highlights the need for geotechnical engineers to develop methodologies to assess the various direct CPT/CPTu methods and ascertain their suitability.

To achieve more accurate and reliable results, it is crucial to perform site-specific calibration, especially if reference load test data (static or dynamic) is available. Site-specific calibration is a vital step that ensures better pile performance and enhanced safety. Geotechnical engineers can apply calibration factors at their discretion to sites exhibiting conditions similar to those encountered in this research. This evaluation can be carried out by comparing the arithmetic average of the CPTu soundings from the calibration to their own CPTu soundings. According to the NCHRP Report 507 (2004), a recommended upper limit of 25% serves as the threshold for low site variability. If the CPTu sounding falls within this threshold, applying calibration factors, and evaluating the sites as similar might be appropriate.

Figure 5.1 illustrates the calculated average plot for the CPTu in-situ data from all six soundings. To supplement the analysis, Figure 5.2 displays the SBT Qtn plot for the site-averaged CPTu sounding, while Figure 5.3 shows probability distributions for cone resistance in the site-averaged CPTu sounding.

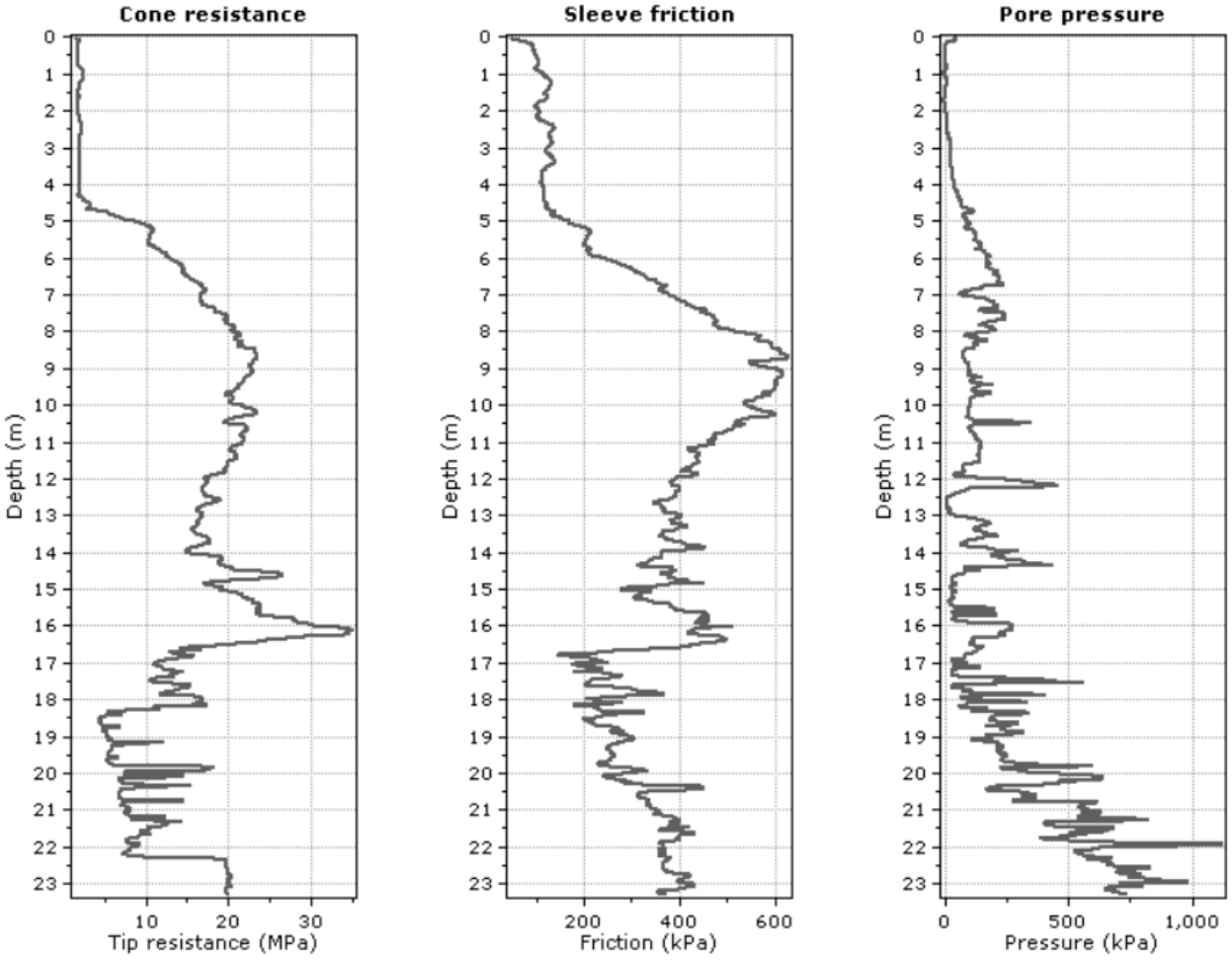

Figure 5.1. Plot of CPTu average in-situ data for the 6 site soundings

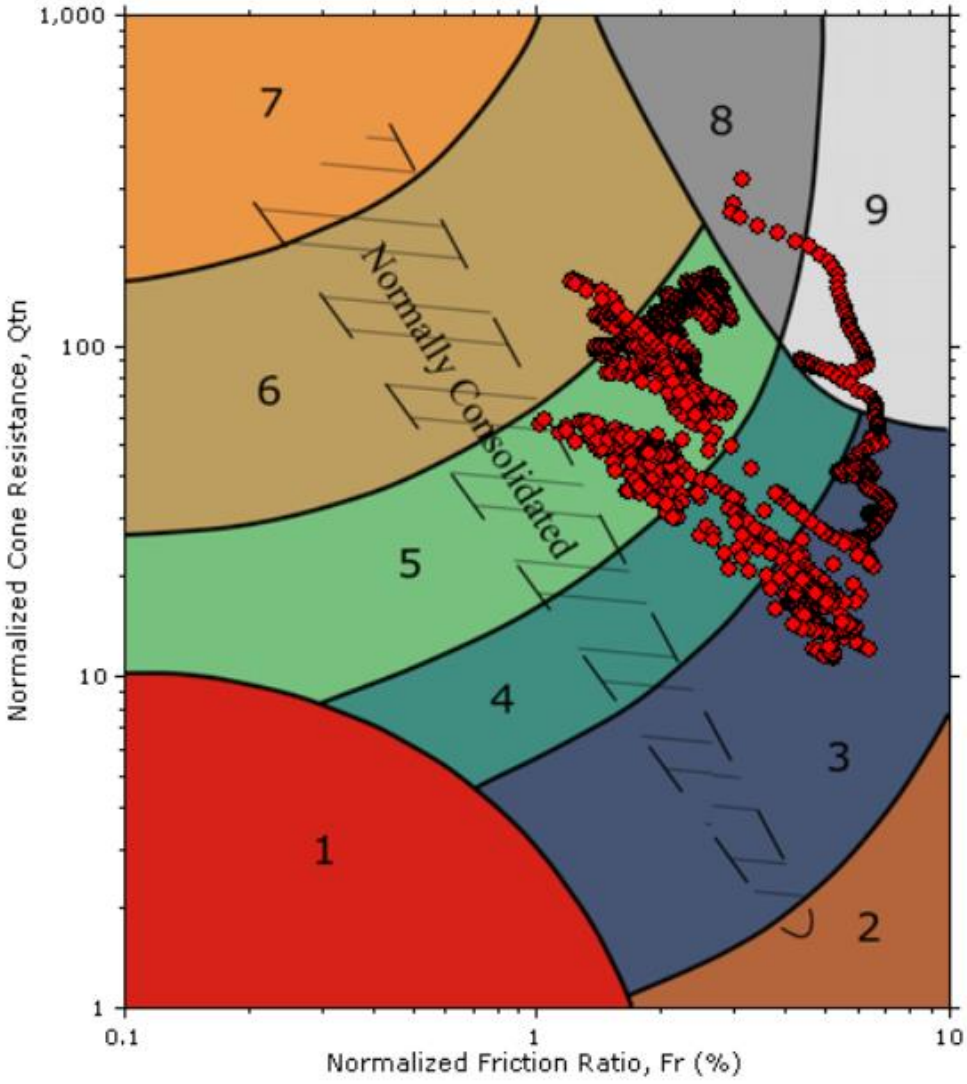

Figure 5.2. SBT Qtn plot for site averaged CPTu sounding

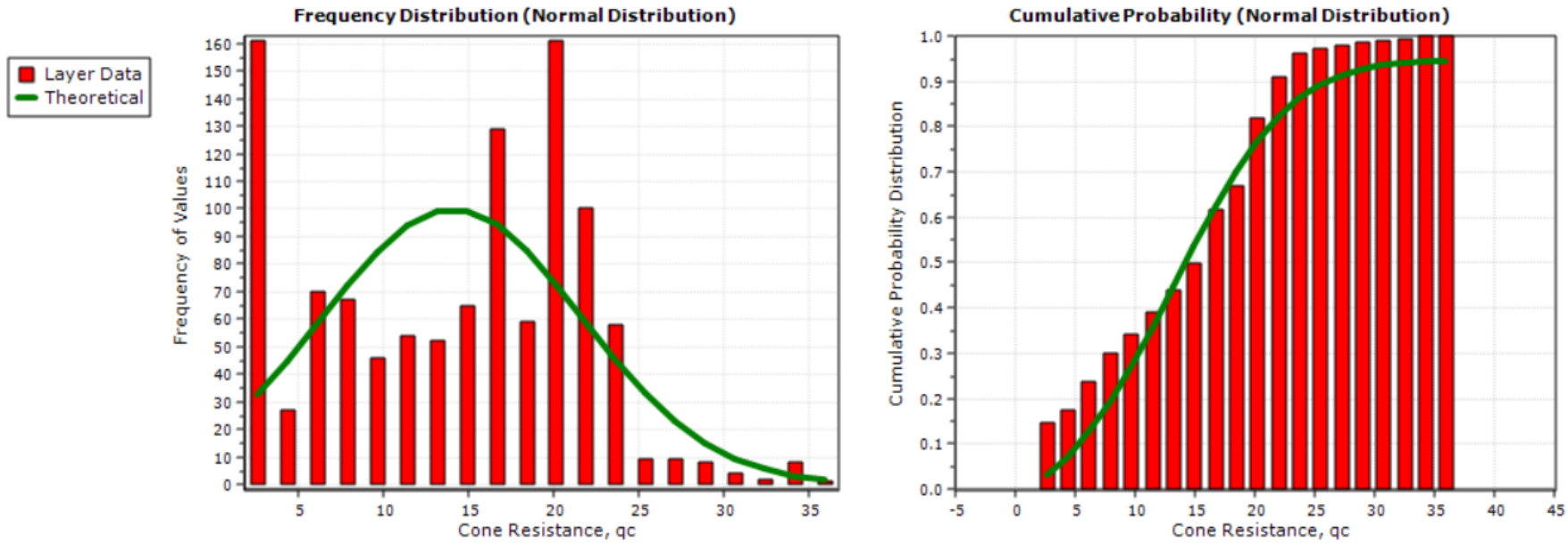

Figure 5.3. Probability distributions for cone resistance for site averaged CPTu sounding

The findings of this research are beneficial for pile design in general as well as pile design specifically in the Condie aquifer region and sites of similar geological conditions.

5.3 RECCOMENDATIONS FOR FUTURE RESEARCH

To further this research a pile database could be created for the region, discretized by pile type and predominant soil conditions. The evaluation of direct CPT/CPTu methods could then take place and the statistical relevance of the results could hold more weight. Preferably this database would include reference load test data from static axial load tests that had gone to failure so that the end bearing capacities of the piles could be evaluated as well. The reference load test data could also be determined by dynamic testing method.

REFERENCES

Abu-Farsakh, M.Y., and Titi, H. H. 2004. Assessment of direct cone penetration methods for predicting the ultimate capacity of friction driven piles. Journal of Geotechnical and Geoenvironmental Engineering, 130(9).

Abu-Farsakh, M.Y., Chen, Q., Haque, N., et al. (2013). Calibration of resistance factors for drilled shafts for the new fhwa design method. Report no., Louisiana Transportation Research Center.

ASTM Standard D1143/D1143M. 2020. Standard Test Methods for Deep Foundation Elements Under Static Axial Compressive Load.

Bartz, J.R. and Blatz, J.A. 2021. Correlation of Cone Penetration Test (CPTu) Pile Design Methods to Predict Shaft Resistance of a Driven Steel H-Pile in Silty Clay.

Briaud, J.L. and Tucker, L.M. 1988. Measured and predicted axial response of 98 piles. Journal of Geotechnical Engineering, 114(9).

Brown, D., Turner, J., Castelli, R., Loehr, E. 2018. Drilled Shafts: Construction Procedures and Design Methods. Adapted from O'Neal, M., and Reese, L. United States Department of Transportation Federal Highway Administration.

Cai, G., Liu, S., Tong, L., and Du, G. 2009. Assessment of Direct CPT and CPTu Methods for Predicting the Ultimate Bearing Capacity of Single Piles. Engineering Geology, 104.

Clisby, M.B., Scholtes, R.M., Corey, M.W., Cole, H.A., Teng, P., and Webb, J.D. 1978. An Evaluation of Pile Bearing Capacities, Volume I, Final Report, Mississippi State Highway Department.

Elbanna, M., Hendry, C., Sharp, J., Woeller, D., and Greig, J. 2007. Axial Pile Capacity: Predicted Versus Measured Response in Southern Alberta Clay Till.

Eslami, A. and Fellenius, B. H. 1997. Pile Capacity by Direct CPT and CPTu Methods Applied to 102 Case Histories. Canadian Geotechnical Journal, 34.

Eslami, A. and Gholami, A. 2006. Analytical Model for the Ultimate Bearing Capacity of Foundations from Cone Resistance.

Eslami, A., Aflaki, E., and Hosseini, B. 2011. Evaluating CPT and CPTu Based on Pile Bearing Capacity Estimation Methods Using Urmiyeh Lake Causeway Piling Records. Scienta Iranica.

Eslami, A., Alimirzaei, M., Aflaki, E., and Molaabasi, H. 2017. Deltaic soil behavior classification using CPTu records. Marine Georesources and Geotechnology 35.

Fellenius, B. H. 2001. From Strain Measurements to Load in an Instrumented Pile. Geotechnical News Magazine, Vol. 19.

Fellenius, B.H. 2002A. Determining the Resistance and Distribution in Piles. Part 1: Notes on Shift of No-Load Reading and Residual Load. Geotechnical News Magazine, Vol. 20, No. 2.

Fellenius, B.H. 2002B. Determining the Resistance Distribution in Piles. Part 2: Method for Determining the Residual Load. Geotechnical News Magazine, Vol. 20, No. 3.

Fellenius, B.H. 1989. Tangent Modulus of Piles Determined from Strain Data. The American Society of Civil Engineers, ASCE, Geotechnical Engineering Division.

Fleming, W.G.K. 1995. The Understanding of Continuous Flight Auger Piling, Its Monitoring and Control. Proceedings of the Institution of Civil Engineers – Geotechnical Engineering.

Fleming, W.G.K. 2009. Piling Engineering. Taylor & Francis, New York.

Gavin, K.G., Chatta, I., and O'Kelly, B.C. 2006. Field Measurements of Horizontal Stress on an Instrumented Pile in Sand. The American Society of Civil Engineers, ASCE, Geotechnical Engineering Division.

Hegazy, Y.A. 1998. Delineating geostratigraphy by cluster analysis of piezocone data. PhD dissertation, School of Civil and Environmental Engineering, Georgia Institute of Technology, Atlanta, Ga.

Kania, J. G., Sorensen, K.K., and Fellenius, B.H. 2020. Analysis of Static Loading Test on an Instrumented Cased CFA Pile in Silt and Sand. International Journal of Geoengineering Case Histories, 5(3).

Kassem, Mahmoud. 2017. Comparative Investigation of Bored and Continuous Flight Auger Piles with Consideration of Green Concrete.

Kee, C.H. 1970. Estimation of the ultimate load of piles from tests not carried to failure. Southeast Asian Society of Soil Engineering, The Second Southeast Asian Conference on Soil Engineering.

Long, J.H. and Wysockey, M.H. 1999. Accuracy of methods for predicting axial capacity of deep foundations. Analysis, Design, Construction, and Testing of Deep Foundations, ASCE.

Lunne, T., Robertson, P.K. and Powell, J.J.M. 1997. Cone Penetration Testing in Geotechnical Practice. Blackie Academic and Professional

Mayne, P., Schneider, J. 2001. Evaluating Axial Drilled Shaft Response by Seismic Cone.

Neely, W. 1991. Bearing Capacity of Auger-Cast Piles in Sand. Journal of Geotechnical Engineering, 117.

Nguyen, T.D., Lee, J.H., Kim, S.R. 2016. Applicability of CPT based methods in predicting toe bearing capacities of driven piles in sand. Acta Geotechnica.

Niazi, F. 2013. An Update on Pile-CPTu Direct Correlations. Georgia Institute of Technology, Atlanta, GA.

Pardoski, K. V. 2008. Pile Bearing Capacity in Glacial Till. 61st Canadian Geotechnical Conference, Edmonton, Alberta.

Paikowsky, S.G., Birgisson, B., McVay, M., Nguyen, T., Kuo, C., Baecher, G., Ayyub, B., Stenersen, K., O'Malley, K., Chernauskas, L., and O'Neill, M. 2004. Load and Rsistance Factor Design (LRFD) for Deep Foundations. NCHRP Report 507, Transportation Research Board Washington.

Price, G. and Wardle, I.F. 1982. A Comparison Between Cone Penetration Test Results and the Performance of Small Diameter Instrumented Piles in Stiff Clay. Proceedings, the 2nd European Symposium on Penetration Testing, Amsterdam.

Robertson, P.K. 2009. Cone penetration testing: a unified approach. Canadian Geotechnical Journal, 46 (11).

Robertson, P.K. and Cabal, K. 2010. Guide to cone penetration testing for geotechnical engineering. Gregg Drilling & Testing.

Saftner, D., Dagger, R., and Mayne, P. 2018. Cone Penetration Testing Guide for State Geotechnical Engineers. Minnesota Department of Transportation and Research Services.

Salgado, R. 2011. The engineering of foundations. McGraw Hill, New Dehli.

Song, C., Kim, S., Bekele, B., Zhang, J., Silvey, A. 2019. CPT-Based Pile Design. Nebraska Department of Transportation (NDOT).

Terzhagi, K. & Peck, R.B. 1967. Soil Mechanics in Engineering Practice. John Wiley & Sons, Inc., New York, London, Sydney.

Titi, H.H. and Abu-Frasakh, M.Y. 1999. Evaluation of Bearing Capacity of Piles from Cone Penetration Test Data. Louisiana Department of Transportation and Development.

Togliani, G. 2008. Pile Capacity Prediction for In Situ Tests.

Togliani, G. 2010. Pile Capacity Prediction using CPT – Case History.

Valsson, S.M. 2016. Detecting quick clay with CPTu. Proceedings, 17th Nordic Geotechnical Meeting, Reykajavik, Iceland: Challenges in Nordic Geotechnics.

Van Impe, W. 2004. Two decades of full-scale research on screw piles: An overview. Published by The Laboratory of Soil Mechanics, Ghent University, Belgium.